Technische Universität München
TUM School of Life Sciences

Hematopoietic cell tracing in mouse models of regeneration and infection

Marcel German Erwin Rommel

Vollständiger Abdruck der von der TUM School of Life Science der Technischen Universität München zur Erlangung des akademischen Grades eines

Doktors der Naturwissenschaften

genehmigten Dissertation.

Vorsitz: Prof. Dr. Aphrodite Kapurniotu

Prüfer*innen der Dissertation:

1. Prof. Angelika Schnieke, Ph.D.

2. Prof. Dr. Benjamin Schusser

3. Prof. Dr. Claudia Waskow

Die Dissertation wurde am 10.01.2023 bei der Technischen Universität München eingereicht und durch TUM School of Life Science am 29.06.2023 angenommen

Summary

All mature blood cells derive from multipotent hematopoietic stem cells (HSCs), which reside in the bone marrow (BM). To maintain life-long and balanced hematopoiesis, HSC fate is tightly regulated between self-renewal, differentiation, and quiescence by extrinsic and intrinsic factors. HSCs are capable to respond efficiently to acute demand like blood loss by proliferation and expansion. One essential signaling pathway controlling HSC maintenance in steady-state hematopoiesis and also HSC expansion in stress hematopoiesis is the thrombopoietin (THPO) / THPO receptor (MPL) pathway. THPO/MPL-signaling is also crucial for megakaryopoiesis and thrombopoiesis. Although MPL expression is restricted to HSCs and megakaryocytes (MKs) and the signaling pathway has been studied mechanistically in detail, the downstream targets are mainly unknown in both cell populations. Furthermore, it remains elusive, how the THPO/MPL signaling axis induces apparently opposing fates, especially in the light that inflammatory stress hematopoiesis studies have identified rapid MK / platelet replenishment directly from HSCs, the so-called emergency megakaryopoiesis. This mechanism strongly supports the close relationship between HSCs and MKs. My study aimed to (1) identify THPO/MPL downstream targets responsible for HSC regeneration in a Mpl-deficient mouse model of aplastic anemia; (2) investigate murine MPL signaling and functionality after stimulation with the human THPO peptide mimetic romiplostim and dissect whether the activation of a specific signal pathway is linked to a particular intracellular residue of MPL and the subsequent functional consequences in megakaryopoiesis; (3) evaluate whether a non-systemic stress hematopoiesis model of respiratory infection with influenza affects HSC quiescence and fate and whether THPO/MPL signaling regulates emergency megakaryopoiesis.

Project 1:

I studied whether predicted Thpo target genes selected from own gene expression analysis were able to rescue the Mpl-deficient phenotype. Therefore, Mpl-knockout (KO) lineage marker-negative (Lin^-) BM cells were transduced with the respective candidate genes and transplanted into Mpl-KO mice. One out of five tested genes were identified, namely the endothelial protein C receptor (EPCR), to expand phenotypic HSCs in Mpl-KO mice and Epcr-transduced Mpl-KO HSCs successfully reconstituted and engrafted in secondary recipients. Epcr-transduced Mpl-KO HSCs homed and re-established quiescence earlier after transplantation and upregulated the expression of the anti-apoptotic gene BcL-XL. Besides re-establishing the HSC pool, Epcr-transduced Mpl-KO hematopoiesis rescued the number of polyploid MKs in the BM without affecting other lineages, however, failed to reestablish

thrombopoiesis. EPCR expression on wild-type (wt) HSCs phenotypically identified the HSC population with superior engrafting potential in the BM. EPCR cell surface expression on fluorescence activated cell sorted (FACsorted) and *in vitro* cultured hematopoietic stem and progenitor cells (HSPCs) was maintained by THPO supplementation, which rapidly declined when THPO was not added. $EPCR^+$ HSCs represent the target population of *ex vivo* gene therapy approaches, where HSC-enriched cells are cultivated for several days for genetic modification. Furthermore, my study underlines the close relationship between HSCs and MKs and supports the hypothesis that the MK-lineage directly branches from HSCs.

Project 2:

Several studies administered the THPO peptide mimetic romiplostim in mouse models, however, mechanistic analysis of murine MPL activation with romiplostim remains unreported. Since romiplostim is specifically selected and designed against the human THPO binding domain of human MPL, there might be differences in signaling activation and functionality. The murine interleukin 3-dependent 32D cell line was utilized to overexpress either murine (m) or human (h) MPL by lentiviral transduction. The activation of wt mMPL with romiplostim lead to balanced AKT, ERK1/2, and STAT5 phosphorylation, however, a four- to five-fold lower phosphorylation intensity at high concentration of romiplostim. This was accompanied by faster murine MPL internalization after romiplostim binding at high concentrations and also coincided with inefficient *in vitro* MK differentiation, maturation, proliferation and polyploidization compared to stimulation with murine THPO. No differences were observed after activation of the human MPL with romiplostim or human THPO. Tyrosine-(Y)-to-phenylalanine-(F) substitution in the intracellular domain of murine MPL at position Y582F caused a gain-of-function in transduced 32D cells with ligand independent ERK1/2 phosphorylation and enhanced proliferation. Furthermore, the Y582F-mMPL mutant variant was unable to rescue *in vitro* megakaryopoiesis from Mpl-deficient Lin^- BM cells. The murine Y582F-mMpl mutant recapitulates the gain-of-function of the human equivalent mutation Y591 identified from myeloproliferative neoplastic (MPN) patients. Phosphorylation of AKT and ERK and cell proliferation was profoundly reduced in 32D cells transduced with murine MPL mutant variants Y616F or Y621F, however, could partly correct Mpl-deficient megakaryopoiesis *in vitro*. Based on my data, I emphasize the predictive role of the murine model in investigation of the signaling of MPL.

Project 3:

Stress hematopoiesis models revealed that pro-inflammatory cytokines regulate HSC fate during infections. Rapid cell consumption and destruction, causing an acute demand of mature blood cells, are frequently observed during respiratory infections, among them influenza A (IAV) infections. IAV infections are associated with alternating platelet counts and excessive cytokine production. Using a non-systemic IAV infection model in mice, I observed that HSPCs in the BM faced elevated levels of pro-inflammatory cytokines and upregulated inflammation marker stem cell antigen 1 (Sca-1). Irrespective of the initial IAV dose, antiviral treatment with oseltamivir or immunization of mice with an experimental vesicular stomatitis virus (VSV) replicon vaccine, at the threshold of $1x10^5$ tissue culture infectious dose 50 ($TCID_{50}$)/g IAV in the lung, $CD41^+EPCR^-$ and $CD41^+EPCR^+$ HSCs lost their quiescence and rapidly entered the cell cycle. In contrast, $CD41^-EPCR^+$ HSCs remained in quiescence (G0-phase) without changes in counts during the acute phase of IAV infection. After viral clearance (>12 days post infection), HSC quiescence was re-established in activated HSC populations. *In vitro* single-cell lineage tracing and transplantation assays proved that $CD41^+$ HS(P)Cs were the MK and platelet source in IAV-induced emergency megakaryopoiesis. Remarkable, emergency megakaryopoiesis was present in IAV-infected Mpl-KO mice, however, mitigated in IAV-infected interleukin-1 (IL-1) receptor knockout mice, indicating that this mechanism is THPO/MPL-signaling independent. Furthermore, the observation of pro-coagulant and immature platelets in the respiratory infection model was linked to fast platelet production by emergency megakaryopoiesis. Inhibition of emergency megakaryopoiesis would be an interesting target to reduce hyper-reactive platelets, which may reduce IAV-induced lung pathology.

In summary, my work strengthens the hypothesis that MKs are produced directly by HSCs in mouse models of regeneration and during non-systemic infection. Furthermore, I provide evidence that IAV-induced emergency megakaryopoiesis is THPO/MPL-independent.

Zusammenfassung

Alle reifen Blutzellen stammen von multipotenten hämatopoetischen Stammzellen (HSZ) ab, die sich im Knochenmark (KM) befinden. Um eine lebenslange und ausgewogene Hämatopoese aufrechtzuerhalten, wird das Schicksal der HSZ durch extrinsische und intrinsische Faktoren zwischen der Selbsterneuerung, die Differenzierung und der Ruhephase streng reguliert. Die Hämatopoese ist in der Lage durch Proliferation, Expansion und Differenzierung der HSZ effizient auf akuten Bedarf, wie Blutverlust, zu reagieren. Ein wichtiger Signalweg, der die Aufrechterhaltung der HSZ in der physiologischen Hämatopoese und auch die HSZ-Expansion in der Stresshämatopoese steuert, ist der Thrombopoietin (THPO) / THPO-Rezeptor (MPL) Signalweg. Der THPO/MPL-Signalweg ist zusätzlich für die Differenzierung von Megakaryozyten (MK) aus HSZ verantwortlich und für die Thrombopoese. Obwohl die MPL-Expression auf HSZ und MK beschränkt ist und der Signalweg mechanistisch im Detail untersucht wurde, sind die nachgeschalteten Zielgene in beiden Zellpopulationen noch weitgehend unbekannt. Außerdem bleibt unklar, wie die THPO/MPL-Signalachse scheinbar gegensätzliche Entwicklungswege auslöst, insbesondere vor dem Hintergrund, dass Studien zur inflammatorischen Stresshämatopoese eine schnelle MK- und Thrombozytenproduktion aus HSZ, der sogenannte Notfall-Megakaryopoese, identifiziert haben. Dieser Mechanismus spricht für eine enge Beziehung zwischen HSZ und MKs. Ziel meiner Studie war es, (1) THPO/MPL-Zielgene zu identifizieren, die für die HSZ-Regeneration in einem Mpl-defizienten Mausmodell der aplastischen Anämie verantwortlich sind; (2) die Signalübertragung und Funktionalität des murinen MPL nach Stimulation mit dem humanen THPO-Peptidmimetikum Romiplostim zu untersuchen und um herauszufinden, ob bestimme intrazelluläre MPL-Domäne mit der Aktivierung eines spezifischen Signalwegs und den funktionellen Folgen für die Megakaryopoese verbunden sind; (3) ob und wie ein nicht systemisches Stresshämatopoese-Mausmodell der respiratorischen Infektion mit Influenza die Blutstammzellruhe und deren Entwicklungsweg beeinflusst.

Projekt 1:

Ich untersuchte, ob Thpo-Zielgene, die aus einer eigenen Genexpressionsanalyse ausgewählt wurden, in der Lage waren, den Mpl-defizienten Phänotyp zu beheben. Dazu transduzierte ich Mpl-knockout (KO) Linienmarker-negative (Lin^-) KM-Zellen mit lentiviralen, für Genkandidaten codierende Vektoren und transplantierten diese Zellen in Mpl-KO-Mäuse. Eines von fünf getesteten Genen wurde identifiziert, nämlich den endothelialen Protein-C-Rezeptor (EPCR), phänotypische HSZ in Mpl-KO-Mäusen zu expandieren, die erfolgreich sekundäre Empfänger rekonstituieren konnten. Epcr-transduzierte Mpl-KO-HSZ fanden früher ins Knochenmark zurück und stellten die HSZ Ruhephase wieder her. Außerdem wiesen diese HSZ eine höhere

Expression des anti-apoptotischen Gens BcL-XL auf. Neben der Wiederherstellung des HSZ-Pools rettete die Epcr-transduzierte Mpl-KO-Hämatopoese in transplantierten Mäusen die Anzahl der polyploiden MK im Knochenmark, ohne andere hämatopoetische Zelllinien zu verändern, konnte jedoch keine Thrombozyten produzieren. Die EPCR-Expression auf Wildtyp-HSZs identifizierte phänotypisch die HSZ-Population im Knochenmark mit überlegenem Transplantationspotential. Die EPCR-Zelloberflächen-expression auf FACsortierten und *in vitro* kultivierten hämatopoetischen Stamm- und Vorläuferzellen (HSPCs) wurde durch die Kultivierung mit THPO aufrechterhalten, während ohne THPO-Zugabe die EPCR-Expression rasch abnahm. EPCR-exprimierende HSZ stellen die Zielpopulation bei Ex-vivo-Gentherapieansätzen dar, bei denen HSZ-angereicherte Zellen mehrere Tage für die genetische Veränderung kultiviert werden. Darüber hinaus hebt meine Studie die enge Beziehung zwischen HSZ und MK hervor und unterstützt die Hypothese, dass sich die MK-Linie direkt von HSZ ableitet.

Projekt 2:

In mehreren Studien wurde das THPO-Peptidmimetikum Romiplostim in Mausmodellen verabreicht, jedoch wurde eine mechanistische Analyse der Aktivierung von murinen MPL durch Romiplostim noch nicht durchgeführt. Da Romiplostim spezifisch gegen die humane THPO-Bindungsdomäne von humanem MPL selektiert und entwickelt wurde, könnte es Unterschiede in der Signalaktivierung und Funktionalität geben. Die murine Interleukin-3-abhängige 32D-Zelllinie wurde für die lentivirale Überexpression von entweder murinem (m) oder humanem (h) MPL verwendet. Die Aktivierung von wildtyp mMPL mit Romiplostim und führte zu einer ausgeglichen AKT-, ERK1/2- und STAT5-Phosphorylierung, jedoch einer vier- bis fünffach geringeren Phosphorylierungsintensität bei hoher Romiplostimkonzentration. Dies ging mit einer schnelleren Internalisierung von murinem MPL nach der Bindung von Romiplostim in hohen Konzentrationen einher und führte auch zu einer weniger effizienten *in vitro* MK-Differenzierung, -Reifung, -Proliferation und -Polyploidisierung im Vergleich zur Stimulation mit murinem THPO. Nach Aktivierung von humanem MPL mit Romiplostim oder humanem THPO wurden keine Unterschiede festgestellt. Tyrosin-(Y)-zu-Phenylalanin-(F)-Substitution in der intrazellulären Domäne von murinem MPL an der Position Y582F führte in transduzierten 32D-Zellen zu einer Funktionszugewinn mit ligandenunabhängiger ERK1/2-Phosphorylierung und verstärkter Proliferation. Darüber hinaus war die Y582F-mMPL-Mutante nicht in der Lage, die *in vitro* Megakaryopoese von Mpl-defizienten Lin^- Knochenmarkszellen zu retten. Die murine Y582F-mMpl-Mutationsvariante rekapituliert den Funktionsgewinn der äquivalenten menschlichen Mutation Y591, die bei Patienten mit myeloproliferativen Neoplasien (MPN) festgestellt wurde. Die Phosphorylierung von AKT und ERK, sowie die Zellproliferation waren in 32D-Zellen, die mit den murinen MPL-Mutationsvarianten Y616F

oder Y621F transduziert wurden, stark reduziert, konnten jedoch die Mpl-defiziente Megakaryopoese *in vitro* teilweise korrigieren. Aufgrund meiner Daten hebe ich die prädiktive Rolle des murinen Modells bei der Untersuchung der Signalübertragung von MPL hervor.

Projekt 3:

Stresshämatopoesemodelle haben gezeigt, dass pro-inflammatorische Zytokine in der Lage sind, das Zellschicksal von HSZ während Infektionen zu regulieren. Rascher Zellverbrauch und -untergang, die einen akuten Bedarf an reifen Blutzellen verursachen, werden häufig bei Atemwegsinfektionen beobachtet, darunter auch bei Influenza-A-Infektionen (IAV). IAV-Infektionen sind mit wechselnden Thrombozytenzahlen und übermäßiger Zytokinproduktion verbunden. In nicht-systemischen IAV-Infektionsmodell bei Mäusen konnte ich erhöhte Werte an proinflammatorischen Zytokinen im Knochenmark, sowie die Hochregulierung des Entzündungsmarkers Stammzellantigen 1 (Sca-1) auf HSPC beobachten. Unabhängig von der initialen IAV-Dosis, der antiviralen Behandlung mit Oseltamivir oder der Immunisierung von Mäusen mit einem experimentellen Impfstoff auf der Vesikularstomatitisvirus (VSV) Replikonpartikelplattform geht die Ruhe von $CD41^{+}EPCR^{-}$ und $CD41^{+}EPCR^{+}$ HSZ ab einer tissue culture infectiouse dose von $1x10^{5}$ (TCID50)/g IAV in der Lunge verloren und lässt diese rasch in den Zellzyklus eintreten. Im Gegensatz dazu blieben die $CD41^{-}EPCR^{+}$ HSZ in der akuten Phase der IAV-Infektion im Ruhezustand (G0-Phase) und in ihrer Anzahl unverändert. Nach Reduktion der Viruslast (>12 Tage nach der Infektion) wurde die Ruhephase in den aktivierten HSZ-Populationen wiederhergestellt. *In vitro* Einzelzell-linienverfolgung und Transplantationen bewiesen, dass $CD41^{+}$ HSPCs die MK- und Thrombozytenquelle in der IAV-induzierten Notfall-Megakaryopoese waren. Bemerkenswert ist, dass die Notfall-Megakaryopoese in IAV-infizierten Mpl-KO-Mäusen auftrat, jedoch in IAV-infizierten Interleukin-1 (IL-1)-Rezeptor-Knockout-Mäusen abgeschwächt war, was darauf hindeutet, dass dieser Mechanismus unabhängig von THPO/MPL-Signalen ist. Darüber hinaus wurde die Beobachtung von gerinnungsfördernden und unreifen Blutplättchen im Atemwegsinfektionsmodell mit einer schnellen Blutplättchenproduktion durch Notfall-Megakaryopoese in Verbindung gebracht. Die Hemmung der Notfall-Megakaryopoese wäre ein interessantes Ziel, um hyperreaktive Blutplättchen zu reduzieren, welche die IAV-induzierte Lungenpathologie verringern könnte.

Zusammenfassend lässt sich sagen, dass meine Arbeit die Hypothese untermauert, dass MKs in Mausmodellen der Regeneration und während nicht-systemischer Entzündungen direkt von HSCs produziert werden. Außerdem liefere ich Beweise dafür, dass die IAV-induzierte Notfall-Megakaryopoese THPO/MPL-unabhängig ist.

Index

Abbreviations

°C	degree Celsius
µL	microliter
5-FU	5-fluorouracil
aa	amino acid
AEC	arterial endothelial cell
aHSC	activated HSC
AKT	protein kinase B
ALI	acute lung injury
ALL	acute lymphatic leukemia
AML	acute myeloid lymphoma
ANG-1	angiopoietin 1
ANOVA	analysis of variation
AP2	adaptor protein 2
aPC	activated protein C
ARNTL1	aryl hydrocarbon receptor nuclear translocator like 1
ATAC-seq	assay for transposase-accessible chromatin using sequencing
BcL-XL	B-cell lymphoma-extra large
BHK	baby hamster kidney
BL6	C57BL6 mice
BM	bone marrow
BMT	bone marrow transplantation
BrdU	5-bromo-2-deoxyuridine
BSA	bovine serum albumin
CALR	calreticulin
CAMT	congenital amegakaryocytic thrombocytopenia
CAR-cell	CXCL12-abundant reticular cell
Cas9	CRISPR associated protein 9
CD	cluster of differentiation
CD110	MPL / thrombopoietin receptor
CD150	signaling lymphocytic activation molecule family member 1
CD317	bone marrow stromal cell antigen 2
CD41	integrin subunit alpha 2b
CD42a	GPIX, glycoprotein 9
CD42b	GPIba, glycoprotein Ib platelet subunit alpha
CD42c	GPIbb, glycoprotein Ib platelet subunit aeta
CD42d	GPV, glycoprotein 5
CD45	protein tyrosine phosphatase receptor type C
CD49b	GPIa, integrin subunit alpha 2
CD53	tetraspanin-25
CD69	C-type lectin domain family 2, member C
CD8	T-Cell surface glycoprotein CD8 alpha chain
CD86	B-lymphocyte activation antigen B7-2
CD9	tetraspanin-29
Cdc42	cell division control protein 42
cDNA	complementary DNA
CFU	colony forming unit

ChIP-seq	chromatin immunoprecipitation DNA sequencing
c-Kit	tyrosine-protein kinase KIT / CD117
CLP	common lymphoid progenitor
CMP	common myeloid progenitor
CRISPR	clustered regularly interspaced short palindromic repeats /
CRM	cytokine receptor module
CSF	colony stimulating factor
CXCR4	CXC-motif-chemokine receptor 4
CXCL12	CXC-motif-chemokine ligand 12
DAB	3,3'-diaminobenzidin
DC	dendritic cell
dHSC	dormant HSC
DMEM	Dulbecco's Modified Eagle's medium
DNA	desoxyribonucleic acid
dpi	days post infection
E. coli	*Escherichia coli*
E. muris	*Ehrlichia muris*
EC	endothelial cell
EDTA	ethylenediaminetetraacetic acid
EdU	5-ethynyl-2'-deoxyuridine
eGFP	enhanced green fluorescent protein
eIF4F	eukaryotic translation initiation factor 4
ELISA	enzyme-linked immunosorbent assay
EPCR	endothelial protein C receptor / CD201
EPO	erythropoietin
ERY	erythrocyte
ESAM-1	endothelial cell-selective adhesion molecule 1
ETV6	ETS variant transcription Factor 6
FACsorted	fluorescence activated cell sorted
FCS	fetal calf serum
ffu	fluorescence forming unit
Fg	fibrinogen
FGF-1	fibroblast growth factor 1
FITC	fluorescein
Fli1	friend leukemia integration 1
FLT3	fms like tyrosine kinase 3 receptor / Flk2 / CD135
FLT3L	fms-related tyrosine kinase 3 ligand
Fox3a	forkhead box O3
FOG1	Friend of Gata 1
Fzd4	Wnt receptor frizzled 4
g	gram
G0 / 1	Gap 0 / 1 phase
G-CSF	granulocyte-colony stimulating factor
GM-CSF	granulocyte monocyte-colony stimulating factor
GFP	green fluorescent protein
GMP	granulocyte-monocyte progenitor
GOI	gene of interest
GRA	granulocyte
GRB2	growth factor receptor bound protein 2
GSEA	gene set enrichment analysis

Gy	gray
h	human
H2B	Histone 2 B
HA	hemagglutinin
HCT	hematopoietic stem cell transplantation
HEK293T	human embryonic kidney 293T
HEL	human erythroleukemia cell
HEPES	4-(2-hydroxyethyl)-1-piperazineethanesulfonic acid
HLA	human leukocyte antigen
Hoxa10	homeobox A10
HRP	horseradish peroxidase
HSC	hematopoietic stem cell
HSPC	hematopoietic stem and progenitor cells
i.p.	intra peritoneal
i.v.	intra venous
IAV	influenza A virus
IAV PR8	influenza A/Puerto Rico/8/34 H1N1
IFN	interferon
IFNAR	interferon alpha receptor
IFNGR	interferon gamma receptor
IGF2	insulin-like growth factor 2
IgG	immunoglobulin G
IL	interleukin
IL1R1	interleukin 1 receptor 1
IL1R1-KO	B6.129S7-Il1r1^{tm1Imx}/J
IL-6 KO	B6.129S2-Il6^{tm1Kopf}/J
ILC	innate lymphoid cell
ISG	interferon stimulated genes
IRES	internal ribosomal entry site
IT-HSC	intermediate-term hematopoietic stem cell
ITP	immune thrombocytopenia
JAK	janus kinase
KO	knockout
KLF1	kruppel like factor 1
L	liter
LCMV	lymphochoriomeningitis virus
LDB1/LMO2	LIM domain binding 1 / LIM domain only 2
Lin$^-$	lineage marker-negative
LMPP	lympho-myeloid primed progenitor
LPS	lipopolysaccharide
LSK	Lineage marker-negative, Sca-1-positive, c-Kit-positive
LSP1	lymphocyte specific protein 1
LRC	label retaining cell
LT-HSC	long-term hematopoietic stem cell
LYN	Lck/Yes-related novel protein tyrosine kinase
m	murine
M. avium	*Mycobacterium avium*
M. tuberculosis	*Mycobacterium tuberculosis*
MAC	macrophage
MAPK	mitogen-activated protein kinase

MCMV	murine cytomegalovirus
MDCK	Madin-Darby canine kidney
MDS	myelodysplastic syndrome
MEM	Eagle's minimal essential medium
MEP	megakaryocyte-erythrocyte progenitor
MERS	middle east respiratory syndrome
MHC	major histocompatibility complex
min	minutes
MK	megakaryocyte
MKP	megakaryocyte progenitor
mL	milliliter
MOI	multiplicity of infection
MON	monocyte
MPL	myeloproliferative leukemia virus oncogene / thrombopoietin receptor
Mpl-KO	B6.129S1-Mpl^{tm1Wsa}/Mpl^{tm1Wsa}
MPN	myeloproliferative neoplasm
MPP	multipotent progenitor
MSC	mesenchymal stem and progenitor cell
mTmG	B6.129-*Gt(ROSA)26Sor*$^{tm4(ACTB\ tdTomato,-EGFP)Luo}$/J
Mycn	neuroblastoma-derived homolog Myc
MyD88	myeloid differentiation primary response protein 88
MYL4	myosin light chain 4
NA	neuraminidase
NFκB	nuclear factor kappa-light chain enhancer of activated B cells
NF-E2	nuclear factor, erythroid 2
NK	natural killer cell
NP	influenza nucleoprotein
P. aeruginosa	*Pseudomonas aeruginosa*
P. berghei	*Plasmodium berghei*
PAMP	pathogen-associated molecular pattern
PAR-1	protease activated receptor - 1 / thrombin receptor
PBS	phosphate-buffered saline
Pbx1	pre–B-cell leukemia homeobox 1
PC	protein C
PCR	polymerase chain reaction
PE	phycoerythrin
PEG	polyethylene glycol
PF4P	platelet factor 4 promotor
PFA	paraformaldehyde
PGK	phosphoglycerate kinase
PI	propidium iodide
PI3K	phosphatidylinositol-3-kinase
polyI:C	polyinosinic:polycytidylic acid
PPR	pattern-recognition receptors
PU.1/Spi1	spleen focus forming virus (SFFV) proviral integration oncogene
PTEN	phosphatase and tensin homolog
qPCR	quantitative polymerase chain reaction
Rac1	Ras-related C3 botulinum toxin substrate 1 GTPase
RCA	Ricinus communis agglutinin
rh	recombinant human

RhoA	Ras homolog family member A
RIPA	radioimmunoprecipitation
RNA-seq	RNA-sequencing
RPMI	Roswell Park Memorial Institute
RSD	RANTES sorting domain
RSP6	ribosomal protein 6
Runx1	runt-related transcription factor 1
SARS-CoV	severe acute respiratory syndrome corona virus
Sca-1	stem cell antigen 1
SCF	stem cell factor / steel factor
SCID	severe combined immunodeficiency
SD	standard deviation
SDF1	stromal-derived growth factor
SEC	sinusoidal endothelial cells
SF	serum-free
SFFV	spleen focus-forming virus
SHC	Src homology 2 domain-containing-transforming protein C1
SIN	self-inactivating
SLAM	signaling lymphocyte activation molecule receptor
SOCS	suppressors of the cytokine signaling
SOS	Son of sevenless Homolog
SP	side-population
STAT	signal transducer and activator of transcription
ST-HSC	short-term hematopoietic stem cell
TACE	TNFα converting enzyme
Tal1	T-Cell Acute Lymphocytic Leukemia Protein 1
TBS	tris-buffered saline
$TCID_{50}$	tissue culture infectious dose 50
td	transduced
TEK	tyrosine protein kinase receptor TEK / angiopoietin 1 receptor
TF	transcription factor
TGFβ1	transforming growth factor beta 1
THPO	thrombopoietin
THPO-R	thrombopoietin receptor
Thy-1	thymocyte differentiation antigen 1
TLR	Toll-like receptor
TMD	transmembrane domain
TNF	tumor necrosis factor
TNFR	tumor necrosis factor receptor
tx	transplanted
VLA-4	very late activation protein 4 receptor, alpha 4 subunit
VSV	vesicular stomatitis virus
vWF	von Willebrand factor
wt	wild-type
wt mouse	C57BL6/J or C57BL/6N
X	any amino acid
x g	g-force
Y	tyrosine

1. Introduction

1.1. Hierarchical organization of hematopoiesis

Hematopoietic stem cells (HSC) ensure lifelong replenishment of mature and functional blood cells. The peripheral blood consists of plasma, short-lived red blood cells (erythrocytes), platelets, myeloid cells like granulocytes (GRA) and mostly long-lived dendritic cells (DC), mast cells, monocytes (MON) and macrophages (MAC) as well as lymphoid cells like B cells, T cells and innate lymphoid cells (ILC) and natural killer (NK) cells. Key functions of blood as defined organ system are transport of oxygen/carbon dioxide to cells and the lung, nutrients/waste products to liver and kidney, immune cells to the side of infection and also the formation of blood clots to prevent blood loss. Concepts and regulatory processes of hematopoiesis are based on intensive mouse studies from bone marrow (BM) and peripheral blood. Nevertheless, hierarchical organization of hematopoiesis is translatable and comparable between mice and humans. If not other indicated, this introduction focuses on murine hematopoiesis.

The HSC is the best characterized adult tissue stem cell. Hematopoiesis was early described in the tree-like hierarchy model, the so-called '**hematopoietic tree**'. This model was developed to explain how a small number of multipotent stem cells give rise to progenies by an unidirectional process through an ordered series of branching points with discrete progenitor states, a model also suited to explain stem cells of other tissues. In this classical model of hematopoiesis, the long-term (LT)-HSCs are at the top of the hematopoietic hierarchy as a homogeneous population residing in the BM (Figure 1A). HSCs are essentially characterized by multipotency and self-renewal (Weissman and Shizuru, 2008; Haas et al., 2018; Laurenti and Göttgens, 2018). Their key feature is the ability to generate the complete spectrum of blood cell lineages while retaining the capacity to generate multipotent progenies in a process called self-renewal. The first *in vivo* evidence of blood stem cell function was based on the short-term rescue of lethally irradiated mice and rats by BM transplantation / exchange in the 1950s (Brecher and Cronkite, 1951; Jacobson et al., 1951), followed by the observation of macroscopic hematopoietic colonies in the spleen (colony forming unit-spleen = CFU-S) in recipient mice (Till and McCulloch, 1961). For the first time the CFU-S assays allowed an estimation of HSC frequency in the BM and their differentiation potential to myeloid blood cell lineages. However, the CFU-S assays allowed only short-term observation (1 to 3 weeks). Therefore, the most stringent proof of HSC functionality are the long-term repopulating assays (Rosendaal et al., 1979; Lemischka et al., 1986). This assay tests the HSCs ability to serially rescue lethal irradiated recipients mice by stable generation of all blood lineages for more than 16 weeks (Purton and Scadden, 2007).

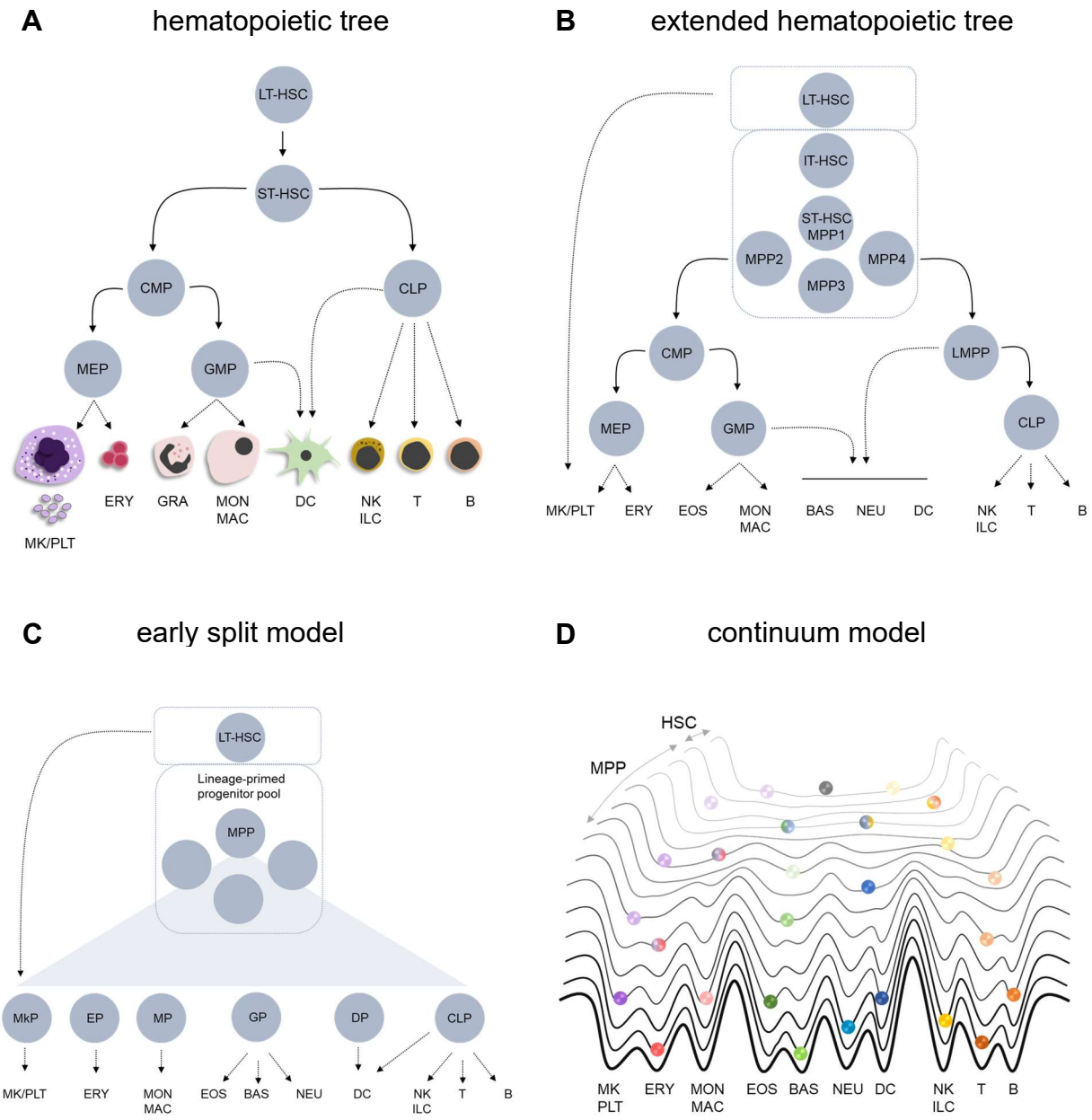

Figure 1 | Hierarchical models of murine and human hematopoiesis. (A) Classical '**hematopoietic tree**' hierarchy with long-term (LT) HSC as a homogeneous population at the top of the hierarchy, with branching points and discrete progenitor populations the common myeloid progenitors (CMP), myeloid-erythroid progenitors (MEP), granulocyte-monocyte progenitors (GMP) and common lymphoid progenitors (CLP). Mature blood lineages are at the bottom of the hematopoietic tree: megakaryocytes (MK), platelets (PLT), erythrocytes (ERY), monocytes (MON), macrophages (MAC), eosinophils (EOS), basophils (BAS), neutrophils (NEU), dendritic cells (DC), natural killer cells (NK), innate lymphoid cells (ILC), T cells (T) and B cells (B). **(B)** '**Extended hematopoietic tree**' taking into account the heterogeneity of the HSC pool with intermediate-term (IT), short-term (ST) HSC and the multipotent progenitor (MPP) 1 to 4. Lymphoid myeloid primed progenitors (LMPP). Short-cut / bypass pathway (indicated as a dashed line) from LT-HSC directly to megakaryocyte progenitors (MKPs). **(C)** '**Early split model**'. Lineage commitment and separation is present already in the MPP pool with bi- to unipotent progenitors for each mature lineage. **(D)** Hematopoietic '**continuum model**' or 'Waddington's landscape' based on single-cell RNA-sequencing data of whole BM. HSC differentiation occurs gradually with lineage-committed transcriptomic states. In this model, HSC or MPPs are not a discrete cell population; they rather represent transitory states in the continuum. Adopted from Haas et al., 2018; Laurenti and Göttgens, 2018.

These characteristics set LT-HSCs apart from their earliest progenitors: intermediate-term HSC (IT-HSCs; Benveniste et al., 2010; Yamamoto et al., 2013), short-term HSC (ST-HSC; Christensen and Weissman, 2001) and multipotent progenitors (MPP; Figure 1B; Morrison et al., 1997a; Wilson et al., 2008). The different cell populations are defined through immuno-phenotypic identification based on cell surface marker expression and functional characterization after transplantation into lethally irradiated recipients. IT-HSC lack the ability to serial repopulate (loss of self-renewal) but give rise to multi-lineage engraftment in the primary recipient. ST-HSC lack serial engraftment potential and only transiently give rise to multi-lineage in the primary recipient. MPPs were first divided into long-term and transiently reconstituting cells in 1997 (Morrison et al., 1997a). Currently MPPs are sub-defined into MPP1 to MPP6 (Wilson et al., 2008; Sommerkamp et al., 2021), whereby MPP1 comprise formerly defined ST-HSC.

In the classical hematopoietic tree, ST-HSCs or MPPs differentiate into oligopotent progenitors, namely common myeloid progenitors (CMP; Akashi et al., 2000) and common lymphoid progenitors (CLP; Kondo et al., 1997) marking the branching into the myeloid lineage and the lymphoid lineage, respectively. Furthermore, CMPs differentiate into bipotent megakaryocyte-erythrocyte progenitors (MEP) restricted to generate megakaryocyte and erythrocyte lineages, and the granulocyte-monocyte progenitors (GMP) restricted to generate granulocyte and macrophage lineages (Akashi et al., 2000). CLPs give rise to progenitor B cells, T cells, NK cells and DC. All progenitor cells explained are ultimately unipotent and generate the individual mature and functional blood cells. In this tree-like model, each cell is required to pass all discrete stages along its developmental path. In murine and human hematopoiesis, the myeloid and lymphoid branching has been estimated to be the final decision point. However, several studies highlighted, that separation of megakaryocyte-erythroid lineage before reaching the myeloid and lymphoid branch, resulting in the identification of lympho-myeloid primed progenitors (LMPP; Adolfsson et al., 2005; Doulatov et al., 2010;). This gave rise to the '**extended hematopoietic tree**' (Figure 1B).

Single-cell RNA-sequencing (RNA-seq) and single-cell *in vitro* and *in vivo* lineage tracing experiments revealed oligopotent CMPs as a mixture of lineage-restricted progenitors with uni-lineage transcriptional profiles. This indicated an earlier lineage separation than anticipated previously, namely in phenotypic HSCs and/or MPPs (Paul et al., 2015; Perié et al., 2015; Notta et al., 2016; Velten et al., 2017). The murine and human hematopoietic tree model has been further challenged by single-cell transplantation and limiting-dilution assays (Müller-Sieburg et al., 2002; Müller-Sieburg et al., 2004; Dykstra et al., 2007; Yamamoto et al., 2013), where it was shown that only a small fraction of highly purified phenotypic HSCs have the potential to generate a balanced multi-lineage output, while in the majority of cases

reconstitution was myeloid- or lymphoid-biased. It has been shown that the lineage bias of one HSC in the primary transplant is also maintained after transplantation into a secondary recipient, indicating that lineage bias is a cell intrinsic feature driven by epigenetic changes (Challen et al., 2010; Benz et al., 2012; Yu et al., 2017). This phenomenon is named as HSC heterogeneity. HSCs with lineage-biased output after transplantation were also identified during steady-state hematopoiesis using *in situ* barcoding or fluorescent tagging methods. These experiments confirmed that, lineage bias is not only an aspect of emergency hematopoiesis but also established under physiological conditions (Yu et al., 2017; Rodriguez-Fraticelli et al., 2018). Single-cell RNA-seq of murine and human HSCs demonstrate a significant correlation between the presence of gene expression patterns and the functional lineage-biased HSCs, which was shown using *in vitro* lineage tracing or transplantation experiments (Grover et al., 2016; Velten et al., 2017). This bolsters the existence of transcriptional lineage priming in phenotypic HSCs, which resulted into the '**early split model**' (Figure 1C). Single-cell transplantation experiments of HSCs have suggested that HSCs have the potential to bypass oligopotent progenitor states and directly undergo uni-lineage restriction (Figure 1B and C). These so-called megakaryocyte- (MK) / platelet-biased HSCs (Sanjuan-Pla et al., 2013; Yamamoto et al., 2013; Haas et al., 2015; Yamamoto et al., 2018) seems to have a high self-renewal capacity but with megakaryocyte-restricted potential. These MK- / platelet-biased HSCs can be identified by expression of high levels of von Willebrand factor (vWF), c-Kit or the integrin subunit CD41 (Gekas and Graf, 2013; Sanjuan-Pla et al., 2013; Grinenko et al., 2014; Shin et al., 2014). *In situ* transposon tagging experiments combined with single-cell RNA-seq analyses in unperturbed steady-state hematopoiesis demonstrated that traditionally defined LT-HSCs are the direct source of MK-restricted progenitors bypassing the classical hematopoietic tree (Rodriguez-Fraticelli et al., 2018).

The classic hematopoietic tree is based on the identification of cell types by cell surface marker detection via flow cytometry. However, single-cell gene expression data from mice, humans and zebrafishes enabled the reconstruction of the hematopoietic differentiation hierarchy (trajectories) *in silico* (Nestorowa et al., 2016; Velten et al., 2017; Tusi et al., 2018). These *in silico* models describe hematopoiesis in a continuous Waddington's landscape (Waddington, 1957), also named as '**continuum model**' (Figure 1D). In this landscape, HSCs still resides at the top, however, multiple pathways in which HSCs are able to follow in hills / valleys separating lineage potential are described. The hills (lineage restriction) in the HSC compartment are initially low and can be passed, but progressively rises in height, indicating the continuous loss of multipotency. This continuum model takes into account that HSC and progenitor cells can acquire, change or lose their fate decision along the continuum until a specific point.

1.2. Identification and characterization of hematopoietic stem cells

Based on the expression levels of immunophenotypic cell surface markers HSCs can be identified using flow cytometry. First identified by negative selection of lineage markers, for B cells (B220), T cells (CD4 and CD8), myeloid cells (Mac-1/CD11b), granulocytes (Gr-1) and erythroid cells (Ter119) murine HSC were named as lineage marker-negative BM cells (Lin^-; Müller-Sieburg et al., 1986; 1988). Other characteristics described are low expression of thymocyte differentiation antigen 1 (Thy-1/CD90), the positive selection for stem cell antigen 1 (Sca-1; Spangrude et al., 1988) and c-Kit (CD117; Ikuta and Weissman, 1992). The '$L^-S^+K^+$' or '$K^+L^-S^+$' population is enriched for HSCs and makes ~0.1% of the whole BM of young mice. Additional markers, as negative selection of the vascular sialomucin CD34 (Osawa et al., 1996), fms like tyrosine kinase 3 receptor (Flt-3/Flk2/CD135; Adolfsson et al., 2001) and including the signaling lymphocyte activation molecule receptors (SLAM) CD48 and CD150 (Kiel et al., 2005) enriched HSCs up to 0.001 to 0.005% of the whole BM. This leads to the widely used and accepted definition of murine LT-HSC as $Lin^-Sca\text{-}1^+c\text{-}Kit^+CD135^-CD48^-CD150^+CD34^-$ (Wilson et al., 2008). Thrombopoietin receptor / c-Mpl (MPL or CD110) as a marker for HSC was identified by the generation of c-Mpl deficient mice (Mpl-KO, Alexander et al., 1996; Yoshihara et al., 2007). In Mpl-KO mice a drastically reduced frequency (90% less compared to wild-type) and count of HSCs was shown, demonstrating a critical role of Mpl in HSC maintenance. DNA-microarray analyses of purified HSCs further suggests a positive selection for endothelial protein C receptor (EPCR/CD201; Balazs et al., 2006; Kent et al., 2009) and endothelial cell-selective adhesion molecule 1 (ESAM-1; Forsberg et al., 2005; Yokota et al., 2009). $EPCR^+$ and $ESAM\text{-}1^+$ HSC have been proved to have a superior long-term engraftment potential. Also based on DNA-microarray profiling, unique genes expressed in HSCs (e.g. *Fgd5* or *Ctnnal1*) were selected to generate fluorescently labeled reporter mice to study HSCs in their BM niche or to isolate isolating them in order to avoid immunostaining, as staining may alter HSC function upon antibody binding (Gazit et al., 2014; Acar et al., 2015). Interestingly, human HSCs are identified by the expression of CD34, while CD34 is absent on murine HSCs (Berenson et al., 1988). Enrichment of human HSCs with CD34 is similar to the murine lineage marker-negative definition with respect to purity and frequency in the BM. In general, only a small subset of cell surface markers are shared between murine and human HSCs, e.g. MPL and EPCR (Ninos et al., 2006; Anjos-Afonso et al., 2022).

HSCs are quiescent, with the majority (>80%) residing in the cell cycle phase G0. The G0-phase state of HSCs can be identified by the low amount of DNA and RNA (Cheshier et al., 1999) or the absence of the nuclear proliferation marker Ki-67 (Wilson et al., 2004; Passegué et al., 2005). The quiescence protects HSCs from gaining and accumulating genetic damage to keep a low mutational burden. To study HSC cycling kinetics over life-time, HSCs can be

chemically labeled (pulse period) with 5-bromo-2-deoxyuridine (BrdU, Bradford et al., 1997; Zhang et al., 2003) or genetically labeled e.g. a transgenic mouse model expressing the fusion protein histone H2B-GFP under the tetracycline-responsive regulatory element and the tTA-S2 transactivator from the endogenous *Scl* locus (Scl-tTA;H2BGFP; Wilson et al., 2008; Foudi et al., 2009). In the chase period, the label is diluted in half with every cell division. A small population of HSCs is capable to retain the GFP label 12 to 20 months, reflecting the persistence of quiescent HSCs upon old age in mice (Bernitz et al., 2016). These HSCs are named label-retaining HSCs (LRC or LR-HSCs) and subdivide phenotypic HSCs in dormant label-retaining (dHSCs) and active non-label retaining HSCs (aHSCs) (Zhang et al., 2003; Wilson et al., 2008). In contrast, only dormant LRCs harbor multi-lineage engraftment potential in serial transplantations and are the most potent LT-HSC. LT-HSCs identified by cell surface markers and the absence of Ki-67 revealed to be a mixture of dormant (30%) and active (70%) HSCs and refelcting HSC heterogeneity (Wilson et al., 2008). Further, dHSC have a low metabolic and biosynthetic profile depending on oxygen-independent glycolysis (Simsek et al., 2010; Takubo et al., 2013), low mitochondrial activity (Ito et al., 2016; Vannini et al., 2016), tightly controlled and low protein synthesis (Signer et al., 2014) and autophagy as degradation mechanism (Ho et al., 2017). In contrast, aHSCs or progenitors (MPPs) are more proliferative and switch to oxidative metabolism with high mitochondrial activity and actively use the proteasome degradation system (Signer et al., 2014; Hidalgo San Jose et al., 2020).

1.3. Regulation of hematopoietic stem cell fate

In adult murine steady-state hematopoiesis, HSCs are primarily located in the trabecular region of the BM with a very small percentage residing in the spleen (Inra et al., 2015), lung (Lefrançais et al., 2017) and also peripheral blood (Méndez-Ferrer et al., 2008) of mice. HSCs are preferentially located in specialized microenvironments, the so-called BM niche (Schofield, 1978; Calvi et al., 2003). Niche cells and distant organs (e.g. liver) provide extrinsic soluble signaling molecules to regulate HSC function like quiescence, self-renewal or differentiation (Morrison and Scadden, 2014; Fröbel et al., 2021). In the murine BM niche, non-hematopoietic cells – as endothelial cells (EC; arterial [AEC], arteriolar and sinusoidal cells [SEC]), mesenchymal stem and progenitor cells (adipogenic and osteogenic MSCs), CXCL12-abundant reticular cells (CAR-cells), osteoblasts, chondrocytes, fibroblasts and very small percentage of neuronal and smooth muscle cells – together with hematopoietic cells – monocytes, macrophages and megakaryocytes - are involved in HSC regulation and their maintenance. Histologically it was shown that HSCs are located close to bone lining osteoblasts in the BM (endosteal niche; Lord et al., 1975; Nilsson et al., 2001) or to sinusoidal endothelial cells (perivascular niche, Méndez-Ferrer et al., 2010; Ding et al., 2012), underlining also that direct cell-to-cell contact is an important regulator of HSCs.

1.3.1. Extrinsic factors – hematopoietic cytokines

Hematopoietic cytokines and factors can be produced permanently or upon induction. There are numerous receptor - ligand interactions (signaling transductions) described based on experiments to expand HSCs *in vitro,* followed by non-conditional, conditional, and inducible knockout mouse models, some of which are lined out here. Signal transduction is able to induce changes of gene expression to regulate HSC function. KIT ligand (stem cell factor [SCF]) and c-Kit receptor regulates HSC and progenitor populations (Zsebo et al., 1990; Ikuta et al., 1991), dependent on the source of SCF. Depletion of SCF produced by MSCs caused the depletion of myeloid-lymphoid lineages while SCF depletion in embryonic cells resulted in depletion of HSC numbers caused by impaired HSC quiescence (Comazzetto et al., 2019). This highlights that the two described niches may play different roles in HSC regulation. Furthermore, SCF or c-Kit knockout mice are not viable due to severe anemia (Russell, 1979). Transforming growth factor beta 1 (TGFβ1) produced by hematopoietic cells and non-hematopoietic niche cells regulates the expression levels of c-Kit on the cell surface of HSCs and subsequently the responsiveness to SCF (Dubois et al., 1994; Sitnicka et al., 1996b). The chemokine CXCL12 (stromal-derived growth factor [SDF1]) and its receptor CXCR4 are key factors for HSC retention in the BM niche and as chemoattractant for murine HSC homing to the BM during transplantation (Sugiyama et al., 2006; Tzeng et al., 2011). CXCL12 is mainly expressed by non-hematopoietic niche cells as AEC, osteoblasts and MSC (Ding and Morrison, 2013; Asada et al., 2017). Antagonizing the CXCR4 receptor (e.g. plerixafor) leads to mobilization of HSCs into the peripheral blood stream. This strategy, currently represents an important method to harvest HSCs for bone marrow transplantations for clinical application in human patients (Broxmeyer et al., 2005). The receptor tyrosine kinase TEK/TIE-2 is solely expressed on quiescent HSCs compared to all other hematopoietic cells (Arai et al., 2004). It's ligand, angiopoietin-1 (ANG-1) is produced by osteoblasts, MSCs and MKs, and enhances HSC quiescence and adhesion in the BM niche (Arai et al., 2004; Zhou et al., 2015). To note, several angiopoietin-like proteins support the *in vitro* expansion of murine and human HSCs (Zhang et al., 2006), however, the receptor is still unknown.

1.3.2. Intrinsic factors – transcription and epeigentics

In response to extracellular signals, the alteration of 'intrinsic' epigenetic and transcriptional factors influence the gene expression pattern of HSCs and therefore HSC fate. Several transcription factors (TF) can be induced by receptor signaling via e.g. Mitogen-activated protein (MAP) kinase, JAK-STAT, SMAD, and other signaling molecules (Lin and Leonard, 2019; Edginton-White and Bonifer, 2022). The combination of bindings and interactions of TFs results in cell-type specific expression patterns. One example of a TF network for regulating HSC gene expression for balancing self-renewal and differentiation is the binding of GATA2,

TAL1, RUNX1, and FLI1 and the bridging factors LDB1/LMO2 (Tijssen et al., 2011; Beck et al., 2013). Additionally, chromatin accessibility via epigenetic changes regulates the activity of genes, which can be transmitted and memorized in HSCs and their progenies (epigenetic memory). In hematopoietic progenitors a gradual decrease of transcriptional accessibility of multi-lineage-associated genes was observed (Cabezas-Wallscheid et al., 2014).

1.4. Thrombopoietin and MPL

The hematopoietic cytokine thrombopoietin (THPO) and its respective receptor myeloproliferative leukemia virus oncogene (MPL or CD110) are a primary regulator of HSC fate and megakaryopoiesis (Gurney et al., 1994; Sauvage et al., 1996; Yoshihara et al., 2007). THPO is one of the extrinsic factors not produced in the BM niche. Although initially RNA transcripts of THPO were identified in BM niche and non-and hematopoietic cells (Sungaran et al., 1997; Yoshihara et al., 2007), it was shown that only THPO produced in parenchymal hepatocytes is essential for regulating HSC number, function and megakaryopoiesis (Qian et al., 1998; Decker et al., 2018). THPO levels in the peripheral blood are regulated at different levels (1) at the transcriptional level through alternative *Thpo* splice variants with different translation efficiencies (Ghilardi et al., 1998), (2) by the platelet count, which buffers the level of THPO via binding to MPL followed by receptor-ligand mediated internalization (endocytosis) and degradation (‘platelet sponging theory’; Kuter and Rosenberg, 1995; Fielder et al., 1996), and (3) by hepatic clearance of aged and desialylated platelets through the Ashwell-Morell receptor (Grozovsky et al., 2015). These feedback loop mechanisms are based on the glycan composition on the cell surface of platelets which acts as one of the degradation mechanism. Aged and desialylated platelets are identified by the Ashwell-Morell receptor and drives mRNA expression of the Thpo in hepatocytes via Janus (tyrosine) kinase JAK2 and the acute phase response signal transducer and activator of transcription STAT3. With the availability of recombinant THPO, it became possible to expand murine and human HSCs *in vitro* by supplementation of THPO in combination with other hematopoietic cytokines like SCF and IL-3 (Ku et al., 1996; Sitnicka et al., 1996a). Regulation of adult HSCs by THPO was further bolstered by the generation of mice lacking Thpo, which have 150-fold reduced HSC numbers (Sauvage et al., 1996; Qian et al., 2007). Comparing the murine (356 amino acids [aa]) and human (353 aa) THPO protein, an identity of 81.6% could be shown. Both proteins have a signal peptide followed by a N-terminal MPL-binding domain and an C-terminal glycan domain (Figure 2A). The N-terminal binding domain to MPL shows a 4-helix bundle connected by cysteine bridges, similar to EPO or growth hormone with to non-identical binding sites for the respective receptors. The C-terminal glycan domain is highly glycosylated and seems to be essential for correct transportation through the secretory system (Linden and Kaushansky, 2000; 2002).

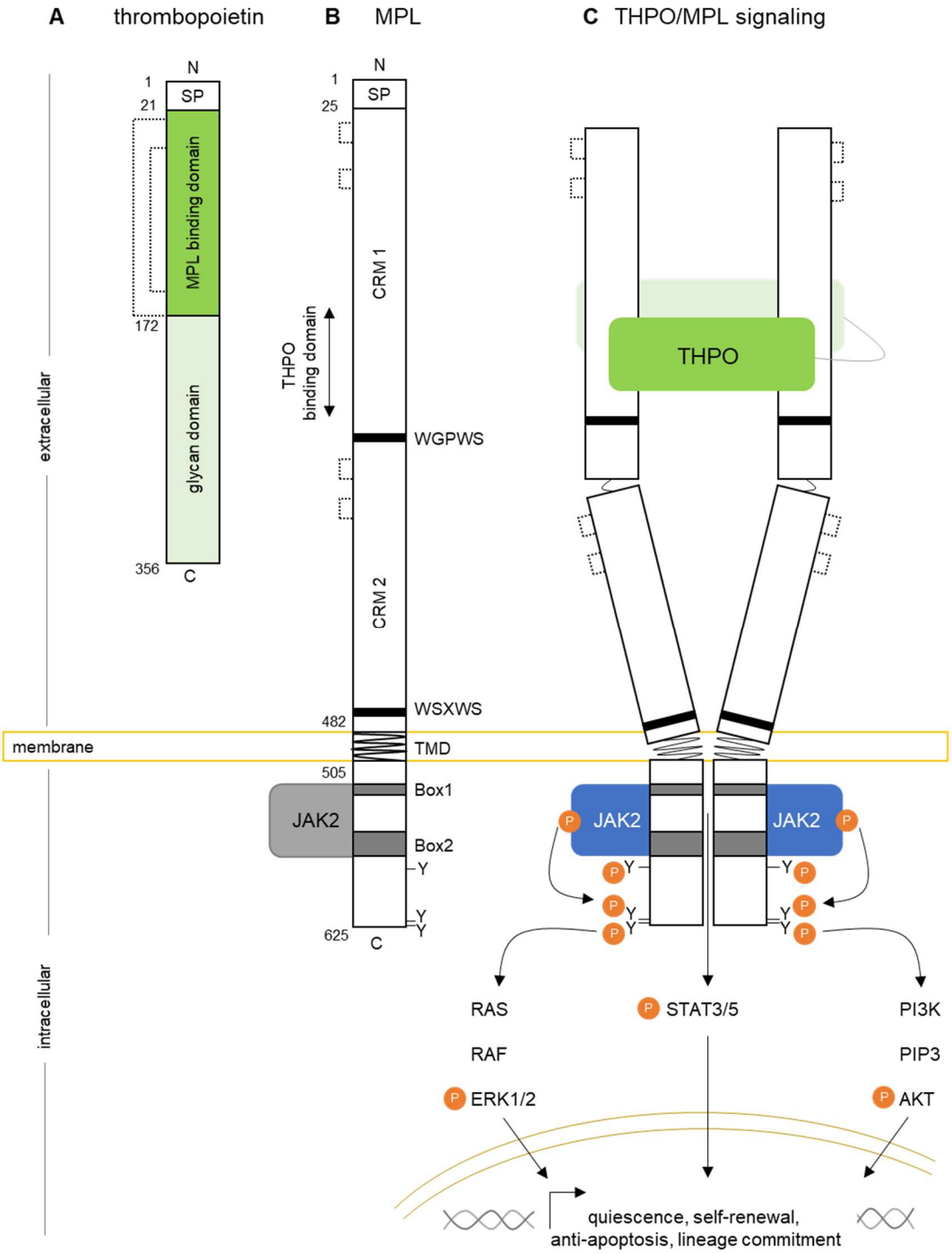

Figure 2 | Schematic representation of murine THPO protein, murine MPL protein and THPO/MPL signaling transduction cascade. **(A)** Thrombopoietin (356 aa) protein with the signal peptide (SP) and MPL-binding domain with disulfide bridges (dotted lines) forming the secondary and tertiary protein structure. **(B)** Mpl monomer protein extracellular domain with SP, cytokine receptor module (CRM) 1 and 2. CRM1 harbors the predicted THPO binding domain. Cytokine class I receptor related structures: four disulfide bridges (dotted lines) and the conserved pentapeptide motif (WSXWS). Single-pass transmembrane domain (TMD). Intracellular conserved Box1 and Box2 motif which facilitates JAK2 binding and C-terminal tyrosine (Y) residues important for imitating signaling transduction. Disulfide bridges are indicted as dotted lines **(C)** THPO-induced MPL activation, with TMD geometry change and induction of JAK2 dependent signaling cascade via the STAT, RAS/MAPK/ERK and PI3K/AKT pathway.

Before identifying THPO as the ligand for MPL (Kaushansky et al., 1994; Wendling et al., 1994) it was known, that mice infected with the murine retrovirus myeloproliferative leukemia virus develop a myeloproliferative disease (granulocytosis, thrombocytosis, erythroblastosis and splenomegaly) two to three weeks after infection (Wendling et al., 1986). The cellular homolog of the myeloproliferative leukemia virus encoded oncogene (c-Mpl) was cloned from an erythroid/megakaryocytic cell line (human erythroleukemia cell [HEL]; Long et al., 1990; Vigon et al., 1992). MPL expression in mice and humans is restricted to hematopoietic cells notably HSCs, MKs and platelets. Defective or reduced expression of MPL (loss-of-function) in humans causes a rare disease named congenital amegakaryocytic thrombocytopenia (CAMT) (Ihara et al., 1999; Ballmaier et al., 2001). Mpl knockout mice reassemble the human disease phenotype, with 5 to 10% the number of platelets, MKs and HSCs compared to wild-type mice (Gurney et al., 1994; Alexander et al., 1996). This phenotype can be reversed by transplantation of HSCs lentivirally transduced with Mpl driven by a lineage specific promotor, restoring functional HSCs, MKs and platelet production (Heckl et al., 2011). Loss-of-function is also associated with point mutations that impair transcription (hMPL P136H) or causing defective trafficking of the receptor to the cell surface (hMPL K39N, R102P, P106L, W154R, R257C, P635L; Plo et al., 2017). Comparison of peptide sequences with Mpl cDNAs from hematopoietic cell lines revealed a high homology to known hematopoietic growth factor receptors (e.g. receptors for EPO or growth hormone). MPL (murine 625 aa and human 635 aa, protein sequence identity 81%) is a member of the cytokine class I receptor sub-family based on the extracellular cytokine binding domain linked by a single-pass transmembrane helix domain to the intracellular domain which provides binding sites for signaling proteins (Figure 2B).

The extracellular domain is structured by two cytokine receptor modules (CRM1 and CRM2): containing two conserved cysteine residues which form disulfide bridges and the juxtamembrane pentapetide motif (WSXWS). Both are features of the cytokine class I receptor family (Spangler et al., 2015). CRM1 harbors the predicted THPO binding domain (Sabath et al., 1999; Chen et al., 2010). The intracellular MPL domain is dominated by a disordered structure with high degree of flexibility. Similar to all type I cytokine receptors, MPL itself lacks intrinsic kinase activity and initiating intracellular signaling depends on phosphorylation of the intracellular tyrosine residues by JAK2. JAK2 interacts by its FERM-SH2 domain with the Box1 and Box2 motifs of the intracellular moiety of MPL (Parganas et al., 1998; Tong et al., 2006). Box1 is characterized by two proline residues (PXXP) whereas Box2 is marked by regions with increased serine and glutamic acid occurrence. Furthermore, JAK2 facilitates MPL stability through enhanced receptor recycling to the cell surface by reduced proteasomal degradation after internalization (Royer et al., 2005).

1.4.1. Thrombopoietin / MPL activation and signaling transduction

Most of cytokine class I receptors including MPL are proposed to exist as pre-formed dimers in the plasma membrane (Syed et al., 1998; Livnah et al., 1999). THPO binding induces conformational changes in the dimer to facilitate JAK2 activation through the plasma membrane. The MPL-binding domain of THPO consists out of two binding sites one presenting a high affinity (nanomolar), which mediates the initial binding to the first MPL binding site and the second site with low affinity (micromolar), which facilitates the interaction with the second MPL binding site (Jagerschmidt et al., 1998; Park et al., 1998; Feese et al., 2004). Studies using artificially dimerized MPL fusion proteins revealed, that the geometry of the TMD helices are important for signal induction. Orientation and rotation of the TMD helices changes the intracellular domain to a more likely JAK2 auto-phosphorylation signaling and are predicted to result in differently expressed target genes in HSCs or MKs (Matthews et al., 2011; Staerk et al., 2011). Mutations in the TMD and juxtamembrane region leads to THPO-independent growth in immortalized cell models via stabilization of an active TMD geometry (Pikman et al., 2006). It was shown that human MPL mutations (gain-of-function) at the position S505 and W515 are responsible for 5 to 10% of classical myeloproliferative neoplasms (MPN). The most prevalent driver mutation in classical myeloproliferative neoplasms (MPN; >60%) is associated with JAK2 V617F mutation. JAK2 V617F and MPL S505 or W151 induce constitutive activation of STAT, AKT and MAPK pathways. Somatic mutations in the chaperone protein calreticulin (CALR) changes the CALR protein structure and its affinity to form stable complexes with MPL at the CRM1 region at the cell surface and allows THPO-independent MPL activation. CALR mutations are responsible for up to 30% of all MPNs (Vainchenker and Kralovics, 2017).

Intracellular THPO/MPL signaling is driven by phosphorylation of intracellular tyrosines by JAK2 providing docking sites for STAT1,3 and 5 (Ezumi et al., 1995), adaptors like SHC, GRB2 and SOS, and leading to the activation of RAS/MAP/ERK1/2-kinase (Rojnuckarin et al., 1999) or phosphatidylinositol-3-kinase (PI3K) / protein kinase B (AKT; Geddis et al., 2001) signaling transduction pathways (Figure 2C). Truncation of the intracellular domain and deleting Box1 and Box2 motifs, abrogates THPO/MPL signaling (Drachman et al., 1999; Kohlscheen et al., 2015). Translocation of dimerized STAT3 and 5 proteins into the nucleus activates transcriptions of mitotic genes like *c-Myc* or *cyclin D1* to promote cell survival and proliferation (Matsumura, 1999). PI3K/AKT activation is also important in the regulation of cell cycle progression (Geddis et al., 2001), e.g. by modulating transcription factors FOXO3a, which inhibits the cell cycle inhibitor p27 and glycogen synthase kinase-3beta (Kaushansky, 2005). Phosphorylated ERK1/2 acts as transcription factor in MKs regulating proliferation, maturation and polyploidization (Ritchie et al., 1999; Rojnuckarin et al., 1999). Strong MAPK signaling in MK cell lines promotes proliferation arrest and differentiation-associated senescence (Racke

et al., 1997; Besancenot et al., 2010). MPL signaling is tightly regulated by the expression levels of MPL and JAK2 in megakaryocytic cells, where at low levels proliferation is seen and at high level cell cycle arrest can be observed (Besancenot et al., 2014). The THPO/MPL signaling complex is internalized after activation to be either recycled or ubiquitinated (ubiquitin ligase CBL), which induces degradation (Saur et al., 2010). Protein phosphatases (PTEN, SHP1 or SHIP1), suppressors of the cytokine signaling (SOCS) proteins, FAK, LYN and LNK proteins, negatively regulate MPL signaling by degrading phosphorylated residues or inhibiting JAK2/MPL association (Starr and Hilton, 1999; Tong and Lodish, 2004; Hitchcock et al., 2008).

1.4.2. MPL receptor agonists

Activating the THPO/MPL axis to improve the generation of MK and platelets has shown to be a promising strategy for the treatment of patients with thrombocytopenia. Recombinant non- and PEGylated human (rh) THPO was administered in clinical trials either in healthy platelet donors (Kuter et al., 2001) and in chemotherapy- or cancer-induced thrombocytopenic patients (Vadhan-Raj et al., 1997; Archimbaud et al., 1999). Although showing high effectiveness with increasing platelet counts after a single dose injection of rhTHPO, there was no improvement or even platelet loss after further administrations. This was based on the development of antibodies against the rhTHPO and also the endogenous hTHPO (Li et al., 2001; Kuter, 2002). Peptide library screenings found a THPO agonist for human MPL without sequence homology to endogenous hTHPO. The approved THPO peptide mimetic romiplostim consists of two identical subunits, two 14 aa peptides with high MPL binding affinity linked with a 5 and 8 aa glycine spacer and fused to the C-terminus of a human immunoglobulin IgG1 Fc-fragment (peptibody; Cwirla et al., 1997). The small-molecule, non-peptide agonists eltrombopag has a juxtamembrane binding affinity to the transmembrane domain of human MPL and do not interfere with the endogenous THPO-binding site (Will et al., 2009). While romiplostim can activate murine MPL, eltrombopag cannot bind to the murine receptor, since the binding region (H499) is not conserved in mice. Both drugs demonstrated a platelet response rate above 60% and reduced bleeding events with good safety and tolerability in patients treated with immune thrombocytopenia (ITP). Since no selective MPL/THPO activation towards MK differentiation is described so far, concerns about clonal evolution and induction of HSC malignancies were raised. However, safety analysis over 10 year usage in clinical routine revealed no neoplastic changes in ITP patients (Ghanima et al., 2019). Eltrombopag and romiplostim showed beneficial results in patients with refractory aplastic anemia to enhance blood production after long term treatment (Olnes et al., 2012; Gill et al., 2017; Lee et al., 2019). Initial concerns that treatment with THPO mimetics might have the potential to induce BM myelofibrosis, observed in pre-clinical mouse models, could be confirmed only in low numbers of patients. However, fibrosis regressed after discontinuation of THPO mimetics (Kuter et al., 2009; 2013).

1.5. Megakaryocytes and platelets

1.5.1. Biogenesis

Platelets represent the majority of mature hematopoietic cells and are generated from megakaryocytes (MK) located in the BM. MK differentiation and maturation is regulated by THPO/MPL signaling. MKs are the largest cells in the BM in mice (up to 50 µm diameter size; Junt et al., 2007) and humans (50 to 100 µm diameter size; Tomer et al., 1987), and account for only 0.05 to 0.1% of cells found in the BM. MK maturation from megakaryocyte progenitors (MKP) is characterized by distinct morphological changes: (1) increase of cell size, (2) replication of DNA without undergoing cytokinesis (endomitosis) to develop multi-lobed polyploid nuclei (2n up to 64n/128n; Deutsch and Tomer, 2006) and (3) cytoplasmic remodeling for efficient platelet production. The cytoplasmic remodeling includes the development of an internal demarcation membrane system, serving as additional membranes necessary for platelet production and storage (Eckly et al., 2014). Further, maturation leads to an increase of the production of granular structures, including dense and alpha granules, which store coagulation factors, cytokines, and adhesion molecules needed for platelet functionality in hemostasis and thrombosis (Koseoglu and Flaumenhaft, 2013). MKPs relocate during the maturation process from the endosteal niche to the vascular niche and are there located in close proximity to vessel sinusoids (Behrens and Alexander, 2018). Microtubal re-arrangements by actin filaments form cellular protrusion at the edges of MKs, where cell organelles and granules are actively transported to (Patel et al., 2005; Richardson et al., 2005). These protrusions are extended through the gaps in the endothelial layer into the vessel lumen. Through shear forces of the blood stream proplatelets are formed, which fragment into platelets in the blood circulation (Italiano et al., 2007; Brown et al., 2018). In the resting phase (non-activated), platelets in the peripheral blood are discoid shaped with a size of 0.5 to 1 µm in mice and 1 to 2 µm humans. In the peripheral blood, murine platelets circulate for 5 days, while human platelets survive up to 10 days (Harker et al., 2000; Fox et al., 2007). Recently, the lung and kidney were discovered and discussed to be a reservoir for platelet producing megakaryocytes (Lefrançais et al., 2017; Pariser et al., 2021; Valet et al., 2022).

In the canonical/classical megakaryopoiesis, MKs differentiate from HSCs through the lineage pathway ST-HSCs, MPPs, CMPs, MEPs to definitive colony forming unit (CFU) MKPs. All cells committed to the megakaryocytic lineage can be identified by the expression of the surface markers MPL and integrin alpha-IIb subunit CD41 at any developmental stage. The progenitor state in mice is usually defined by the additional presence of CD150 and CD9 (Ng et al., 2012). The glycoproteins of the multi-protein CD42 (GPIb-IX-V) complex - GPV (CD42d), GPIX (CD42a), GPIba (CD42b) and GPIbb (CD42c) – and the integrin alpha 2 (CD49) are used to define maturation stages of MKs which they share with platelets (Figure 3).

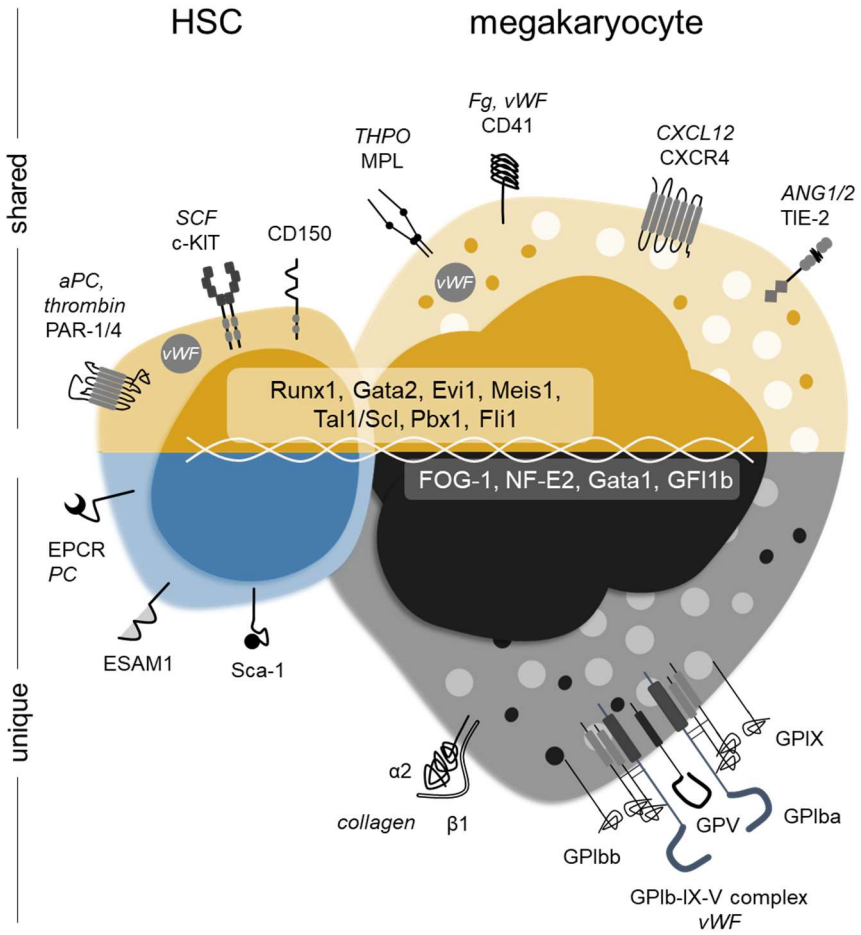

Figure 3 | Murine HSCs and megakaryocyte shared and unique molecules. Shared and unique surface proteins, transcription factors and cytoplasmic proteins of HSCs and MKs. The ligand of each receptor is written in *italic*. Ligand proteins: *SCF* = stem cell factor, *THPO* = thrombopoietin, *Fg* = fibrinogen, *vWF* = von Willebrand factor, CXCL12 = C-X-C motif chemokine 12, ANG1/2 = angiopoietin 1 and 2 and *aPC* = activated protein C. Receptor protein: integrin α2 = CD49b, integrin β1 = CD29, PAR-1 = protease activated receptor 1 (thrombin receptor), CD41 = integrin subunit alpha 2b, CXCR4 = C-X-C motif chemokine receptor 4, GPIb-IX-V complex = von Willebrandt factor receptor. Transcription factors: Runx1 = Runt-Related Transcription Factor 1, Evi1 = ecotropic virus integration site 1 protein homolog, Meis1 = myeloid ecotropic viral integration site 1 homolog, Tal1/Scl = T-cell acute lymphocytic leukemia protein 1, Pbx1 = pre-B-cell leukemia transcription factor 1, Fli1 = friend leukemia integration 1, FOG-1 = friend of GATA-1, NF-E2 = nuclear factor, erythroid 2 and GFI1b = growth factor independent 1B transcriptional repressor.

By the recognition of HSC heterogeneity it was found that HSCs expressing CD41, MPL, vWF or GATA1 (Månsson et al., 2007; Gekas and Graf, 2013; Sanjuan-Pla et al., 2013; Yamamoto et al., 2013) and the MPP2 population (Cabezas-Wallscheid et al., 2014; Pietras et al., 2015) are biased or even committed to the myeloid and megakaryocyte/platelet lineage. Recently, it was proven that megakaryocyte-biased HSCs and MPP2 exist during steady-state hematopoiesis and are the direct sources for MKs by tracking inducible random transposon integration sites (Rodriguez-Fraticelli et al., 2018; Weinreb et al., 2020). This study also bolsters the theory that MEP are mainly erythroid committed since no MK shared an integration with erythroblasts.

1.5.2. Regulation – cytokines and transcription factors

The fact that megakaryopoiesis is dependent on THPO/MPL signaling is also reflected by the respective knockout mice with very small (yet sufficient) numbers of platelets (Mpl-KO ~200x10^3/µL, Thpo-KO ~100x10^3/µL and wt BL6 ~1200x10^3/µL; mean platelet number of mice at an age of 12 weeks, own data). A similar reduction in platelet numbers could be found in CAMT patients (CAMT: <21x10^3/µL; van den Oudenrijn et al., 2000; healthy: 150-450x10^3/µL). Because platelets are still generated, although at low numbers, a THPO-independent megakaryocyte and platelet production must exists in mice and humans. Important to note, platelet producing MKs are not the most polyploid and mature MKs and platelet release is not fully dependent on THPO/MPL signaling (Ng et al., 2014). In fact, the injection of interleukin (IL)-1β or IL-6 increased platelet production *in vivo* (Kimura et al., 1990; Kaser et al., 2001), however, it was proven later that these interleukins indirectly stimulate THPO production. Although IL-6, IL-11 and leukemia inhibitory factor (Ishibashi et al., 1989; Burstein et al., 1992) have shown to promote cell size and polyploidy of MKs *in vitro*, crossing Mpl-KO mice with the respective cytokine receptor-deficient mice revealed that they were dispensable for steady-state megakaryopoiesis (Gainsford et al., 2000). Only for IL-1α, a THPO-independent platelet production by MK rupture *in vivo* instead of proplatelet formation was described (Nishimura et al., 2015). The insulin-like growth factor 1 enhances the maturation of MKs and proplatelet formation *in vitro* via AKT and ERK1/2 signaling and promotes platelet production in Mpl-KO mice after application (Chen et al., 2018).

HSC lineage commitment to MKs is further coordinated by the temporal and specific action of various TFs (Figure 3). Namely Runx1, GATA2, Evi1, Fli1, SCL/TAL1, Meis1, Pbx1 and Ets family TFs (Huang and Cantor, 2009). Knockout of one of these factors in mice results in embryonic lethality due to the failure of definitive hematopoiesis, conditional knockouts or haplo-insufficiency leads to the reduction or loss of HSCs and/or in defective maturation of MKs by low polyploidy, undeveloped demarcation membrane system and granule formation. Balanced expression of GATA1 and PU.1/Spi1 promotes one of the first steps of HSC commitment to the myeloid lineage (Rekhtman et al., 1999). The canonical MEP commitment to MKPs or erythroid cells is coordinated by dose- and time-dependent expression of a TF network. NF-E2, SCL/TAL1, GATA1, GATA2, ETV6 and KLF1 are expressed in the MEP population, were only the expression of Fli1 and Runx1 are exclusively expressed in MKs and KLF1 in erythroid cells. Certain transcription factors actively repress the expression of lineage committing TF, e.g. Runx1 repress erythroid-specific transcription of KLF1 to increase the ratio towards Fli1 thereby boosting MK fate (Athanasiou et al., 2000; Bouilloux et al., 2008; Doré and Crispino, 2011; Kuvardina et al., 2015). MK maturation markers as GPIX and GPIba are regulated by the TF Fli1 (Martin et al., 1993; Kwiatkowski et al., 1998; Bastian et al., 1999).

GATA1 and GATA2 expressed in hematopoietic cells have reciprocal/antagonistic roles during hematopoiesis, also known as the 'GATA switch model' (Bresnick et al., 2010). While GATA2 is required for self-renewal and multipotency of HSCs (Tsai and Orkin, 1997), balanced GATA2/GATA1 expression in combination with the cofactor Friend of Gata 1 (FOG1) regulate myeloid commitment to CMP and MEPs. GATA1 knockout mice are incompetent to promote definitive erythropoiesis (Ikonomi et al., 2000b; Cantor and Orkin, 2002), while GATA2 knockouts are able to undergo erythroid and myeloid differentiation (Ikonomi et al., 2000a; Galloway et al., 2005). However, GATA1 expression is crucial for late-stage MK maturation steps in granule and proplatelet formation (Shivdasani et al., 1997; Tubman et al., 2007). Similarly, the TF NFE2 is essential for proplatelet formation (Shivdasani et al., 1995), since NFE2 deficient mice have a malfunctioning platelet production due to dysregulation of microtubules for cellular re-arrangement (Levin et al., 1999).

Adding another layer of complexity, a genome-wide ChIP-sequencing of GATA1, GATA2, SCL, Fli1 and Runx1-targeted promoters demonstrated, that these TF bind promoters simultaneously in various combinations and can act as transcriptional repressors and activators (Tripic et al., 2009; Tijssen et al., 2011). Screening for genes regulating MK differentiation by CRISPR/Cas9-mediated gene deletion additionally highlighted histone modifiers (histone deacetylates) as modulators of chromatin accessibility at the epigenetic level (Zhu et al., 2018). Based on FACsorted hematopoietic cells from murine BM in combination with transcriptome profiles (RNA-seq), genome-wide profiles of chromatin accessibility (ATAC-seq), histone modifications (ChIP-seq), and DNA methylation (MBD-seq), it was found that HSC, MKPs and MKs exhibit a strong overlapping open chromatin signature (Heuston et al., 2018). 89% of active regulatory regions in MKPs are also present in HSCs. The most significant differences between MKPs and HSCs were identified in *de novo* DNA-methylations in MKPs bolstering epigenetic regulation as important MK differentiation driver. In addition, the shared open chromatin sites correspond with MK, MKPs and HSC specific TF-binding sites, which were absent amongst erythroid progenitors. This was further supported by the finding of the existence of CD41-positive megakaryocyte-biased HSCs expressing high levels of GATA1, GFI1b, GATA2, and Fli1 (Sanjuan-Pla et al., 2013; Shin et al., 2014) and showing few differences in transcriptional signature to differentiated MKs (Rodriguez-Fraticelli et al., 2018).

1.6. Stress and emergency hematopoiesis

Hematopoiesis is under stress when HSCs divide more than required, e.g. during the acute demand of a certain type of blood cell. In this case, quiescent HSCs are then pushed into the cell cycle to proliferate, differentiate, and/or self-renew to re-establish hematopoiesis. Extreme stressors of hematopoiesis are blood loss, irradiation or chemotherapy (Morrison et al., 1997b; Wright et al., 2001; Cheshier et al., 2007). Similar, blood cell consumption, destruction, and demand could also be detected during infections. In between, it is known that HSPCs can sense and respond to infections by direct infection or recognition of the pathogen, or indirectly via inflammatory cytokines or changes in the BM niche (King and Goodell, 2011). Inflammation is a crucial part of the protective immune response to tissue damage or infection, and is orchestrated by pro-inflammatory cytokines and chemokines that regulate local or systemic responses (Medzhitov, 2008). During the last two decades, the sensing of inflammatory cytokines and their effect on HSC biology and functionality has been studied in detail, highlighting HSCs as responders to infection and their potential role in immune defense.

1.6.1. Direct and indirect stressor of hematopoiesis

The innate immune system recognizes pathogens through pattern-recognition receptors (PPR), amongst them the Toll-like receptors (TLR), which signal after the detection (extra- or intracellular) of pathogen-associated molecular patters (PAMPs). PPRs are expressed in non-hematopoietic and hematopoietic BM niche cells especially in MSCs, macrophages and dendritic cells. It has been recognized that HSPCs express TLR and sense systemic administered lipopolysaccharide (LPS; Nagai et al., 2006; Takizawa et al., 2011) or systemic bacterial infections (Esplin et al., 2011). Direct pathogen sensing leads to the production of granulopoietic cytokines, such as granulocyte colony stimulating factor (CSF) G-CSF, granulocyte macrophage GM-CSF and IL-6 (Zhao et al., 2014). HSPCs respond with increased cell cycling, mobilization of HSPCs into the peripheral blood and lineage skewing towards myeloid cells after pathogen sensing (Megías et al., 2012). During bacterial infection, the myeloid output replenishes in particular granulocytes, and is described as ‘emergency granulopoiesis’ (Manz and Boettcher, 2014).

Pro-inflammatory cytokines produced during infections are crucial HSC regulators, amongst them are type I (IFNα and IFNβ) and type II (IFNγ) interferons, tumor necrosis factor (TNF) and interleukin-1 (IL-1). Initial studies were performed *in vivo* by the application of the respective cytokine intraperitoneal or intravenous in mice. IFNs are antiviral cytokines mostly produced by innate immune cells in response to pathogens which transmit signals through the hetero-dimerization of the interferon alpha and beta receptors (IFNAR1/2) or the interferon gamma receptor (IFNGR). IFN receptors also signal through the JAK/STAT pathway inducing IFN-

stimulated genes (ISGs; Decker et al., 2005). A single injection of IFNα induced HSC (LSK side population [SP]) proliferation (Sato et al., 2009), the loss of HSC (LSK $CD150^{+}CD34^{-}$) quiescence through STAT1 and AKT signaling and the increased expression of Sca-1 on HSPCs (Essers et al., 2009). Not only HSPCs upregulate Sca-1 expression, but also CMPs and GMPs, which are defined by the absence of Sca-1 in steady-state hematopoiesis and shift into the LSK gate. HSC functionality is impaired under chronic exposure (2 weeks simulation) to IFNα which was detected by compromised HSC repopulation capacity in competitive repopulation assays. However, chronically (30 days stimulation) IFNα-exposed HSCs (LSK $Flt3^{-}CD150^{+}CD48^{-}$) do not alter in numbers and re-established their quiescence, but upon transplantation the cells activate a p53-dependent pro-apoptotic program, which results in reduced HSC engraftment (Pietras et al., 2014). Both studies utilized the double stranded RNA and virus mimicking agent polyinosinic:polycytidylic acid (polyI:C), which triggers IFNα production *in vivo* though activation of Toll-like receptor 3 (TLR3) expressing hematopoietic cells including macrophages, dendritic cells and B lymphocytes (Marshall-Clarke et al., 2007). Interestingly, although IFNα is able to induce cell cycle activation of HSCs *in vivo,* in *in vitro* culture with and without bone marrow stromal cells, HSC activation was not observed.

Type II interferon IFNγ enhances the proliferation of HSPCs (LSK cells) *in vitro* and upon injection in mice. This observation was strengthened by an *in vivo* mouse model of *Mycobacterium avium* (*M. avium*) infection (i.v.), were IFNγ was identified to be the cause of HSC alteration. HSCs (LSK $CD150^{+}$) lost quiescence, were mobilized to the peripheral blood and exhibited a heavily reduced engraftment potential (LSK SP; Baldridge et al., 2010). Activation of HSCs (LSK SP) was recapitulated by single injection of IFNγ, yet mild reduction of engraftment potential. Even with stringent immunophenotypic HSC characterization (LK $CD150^{+}$ $CD48^{-}$ $EPCR^{+}$), HSCs divide upon acute lymphochoriomeningitis virus (LCMV) infection, which induces IFNα and IFNγ production (Matatall et al., 2014). Especially myeloid-biased HSCs (LSK SP^{low} $CD150^{+}$; Challen et al., 2010) with high IFNGR expression are activated, differentiated and were almost depleted from the BM during *M. avium* infection. Chronic infection with *M. avium* in mice leads to pancytopenia, due to severe depletion of HSPCs as a response to IFNγ signaling (Matatall et al., 2016). Loss of HSC quiescence and reduced engraftment potential was observed in mouse models of systemic viral (VSV and murine cytomegalovirus [MCMV]; Hirche et al., 2017) or protozoan (*Plasmodium berghei*, Haltalli et al., 2020) infections caused by elevated IFNγ levels in the BM.

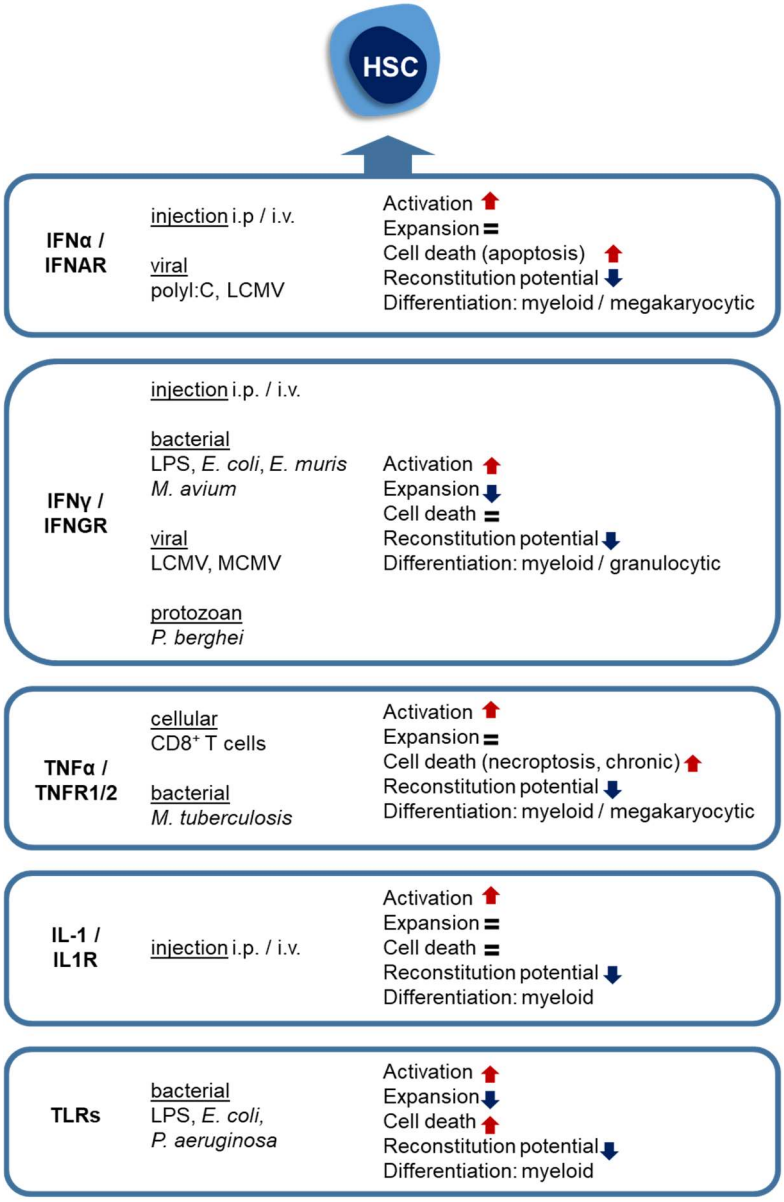

Figure 4 | Effects of pro-inflammatory cytokines and Toll-like receptor (TLR) signaling on murine HSC fate. Summary of reported stressors and the effect on HSC fate *in vivo* (mouse models) and *in vitro*. 'Activation' means the loss of HS(P)C quiescence, 'expansion' means the change of HSCs in numbers in the treated / infected mice, 'reconstitution potential' describes the engraftment potential in primary and sometimes secondary transplantations and 'differentiation' describes the lineage skewing / lineage output of mature blood cells observed in the treated / infected mice. polyI:C = polyinosinic:polycytidylic acid, LCMV = lymphocytic choriomeningitis virus, *E. coli* = *Escherichia coli*, *E. muris* = *Ehrlichia muris*, *M. avium* = *Mycobacterium avium*, MCMV = murine cytomegalovirus, *P. berghei* = *Plasmodium berghei*, *M. tuberculosis* = *Mycobacterium tuberculosis* and *P. aeruginosa* = *Pseudomonas aeruginosa*.

The pro-inflammatory cytokine tumor necrosis factor alpha (TNFα) is produced upon infection by activated macrophages and monocytes, endothelial cells, fibroblasts and osteoclasts. TNFα is generated as a membrane-bound prohormone, and is released through TNFα converting

enzyme (TACE). It binds to two receptors (1) the ubiquitous expressed TNF receptor (TNFR) 1, mediating the pro-inflammatory and apoptosis pathway and (2) the TNFR2 expressed on hematopoietic cells, regulating tissue repair and angiogenesis (Naudé et al., 2011). TNFR activation leads to the activation of the NFκB or caspase signaling. The role of TNFα in HSC regulation is under controversial debate based on opposing findings. *In vitro* stimulation of murine and human HSPCs (murine LSK; human $CD34^+CD38^-$) showed inhibition of proliferation and reduction in colony-formation and reconstitution potential (Broxmeyer et al., 1986; Selleri et al., 1995; Bryder et al., 2001). However, there are reports based on *in vitro* assays showed, that stimulation of HSPCs by TNFα released from co-cultured BM-derived CD8 T cells enhances HSPC engraftment by suppressing apoptosis (Rezzoug et al., 2008). Contradictory to that, transplantation of whole BM cells from TNFR1 and TNFR2 double knockout mice had a competitive advantage in reconstitution potential compare to BM cells from wild-type HSCs (Pronk et al., 2011).

IL-1α and IL-1β are two pro-inflammatory cytokines with similar biological activities. Both signal via the interleukin 1 receptor (IL1R) to activate MyD88 responses and NF-κB, MAPK and JNK, signaling pathways. Before the identification that IL1R is expressed on adult HSPCs (LKS cells; McKinstry et al., 1997), acute IL-1 signaling has been associated with myeloid cell production *in vitro* and *in vivo*, e.g. low dose IL-1α administration prevented irradiation or chemotherapy-induced myelosupression (Morrissey et al., 1988; van der Meer et al., 1988; Damia et al., 1992). IL1R1-KO mice treated with the chemotherapeutic agent 5-fluorouracil (5-FU) show a prolonged myeloid recovery compared to treated wild-type mice (Pietras et al., 2016). Initial studies report that chronic IL-1β exposure drastically reduced HSC (LSK $Flt3^-CD48^-CD150^+$) engraftment potential, however, this effect can be reverted upon treatment stop (Pietras et al., 2016). The cytokines IFNα, TNFα and IL-1 are associated with the activation of CD41-expressing HSCs to rapidly differentiate towards megakaryocytes and platelets to counter act inflammation-induced platelet loss (Haas et al., 2015; Pietras et al., 2016). This mechanism is described as ‘emergency megakaryopoiesis’.

1.6.2. Viral infections and stress hematopoiesis

The analysis of blood cell counts is part of the routine diagnostic of hospitalized patients with symptoms of infectious diseases. Lymphocytopenia combined with mild ($<150x10^3$/µL) to severe ($<20x10^3$/µL) thrombocytopenia can be initial findings during an acute viral or bacterial infection. Amongst them flaviviruses (arboviruses) causing potential hemorrhagic fevers, blood-borne viruses (hepatitis B and C) associated with liver failure and hepatocellular carcinoma and mostly respiratory viruses, like influenza A or B, corona, respiratory syncytial and adeno viruses causing a thrombotic milieu in the lung capillaries (Raadsen et al., 2021). Virus infections affect the levels of platelets (1) by decreased platelet production due to direct

infection of HSCs and MKs in the BM (systemic viruses) or (2) by platelet destruction due to platelet infection, activation and coagulation or enhanced platelet clearance (Assinger, 2014). Respiratory viral infections with influenza are rarely viremic and systemic, however, patients suffer from thrombocytopenia or thrombocytosis during the acute phase of infection (Kim et al., 2016). Influenza viruses, also commonly known as the 'flu' virus, appear in seasonal endemic outbreaks in the cold-seasons. Through the zoonotic spread from avian or porcine hosts to humans, influenza A virus (IAV) exhibits a high pandemic potential. Excessive IAV replication in the epithelial cells of the lower respiratory tract leads to production of pro-inflammatory cytokines potentially causing a 'cytokine storm' (IFNα and IFNγ, TNFα, IL-1, IL-6, IL-17 and IL-18) and epithelial-endothelial dysfunction leading to pro-thrombotic milieu.

1.7. Bone marrow transplantation in disease treatment

Since decades bone marrow transplantation (BMT) has been established as strategy for the treatment of leukemia. Leukemia patients in the United States (Thomas et al., 1957) and France (Mathé et al., 1965) were infused with frozen BM samples from fetuses or adults and a complete remission from leukemia was observed for a short-period of time, before patients died. By identification and recognition of human homologs of the murine histocompatibility complexes (MHC), the human leukocyte antigens (HLA), HLA-typing was included in the search of allogenic donors. This lead to the first successfully BMT in human as therapy hematological disorders. A child diagnosed with severe combined immunodeficiency (SCID) was treated by HLA-matched BM and blood transfusion from one of its siblings and remained cured from the SCID diagnosis (Gatti et al., 1968). BMT or hematopoietic stem cell transplantation (HCT) as a curative therapy for other hematological diseases faces the immune system reaction (1) from host immune cells (host-versus-graft-reaction) and (2) from newly generated graft immune cells (graft-versus-host reactions). Conditioning regimes with myeloablative and immunosuppressive treatments next to total body irradiation of the patients have provided sufficient immunoablation and reduced tumor burden. In Europe, the number of patients receiving allogenic or autologous HCT per year rose from ~6,000 in 1990 to ~50,000 in 2019 (Passweg et al., 2021). The main indications for allogenic HCT (~40-50% of all HCT) are myeloid malignancies like acute myeloid lymphomas (AML), myelodysplastic syndromes (MDS) or MPNs as well as lymphoid malignancies like acute lymphatic leukemia (ALL), while autologous HCTs (~50-60%) are mainly indicated for lymphoid malignancies (>90%) like plasma cell disorders, non- and Hodgkin lymphomas. Stem cell sources for allogenic transplantations are mobilized HSCs (80%) and BM aspirates (20%) and rarely cord blood-derived HSCs (<1%).

2. Aim

HSCs provide constant supply of progenitor cells and mature blood cells. The rare but specialized HSCs in the BM are characterized by self-renewal capacity, a high proliferative potential, and the ability to differentiate into all mature blood cells. At steady-state the THPO/MPL signal pathway is an important regulator of HSC fate by promoting either HSC maintenance and self-renewal or megakaryopoiesis and thrombopoiesis. Although the Thpo/Mpl-pathway has been studied for years, downstream targets have barely been identified. Stress hematopoiesis studies with inflammatory agents, have strengthened the hypothesis that the MK-lineage branches directly from HSCs or MPPs, bypassing several precursor stages. This highlights the close relationship between HSCs and MKs, which not only share similar transcription factors and cell surface receptors. In this respect, I aimed to identify THPO/MPL-downstream targets to elucidate, how one signal pathway can regulate apparently opposing functions in steady-state, regeneration and during inflammation.

Project 1: Studying potential THPO/MPL downstream genes in the Mpl-deficient mouse model for their regenerative capacity on HSCs and MKs

Thpo candidate target genes from own gene expression DNA-microarray experiments of Mpl-regenerated Mpl-deficient LSK cells and wt Mpl-inhibited LSK cells were selected. To investigate the identified gene candidates on HSC regeneration and megakaryopoiesis the cDNA of the respective gene candidate was inserted in third generation self-inactivating (SIN) lentiviral vectors, transduced Lin^- BM cells from Mpl-KO mice and transplanted them into Mpl-KO mice. The hypothesis was, that lentiviral overexpression of potential Thpo target genes in Mpl-KO mice should rescue HSC engraftment and pool in Mpl-KO mice. Effects of the candidate genes were evaluated on peripheral blood reconstitution and regeneration of HSC pool in the BM and compared to the potential of wt and Mpl-KO control transduced and transplanted Mpl-KO Lin^- BM cells. HSC key features like quiescence and self-renewal in HS(P)Cs were evaluated by flow cytometry and gene expression at different time points of reconstitution/homing in the BM and spleen. Rescue of megakaryopoiesis was assessed by patho-histological analysis in BM-sections of Mpl-KO mice transplanted with transduced Lin^- MPL-KO BM cells. In addition, I intended to verify the target gene as a direct transcriptional target in ex vivo culture assays of FACsorted LSK cells.

Project 2: Mechanistic investigation of the THPO mimetic romiplostim and THPO on signal transduction of wild-type and mutated variants of the murine thrombopoietin receptor

The aim of this project was to uncover whether stimulation of murine Mpl with the human THPO mimetic romiplostim would result in differential activation. This would shed light on the question how Thpo/Mpl-signaling results in HSC maintenance or megakaryopoiesis. I made use of the murine interleukin 3-dependent 32D cell line, lentivirally overexpressing either murine (m) or human (h) MPL. To identify potential differences between 32D-mMpl and -hMPL cells stimulated with romiplostim, recombinant mTHPO and hTHPO, I analyzed signal transduction activity by flow cytometry based phosflow assays and cell proliferation by cell trace and cell viability assays. *In vitro* megakaryocyte differentiation potential of Lin^- BM cells from wt mice after stimulation with romiplostim and mTHPO was examined by identification of MK maturation cell surface markers and ploidy state by flow cytometry and morphological characterization of cytospins. Tyrosine-to-phenylalanine mutant versions were created by site-directed mutagenesis and truncated mutant versions in the intracellular moiety of mMPL to shed light on the question whether intracellular residues of mMPL are linked to specific signal pathways for the induction of megakaryopoiesis. The signal transduction of mMPL mutant variants in transduced 32D cells after stimulation with mTHPO and romiplostim was assessed by phosflow assays and Western blots. In addition, I evaluated the rescue of MPL-deficient megakaryopoiesis from Mpl-KO Lin^- BM cells transduced with the mMPL mutant variants. This included the analysis of MK morphology by cytospins, maturation cell surface markers and polyploidy by flow cytometry.

Project 3: The role of THPO/MPL signaling during stress hematopoiesis during influenza infection

In the recent years, stress hematopoiesis has been linked to inflammation. Various systemic infection models, from cytokine administration up to infections with pathogens has been shown to induce HSC activation and functional defects as well as myeloid lineage-biased differentiation. Whether a non-systemic and respiratory infection with a clinically relevant virus could have a similar influence on HSC fate has been not addressed so far. Since influenza infections are associated with altered platelet counts in the peripheral blood in severely infected patients, the hypothesis was, that THPO/MPL signaling may play a key role in HSC activation but also in platelet replenishment. Therefore, mouse models of influenza A (IAV) infections with different initial dosages, antiviral drug treatments or immunized mice were conducted. In these mice, IAV-induced lung pathology, changes in peripheral blood and BM compartment composition and counts were analyzed. Specifically, I addressed the cell cycle status of

phenotypically quiescent HSCs by flow cytometric analysis and the levels of pro-inflammatory cytokines by multiplex-ELISA in BM samples of IAV-infected mice. CD41 expression on HSPCs was utilized to identify and evaluate potential myeloid or platelet-biased differentiation in IAV-infected mice. In the following, myeloid or platelet-biased HSC potential was validated by performing *in vitro* single-cell trace assays and bone marrow transplantations of CD41-expressing HSPCs from non- and IAV-infected mice. The global transcriptome of $CD41^+$ or $CD41^-$ HSPCs by RNA-seq was investigated to characterize and identify specific changes, which could define platelet-biased HSC potential in non-infected and IAV-infected mice. In addition, IAV infections in cytokine- or cytokine receptor-knockout mice were conducted to narrow down potential cytokine(s) responsible for HSC activation and myeloid or platelet-biased HSC differentiation during IAV infection. I raised the question whether platelets produced during IAV infection have a beneficial or patho-physiological role. Subsequently platelet phenotype was characterized by flow cytometry and platelet function by activation and spreading assays.

3. Methods

3.1. Molecular biological methods

3.1.1. Generation of lentiviral vectors

Third generation SIN lentiviral vectors were constructed by inserting the coding sequences of the respective gene of interest (GOI) into the pRRL.PPT.pre vector (Schambach et al., 2006). The complementary (c)DNAs (Table 1) were expressed by either the internal spleen focus-forming virus (SFFV) promotor, the human phosphoglycerate kinase (PGK) promoter or murine platelet factor 4 promoter (mPF4P) (Table 1). Transduction rates were determined by co-expression of the enhanced green fluorescent protein (eGFP) via an internal ribosomal entry site (IRES) or the insertion of a hemagglutinin (HA) –tag into the protein.

Table 1 | List of lentiviral vectors used in experiments.

Project/Experiment	Vector	Reference
4. Results Publication 1	RRL.PPT.PGK.IRES.eGFP.pre RRL.PPT.PGK.Pbx1.IRES.eGFP.pre RRL.PPT.PGK.Fzd4.IRES.eGFP.pre RRL.PPT.PGK.Hoxa10.IRES.eGFP.pre RRL.PPT.PGK.Epcr.IRES.eGFP.pre RRL.PPT.PGK.Mycn.IRES.eGFP.pre	Designed and generated in Publication 1
4.Results Publication 2	RRL.PPT.SFFV.HA-murine(m)Mpl.pre	Heckl et al., 2011
	RRL.PPT.SFFV.HA-human(h)Mpl.pre	Heckl et al., 2011
	RRL.PPT.SFFV.HA-mMplY616F.pre RRL.PPT.SFFV.HA-mMplY621F.pre RRL.PPT.SFFV.HA-mMplY616F_Y621F.pre RRL.PPT.SFFV.HA-mMplY616F.pre RRL.PPT.SFFV.HA-mMplY582F.pre RRL.PPT.SFFV.HA-mMplΔ53F.pre RRL.PPT.SFFV.HA-mMplΔ69.pre	Designed and generated in Publication 2
4. Results Publication 3	RRL.PPT.PF4P.RSD.IRES.eGFP.pre RRL.PPT.PF4P.RSD.IFN-alpha.IRES.eGFP.pre	Woods et al., 2022

Internal ribosomal entry site (IRES), enhanced green fluorescent protein (eGFP), pre–B-cell leukemia homeobox 1 (Pbx1), Wnt receptor frizzled 4 (Fzd4), homeobox A10 (Hoxa10), endothelial protein c receptor (Procr/EPCR), neuroblastoma-derived homolog Myc (Mycn), cellular myeloproliferative leukemia virus oncogene (c-Mpl), hemagglutinin (HA) –tag, platelet factor 4 promotor (Pf4P), RANTES sorting domain (RSD) and interferon alpha (IFN-alpha).

3.1.2. RNA isolation and quantitative PCR

The RNA was isolated from FACsorted hematopoietic cells or the liver using the Direct-zol RNA MicroPrep Kit (Zymo Research, #R2060) and reverse transcribed to cDNA using RevertAid H Minus Reverse Transcriptase (ThermoFisher, #EP0451) according to the manufactures' protocol. qPCR reaction was performed with TaqMan primer and probe sets

(ThermoFisher). Gene expression of the respective gene was normalized to the β-actin housekeeping gene and calculated using the ΔΔ-ct method.

3.2. Cell culture – stable/immortalized cell lines

3.2.1. Cultivation of stable cell lines

Stable cell lines were cultivated and maintained in an incubator at 37°C, 5% CO_2 and saturated relative humidity. The respective culture medium of each cell line is listed in Table 2. Adherent cell lines were passaged three times a week by de-attaching them with 0.5 g/L trypsin in PBS-ethylenediaminetetraacetic acid (EDTA) for2 to 5 min at 37°C in a split ratio of 1:8. Suspension cell lines were passaged two times a week in a split ratio of 1:10.

Table 2 | Stable cell lines used in experiments.

Stable cell line	Organism / tissue /morphology	Culture medium	Reference
HEK239T	human / kidney, embryonal / epithelial cell-like / adherent	90% DMEM 10% FCS 2 mM L-glutamine	Graham et al., 1977
SC-1	mouse / embryonal / fibroblast / adherent	90% DMEM 10% FCS 2 mM L-glutamine	Hartley and Rowe, 1975
32D	mouse / bone marrow / myeloblast cell-like / suspension	90% RPMI 1640 10% FCS 2 mM L-glutamine 10 mM HEPES 1 mM sodium pyruvate 1 ng/mL murine IL-3	Greenberger et al., 1983
HEL	human / bone marrow / erythroblast / suspension	90% RPMI 1640 10% FCS 2 mM L-glutamine 10 mM HEPES 1 mM sodium pyruvate	Martin and Papayannopoulou, 1982
MDCK	dog / kidney / epithelial / adherent	90% DMEM 10% FCS 2 mM L-glutamine	Madin and Darby, 1958
BHK-21	hamster / kidney / fibroblast / adherent	90% MEM 10% FCS 2 mM L-glutamine	Macpherson and Stoker, 1962
BHK-G43	hamster / kidney / fibroblast / adherent	90% MEM 10% FCS 2 mM L-glutamine	Hanika et al., 2005

Dulbecco's Modified Eagle's medium (DMEM), Roswell Park Memorial Institute (RPMI)-1640 medium, Eagle's minimal essential medium (MEM), fetal calf serum (FCS), 4-(2-hydroxyethyl)-1-piperazineethanesulfonic acid (HEPES) and interleukin 3 (IL-3).

3.2.2. Lentiviral vector production and titration

Viral vector particles were produced in human embryonic kidney (HEK293T) cells (10 cm culture dishes) cultivated in Dulbecco's Modified Eagle's medium (DMEM) medium supplemented with 10% fetal calf serum (FCS), 2 mM L-glutamine, 1% penicillin / streptomycin, 20 mM 4-(2-hydroxyethyl)-1-piperazineethanesulfonic acid (HEPES), 25 µM chloroquine. HEK293T cells (one 10 cm dish) were transfected with 10 µg vector plasmid, 10 µg of gag/pol plasmid (pCDNA3.GP.4xC plasmid), 5 µg of rev-encoding plasmid (pRSV-REV plasmid), and 1.5 µg plasmid encoding the VSV G protein (VSV-G) envelope protein (pMD.G plasmid) using the transient calcium-phosphate transfection method. 36 and 48 hours after transfection the supernatant was collected, filtered (0.22 µm filter), when need concentrated through high-speed centrifugation at 80,000 x g for 2 hours, re-suspended in serum-free (SF) StemSpan SFEM (StemCell Technologies; #09650) and stored at -80°C until use. Murine fibroblast SC-1 cells were utilized for evaluating the viral vector transducing titers (infectious particle/mL) by serial dilution of the supernatant in presence of protamine sulfate (4 µg/mL) as transduction enhancer. Three days after transduction, SC-1 cells were analyzed for the expression via eGFP by direct fluorescence or Mpl by staining the HA-tag using flow cytometry. Cells transduced with MPL or MPL mutant variants were identified by staining with a primary anti-HA-Biotin (1:100, Roche, clone: N.A., #12158167001) and secondary Streptavidin-phycoerythrin (PE; 1:100; BioLegend, clone: N.A., #405204). Only cultures with an expression between 1-30% were used for titer calculation.

3.2.3. Influenza virus production

Madin-Darby canine kidney (MDCK) cells or eleven days old embryonated chicken eggs were utilized to grow the mouse-adapted influenza A/Puerto Rico/8/34 H1N1 (IAV PR8 or IAV in this work) as described by (Walz et al., 2018). In brief, for cell-culture grown IAV stocks MDCK cells were infected with IAV, cultivated serum-free in DMEM with tosylsulfonyl phenylalanyl chloromethyl ketone-treated Trypsin (Sigma-Aldrich, #4352157). Supernatant was harvested when the cytopathic effect was widespread, clarified by centrifugation, and stored at -80°C. For chicken egg-derived IAV, the allantoic fluid was infected with IAV ($1x10^3$ $TCID_{50}$), incubated for 2 days and harvested from allantoic fluid. IAV were purified via ultracentrifugation (135,000 x g, 2 hours, 4°C) in 20% sucrose (Sigma-Aldrich, #S0389). Before storage at -80°C the hemagglutinin titer was determined by standard procedure describe by the WHO (World Health Organization, 2002).

3.2.4. Influenza virus titration

After one freezing cycle the IAV titers were quantified. MDCK cells were seeded in a 96-well plate format. In serial 10-fold dilutions the supernatant of homogenized and clarified lung and tracheal tissue or IAV vector stocks were titrated in quadruplicates on 80 to 90% confluent

MDCK cells. Two days post infection, IAV-infected cells were detected by ferret anti-pdm09 H1N1 serum (1:500; Veronika von Messling, Paul-Ehrlich-Institute) and secondary goat anti-ferret IgG conjugated with a horseradish peroxidase (HRP, 1:750, Bethyl Laboratories, #A140-108P). Red colored cells from 3-amino-9-etyhl-carbazole (AEC, Sigma-Aldrich, #A6926) deposits visualized IAV-infected (positive) cells. The 50% tissue culture infectious dose per mL ($TCID_{50}$/mL) for IAV stocks was calculated based on Spearman and Kaerber. IAV load in lung and tracheal tissue was normalized to the weight ($TCID_{50}$/g).

3.2.5. Vesicular stomatitis virus replicon particle propagation and titration

The vesicular stomatitis virus (VSV) vector platform expressing GFP and lacking the surface glycoprotein VSV-G (pVSV∗ΔG) was used to generate VSV replicon particles. Walz et al., 2018 generated a pVSV∗ΔG expressing a neuraminidase of influenza A/chicken/Yamaguchi/7/ 2004 H5N1 (pVSV∗ΔG(NA_{H5N1})), which was used to immunize mice for IAV challenge. The helper cell line baby hamster kidney cells (BHK-21) providing the VSV G protein in *trans* (BHK-G43), were infected with recombinant vaccinia virus ankara expressing the T7 phage RNA polymerase and cultivated in Eagle's minimal essential medium (MEM, Sigma-Aldrich, # 51412C) supplemented with 10% FCS, 2 mM L-glutamine with 1 nM mifepristone (Sigma-Aldrich, #M8046) for VSV G expression. The cells were co-transfected with the VSV helper plasmids (VSV-N, -P and -L) and the plasmid encoding the pVSV∗ΔG(NA_{H5N1}), which are all controlled by the T7 promotor. After 24 hours co-transfected BHK-G43 cells were detached with trypsin, seeded with fresh BHK-G43 cells and cultivated for additional 24 hours in the presence of mifepristone. The VSV replicon particle containing supernatant was collected, clarified by low-speed centrifugation (1000 x g, 15 min, 4°C) and stored at -80°C. For large scale amplification of the VSV replicon, BHK-G43 cells were cultivated in the presence of 1 nM mifepristone and were infected with the VSV replicon particles. After 48 hours post infection and when the GFP expression was widespread the supernatant was collected, low-speed clarified, purified with high-speed centrifugation (100,000 x g, 1 hour, 4°C) with a 20% sucrose (Sigma-Aldrich, #S0389) cushion, re-suspended in sterile PBS and stored at -80°C. VSV replicon particles were titrated on 90% confluent BHK-21 cells seeded in a 96-well plate format. Titration was performed in 10-fold serial dilution in duplicates and after 12 hour incubation (37°C, 5% CO_2, saturated humidity) the cells were analyzed for GFP expression under the fluorescence microscope (ECLIPSE Ti-S, Nikon) . VSV replicon particle titers were calculated as number of GFP-expressing cells in an appropriate dilution × dilution factor × volume of inoculums/mL and expressed as fluorescence forming unit per milliliter (ffu/mL).

3.2.6. MPL and MPL-mutant variant signal transduction pathway analysis

The murine myeloblast-like 32D cell line was used to the compare signaling capacity of the murine (m)Mpl, mMPL-mutant variants or human (h)MPL. 32D cells were cultured at 37°C saturated relative humidity and 5% CO_2 in Roswell Park Memorial Institute (RPMI)-1640 medium with 10% FCS, 2 mM L-glutamine, 1 mM sodium pyruvate and 1 ng/mL murine IL-3. For signaling transduction analysis 32D cells were transduced with the respective lentiviral vector and FACsorted to >99% HA-mMPL, HA-mMPL mutant variants or HA-hMPL expression (Table 1). 32D cells expressing mMPL, mMPL mutants or hMPL were serum (0.5% FCS) and cytokine (without IL-3) starved in RPMI-1640 medium for 14-16 hours before stimulation with increasing doses of murine (m)THPO, human (h)THPO or romiplostim (Nplate®, Amgen, PZN 06648759). Small-molecule inhibitors were added 1 hour before stimulation in increasing concentrations (ruxolitinib/JAK-inhibitor, StemCell Technologies, #73402; LY294002/PI3K inhibitor, StemCell Technologies, #72152; PD98049/MEK inhibitor, StemCell Technologies, #72172; and SCH772984/ERK-inhibitor SelleckChem, #S7101).

Phosflow analysis

Starved and stimulated 32D cells were stopped with ice-cold 4% paraformaldehyde (PFA, 15 min, on ice) and permeabilized with 100% methanol (-20°C, 45 min, on ice). Samples were split for single staining (30 min, on ice) with anti-mouse pY694-STAT5 (clone 47, #562077), anti-mouse pS473-AKT (clone M89-61, #561670) or anti-mouse pT202/pY204-ERK1/2 (clone 20A, #612566) antibodies (AlexaFluor 647, BD Bioscience) and acquired using flow cytometry (Cytoflex, Beckman Coulter).

Western Blot

Starved and stimulated (20 ng/mL mTHPO) 32D cells transduced with mMPL and MPL_Y582F were washed in ice-cold PBS and lysed in radioimmunoprecipitation assay (RIPA) buffer (Abcam, #ab156034) with protease and phosphatase inhibitors and sonication. Equal amounts of protein were separated in a 12% sodium dodecyl sulfate-polyacrylamide gel electrophoresis (SDS-PAGE), blotted on a nitrocellulose membrane, blocked in 5% bovine serum albumin (BSA) in tris-buffered saline with 1% Tween20 (TBS-T). The blocked membranes were incubated (4°C, overnight, 5% BSA in TBS-T) with rabbit-anti-mouse pERK (p44/42, T202/Y204, 1:750, Cell Signaling Technology, #9101S), rabbit-anti-mouse panERK (1:1000, Cell Signaling Technology,#4695T) or rabbit-anti-mouse GAPDH (1:1000, ThermoFisher Scientific, #MA5-15738) for loading control. Washed membranes were incubated (1 hour, RT, 5% BSA in TBS-T) with a secondary antibody goat-anti-rabbit IgG HRP (1:5000, Abcam, #ab6721). Enhanced chemiluminescence (ECL) solution (Bio-Rad Laboratories) and membranes were incubated (5 min, RT, dark) and visualized using the MicroChemi 4.2 chemiluminescent imaging system (DNR Bio Imaging Systems).

3.2.7. Surface receptor internalization

Starved and stimulated (50 ng/mL mTHPO, hTHPO or romiplostim) mMpl- and hMpl-32D cells were fixed at different time points with PBS 4% PFA (10 min, ice-cold) and surface expression of MPL was detected using flow cytometry by staining the HA-tag (see 3.2.2).

3.2.8. Proliferation and cell division assay

Starved 32D cells (2 x 10^4 cells/well) were seeded in 96-well plates and cultured (48 hours) with increasing doses with either mTHPO, hTHPO, romiplostim or mIL-3. Proliferation of cells were determined by metabolic activity through incubating the cells with PrestoBlue (30min up to 24 hours, 37°C, ThermoFisher, #A13261). The metabolization (reduction) of PrestoBlue from non-fluorescent resazurin to highly fluorescent resorufin was acquired by the fluorescence emission signal at $\lambda_{em} = 590$ nm with a microplate reader (Infinite 200, Tecan). The proliferation rate of mMPL mutants was normalized to the proliferation rate of wild-type mMPL 32D cells stimulated with mIL-3. Cell divisions upon stimulation were determined by labeling starved cells with 1 µmol/L Celltrace far red (ThermpFisher, #C34572). Cell proliferation was analyzed by label dilution after 48 hours of cultivation via flow cytometry.

3.3. Cell culture – primary murine cells

3.3.1. Mouse strains

Table 3 | Mouse strains used for animal experiments or tissue and organ harvesting.

Mouse strain	Experiment	Source	Reference
C57BL/6J (BL/6J or CD45.2)	IAV challenge; BM transplantation (donor and supportive BM); *In vitro* MK differentiation	Charles River #000664	N/A
C57BL/6NRj (BL/6N)	IAV challenge	Janvier Labs	N/A
B6.SJL-*Ptprc*^{a} *Pepc*^{b}/BoyJ (CD45.1)	BM transplantation (recipient)	Charles River #02014; PEI, in-house breeding	N/A
B6.129S1-Mpl^{tm1Wsa}/Mpl^{tm1Wsa} (Mpl-KO CD45.2)	IAV challenge; BM transplantation (donor); *In vitro* MK differentiation	PEI, in-house breeding	Alexander et al., 1996
B6.129S1-Mpl^{tm1Wsa}/Mpl^{tm1Wsa}; *Ptprc*^{a} (Mpl-KO CD45.1)	BM transplantation (recipient); *In vitro* MK differentiation;	PEI, in-house breeding	Kohlscheen et al., 2019
B6.129-*Gt(ROSA)26Sor*$^{tm4(ACTB\ tdTomato,-EGFP)Luo}$/J (mTmG)	IAV challenge; Bone marrow transplantation (donor)	PEI, in-house breeding	Muzumdar et al., 2007
B6.129S7-Il1r1^{tm1Imx}/J (IL1R1-KO)	IAV challenge	PEI, in-house breeding	Glaccum et al., 1997
B6.129S2-Il6^{tm1Kopf}/J (IL-6-KO)	IAV challenge	Jackson Lab #002650	Kopf et al., 1994

3.3.2. Bone marrow cells

Isolation of mononuclear cells and lineage marker-negative BM cells

From each mouse, the BM cells were isolated from femora, tibia and coxae. For BM cell analysis of individual mice the cells were flushed with 10 mL SF Iscove's Modified Dulbecco's Medium (IMDM) medium supplemented with 10% FCS, 2 mM L-glutamine and 1% penicillin / streptomycin with a 1 mL syringe fitted with a 23G cannula. Alternatively, bones from multiple mice were pooled and crushed three-times in the same media. BM cell suspension was filtered through a 70 µm strainer (Corning or Miltenyi-Biotech).

Mononuclear cells (MNC) were isolated from filtered BM cells performing density gradient centrifugation (800 x g, RT, 20 min without acceleration and break; Histopaque-1803, Sigma-Aldrich, #10831). MNCs were collected from the interphase of PBS and Histopaque-1083, washed and counted. Counting was performed with a hemocytometer and trypan blue staining. MNCs were used for FACsorting HSCs, MPPs and LSK cells.

Lineage marker-negative (Lin^-) BM cells were isolated by lineage-depletion by magnetic cell-sorting (MACS), according to the protocol of the mouse lineage depletion kit (Miltenyi Biotech, #130-090-858). In brief, Fc-receptor blocked MNCs were stained with lineage-specific anti-mouse CD5, CD45R (B220), CD11b, Gr-1 (Ly-6G/C), 7-4 (Ly-6B.2), and Ter-119 biotin antibodies (30 min, 4°C, shaking), followed by adding the streptavidin magnetic beads (30 min, 4°C, shaking) and separated in the flow-through by a magnetic separation column. Lin^- BM cells in the flow-through were collected and counted.

LSK cell stimulation

Fc-receptor blocked (1:100, eBioscience, clone 93, #14-0161-82) MNCs were stained for LSK cells (Table 4) and were FACsorted with a 70 µm nozzle in a bulk. LSK cells were seeded at density of $1x10^4$/well in a 96-well plate and were cultivated with SF StemSpan SFEM, 2 mM L-glutamine, 1% penicillin / streptomycin with murine mSCF (10 ng/mL, PeproTech) alone or murine mSCF (10 ng/mL) and murine THPO (100 ng/mL, PeproTech). At 36 and 60 hours of cultivation EPCR expression (Table 4) was analyzed by flow cytometry (Cytoflex, Beckman Coulter).

Table 4 | Antibodies and reagents used for FACsorting LSK cells and FC analysis after stimulation. Clone of the respective antibody in bracket, e.g. anti-mouse TER-119 (Ter-119)

Antibodies / Reagent	Conjugate	Con.	Source	Identifier
FACS				
live / dead (DNA)	DAPI	1:1000	Sigma-Aldrich	Cat# D9542
Lineage marker panel anti-mouse TER-119 (Ter-119) anti-mouse CD11b (M1/70) anti-mouse Ly-6G/Ly-6C (RB6-8C5) anti-mouse CD3ε (17A2) anti-mouse CD45R/B220 (RA3-6B2)	Pacific Blue	1:10	BioLegend	Cat# 133310
anti-mouse c-Kit (2B8)	APC	1:100	eBioscience	Cat# 17-1171-83
anti-mouse Sca-1 (D7)	PerCP-Cy5.5	1:100	eBioscience	Cat# 45-5981-82
Flow cytometry				
live / dead (DNA)	DAPI	1:1000	Sigma-Aldrich	Cat# D9542
anti-mouse EPCR (eBio1560)	PE	1:200	eBioscience	Cat# 12-2012-82

Cell cycle analysis via BrdU labeling

2,000 FACsorted HSCs (LSK $CD150^{+}CD48^{-}CD34^{-}$) and 2,000 FACsorted MPPs (LSK $CD150^{+}CD48^{+/-}CD34^{+}$) were cultured (36 hours) in 100 µL StemSpan SFEM supplemented with 2 mM L-glutamine, 1% penicillin/streptomycin, bromodesoxyuridine (BrdU, 5 µM, Sigma-Aldrich, #H27260), mSCF (50 ng/mL) alone or mSCF (50 ng/mL) with either mTHPO, mIL-1α, mIL-6 or mIFNγ (100 ng/mL, all PeproTech) in an 96-well plate format. 500,000 MNCs were cultured (24 hours) in 1 mL StemSpan SFEM with equal supplementation in a 24-well format.

To prevent HSC and MPP loss during staining procedures, 150,000 human erythroleukemia (HEL) cells were added. Human and murine cells were distinguished with the anti-human HLA-A, B, C– APC antibody (1:100, clone W6/32, BioLegend, #311410). HSCs or MPPs in the MNC bulk were surface stained for LSK CD150 CD48 CD34 and FACSsorted HSC and MPPs were surface stained for LSK CD150 CD48 with the antibodies according to Table 5. Cells were fixed (40 min, on ice; 1:4 dilution of the fixation/permeabilization concentrate (PFA based) in fixation/permeabilization diluent) using the Foxp3/transcription Factor Staining Buffer Set (eBioscience, #00-5523-00). After fixation the cells were permeabilized two times with the permeabilization buffer (30 min, RT; 1x Permeabilization buffer (saponin based) in dH_20), followed by DNA digestion with DNAse I (4 U/mL) in Dulbecco's PBS for 1 hour at 37°C. Intracellular BrdU (1:20, anti-mouse BrdU-FITC, clone BU20A, eBioscience, #11-5071-42) and Ki-67 were stained for 1 hour at room temperature, followed by DNA straining by undiluted 7-AAD for at least 30 min. Cells were acquired with the LSR SORB II, Fortessa or Symphony A3 flow cytometer (BD Bioscience).

Table 5 | Antibodies and reagents used for cell cycle analysis.

Antibodies / reagent	Conjugate	Con.	Source	Identifier
Extracellular / surface				
Lineage marker panel anti-mouse TER-119 (Ter-119) anti-mouse CD11b (M1/70) anti-mouse Ly-6G/Ly-6C (RB6-8C5) anti-mouse CD3ε (17A2) anti-mouse CD45R/B220 (RA3-6B2)	Biotin	1:100	BioLegend	Cat# 133307
anti-mouse c-Kit (2B8)	SP702	1:100	eBioscience	Cat# 67-1171-82
anti-mouse Sca-1 (D7)	BV510	1:100	BioLegend	Cat# 108129
anti-mouse CD150 (TC15-12F12.2)	BV605	1:100	BioLegend	Cat# 115927
anti-mouse CD48 (HM48-1)	AF700	1:50	BioLegend	Cat# 103426
anti-mouse CD34 (RAM34)	eF660	1:10	eBioscience	Cat# 11-0341-85
anti-mouse CD201 (EPCR) (eBio1560)	PE	1:200	eBioscience	Cat# 12-2012-82
anti-mouse CD41a (MWReg30)	eF450	1:75	eBioscience	Cat# 48-0411-82
anti-mouse CD16/CD32 (93)	APC-Cy7	1:75	eBioscience	Cat# 25-0161-82
anti-mouse CD9 (eBioKMC8)	AF700	1:75	eBioscience	Cat# 56-0091-82
Streptavidin	BV570	1:100	BioLegend	Cat# 405227
Intracellular				
anti-mouse Ki-67 (SolA15)	PE-Cy7	1:100	eBioscience	Cat# 25-5698-82
DNA	7-AAD	Undiluted	BioLegend	Cat# 420403

In vitro lineage tracing of HSCs

BM cells from single mice were isolated by crushing hips, femora, tibias and spines three-times in 10 mL SF-IMDM and filtered through a 70 µm strainer. Lineage marker-positive cells were depleted by magnetic separation by incubation with rat anti-mouse monoclonal antibodies against CD11b, Gr-1, CD4, CD8a, Ter119 and B220 (45 min, 4°C) and followed by the incubation with anti-rat IgG coated Dynabeads for 45 min (4.5 µm supermagnetic polystyrene beads (Invitrogen), 1mL of beads / $3x10^8$ bone marrow cells). Lin^- BM cells were stained according to Table 6 and single HSCs were sorted (single-cell mode and index mode) with a 100 µm nozzle directly in 200 µL SF StemSpan SFEM , supplemented with 1% L-glutamine, 1% penicillin / streptomycin, 10 ng/mL hFlt3-ligand, 50 ng/mL mSCF, 10 ng/mL mTHPO, 5 ng/mL mIL-3, 10 ng/ml mIL-11, 22.2 ng/mL mIL-7 (all PeproTech) 0.3 IU/mL rhEPO (Janssen, PZN 06301240) of a round bottom 96-well plate. Cells were cultivated under normoxic conditions (37°C, 5% CO_2). Small and large (>500 cells) colonies from sinlge HSCs were analyzed based on their morphology (cytospin, 300 x g, 7 min, May-Grünwald Giemsa, Carl-Roth, #7863.2 and #7862.2) and larger colonies via flow cytometry (HTS 96-well plate, Fortessa, BD Bioscience) for myeloid cells, megakaryocytes, and erythroid cells (Table 6).

Table 6 | Antibodies used for single-cell sorting of HSCs and generated colonies.

Antibodies / Reagents	Conjugate	Con.	Source	Identifier
FACS				
live / dead (DNA)	7-AAD	1:300	BioLegend	Cat# 420403
Lineage marker panel anti-mouse TER-119 (Ter-119) anti-mouse CD11b (M1/70) anti-mouse Ly-6G/Ly-6C (RB6-8C5) anti-mouse CD3ε (17A2) anti-mouse CD45R/B220 (RA3-6B2)	Pacific Blue	1:10	BioLegend	Cat# 133310
anti-mouse c-Kit (ACK2)	BV711	1:100	BD Bioscience	Cat# 752698
anti-mouse Sca-1 (D7)	APC-Cy7	1:100	BD Bioscience	Cat# 560654
anti-mouse CD150 (TC15-12F12.2)	PE-Cy7	1:100	BioLegend	Cat# 115914
anti-mouse CD48 (HM48-1)	BUV395	1:200	BD Bioscience	Cat# 740236
anti-mouse CD34 (RAM34)	FITC	1:20	eBioscience	Cat# 11-0341-85
Anti-mouse CD41 (MWReg30)	APC	1:100	eBioscience	Cat# 17-0411-82
anti-mouse EPCR (eBio1560)	PE	1:100	eBioscience	Cat# 12-2012-82
FC colonies				
live / dead (DNA)	7-AAD	1:300	BioLegend	Cat# 420403
anti-mouse CD42d (1C2)	APC	1:200	eBioscience	Cat# 17-0421-82
anti-mouse CD41 (MWReg30)	FITC	1:200	BioLegend	Cat# 13390
anti-mouse CD71 (R17 217.1.4)	PE	1:200	eBioscience	Cat# 12-0711-83
anti-mouse Ter119 (TER-119)	PE-Cy7	1:200	eBioscience	Cat#25-5921
anti-mouse CD11b (M1/70) anti-mouse Gr-1 (RB6-8C5)	APC-Cy7	1:200	eBioscience	Cat# 47-0112; Cat# 47-5931

Differentiation potential of HSCs towards myeloid, megakaryocytic and erythroid lineages (uni-, bi- or multi-lineage) were assessed computationally based on the flow cytometry data and verified by morphology. Unipotent cells show the generation of only one lineage (>80% of one lineage), bipotent cells generate two lineages with approximately 50% each and multipotent cells generate a balanced output of all three lineages. R-scripts were used for computational analysis described by Bogeska et al., 2022. CD41 and EPCR fluorescence intensity values of HSC were assigned from the FACsort index data to the respective colony grown from the respective HSC.

Colony Forming Unit Assay

After erythrocyte lysis, 40,000 erythrocyte-lysed whole BM cells were seeded in semi-solid methylcellulose media (R&D Systems #HSC007, containing 100 µg/mL human transferrin, 200 µg/mL human insulin, 50 ng/mL human SCF, 10 ng/mL murine IL-3, 10 ng/mL murine IL-6 and human 5 IU/mL EPO) in three centimeter culture dishes in triplicates and cultivated for 12 to 14 days under normoxic conditions. Colonies were counted and their morphology assessed by two persons by light microscope (5x magnification) in a 2 x 2 cm area. Cell morphologies of the colonies were confirmed by isolating single colonies from the methylcellulose assays in cytospins (300 x g, 7 min) and May-Grünwald-Giemsa staining as well as by flow cytometry (Table 7).

Table 7 | Antibodies and reagents used to characterize CFU composition via FC.

Antibodies / Reagent	Conjugate	Con.	Source	Identifier
live / dead (DNA)	7-AAD	1:300	BioLegend	Cat# 420403
Anti-mouse CD11b (M1/70)	APC	1:100	BioLegend	Cat# 101212
Anti-mouse CD41 (MWReg30)	FITC	1:100	BioLegend	Cat# 13390
Anti-mouse Gr-1 (RB6-8C5)	eF450	1:100	eBioscience	Cat# 48-5931-82
Anti-mouse F4/80 (BM8)	PE	1:100	BioLegned	Cat# 123110

In vitro generation of megakaryocytes and analysis

Lin$^-$ BM cells were purified as described. To differentiate megakaryocytes *in vitro* from either transduced or non-transduced Lin$^-$ BM cells 50 ng/mL mTHPO or 50 ng/mL romiplostim were added to the SF medium (StemSpan SFEM) for up 3 weeks. Megakaryocyte differentiation 8 days after cultivation with mTHPO or romiplostim was analyzed by staining cells on cytospins (300 x g, 7 min, May-Grünwald Giemsa staining) and evaluating the morphology. Large and small megakaryocytes were enumerated per field of view from eight-to-nine slides (40x magnification). Megakaryocyte maturation was determined by the expression of cell surface markers (Table 8) and state of polyploidization after 3 weeks of cultivation. For this analysis cells were fixed and permeabilized with -20°C cold 100% ethanol overnight, washed two times and the amount of DNA was stained with propidium iodide (PI) solution (1 hour, 37°C) containing 50 µg/mL PI, 0.1 mg/mL RNase A, 0.05% Triton-X-100 in PBS.

Table 8 | Antibodies used to determine megakaryocyte differentiation and maturation.

Antibodies / Reagent	Conjugate	Con.	Source	Identifier
anti-mouse CD41 (MWReg30)	PE	1:100	BioLegend	Cat# 133906
anti-mouse CD42d (1C2)	APC	1:200	eBioscience	Cat# 17-0421-82

3.4. Animal experiments

All animal experiments were conducted according to the German Animal Welfare Act and were authorized by the local animal welfare committee (Hesse, Germany). Mice were kept specific pathogen-free in individually ventilated cages with food and water (ad libitum) in the animal facilities of the Paul-Ehrlich-Institute.

3.4.1. IAV infection, vaccination and antiviral treatment

Male and female BL/6J or BL/6N, mTmG, Mpl-KO, IL1R1-KO and IL-6-KO mice at an age of eight-to-twelve weeks were anesthetized and infected via intranasal application (30 µL) of IAV PR8. BL/6J or BL/6N were infected with increasing doses 1×10^2, 1×10^3 or $1x10^4$ $TCID_{50}$ of IAV PR8 in DMEM or DMEM without additives (vehicle, control group). One group of six week old BL/6J or BL/6N mice were immunized one time intramuscular with $1x10^6$ ffu of

VSV∗ΔG(NA_{H5N1}) replicon particles diluted in PBS (30 µL per injection). Four weeks after the immunization, animals were anesthetized and infected via intranasal application with $1x10^4$ $TCID_{50}$ IAV PR8 (30 µL in DMEM). Another group of eight-to-twelve week old BL/6J or BL/6N mice infected with $1x10^4$ $TCID_{50}$ IAV PR8 were treated with the neuraminidase inhibitor oseltamivir phosphate (Tamiflu®, Roche, PZN: 00890287) suspended in PBS via oral gavage at 100 mg/kg of body weight twice a day starting 2 hours before IAV challenge and continued for 5 days. IAV challenges in Mpl-KO, IL1R1-KO and IL-6-KO mice were performed with $1×10^4$ $TCID_{50}$ of IAV PR8. Infected mice were daily monitored in the morning according to a designed score sheet (ranging from category 1 (no symptoms) to 6 (severely moribund)) to evaluate clinical signs, differences in breathing, behavior, appearance, body weight and pain level. Infected mice were euthanized when three of five categories were assessed in category 3 of the score sheet, weight loss reached 20% for mice infected $1x10^4$ $TCID_{50}$ or 25% for mice infected with $1×10^3$ or $1×10^2$ $TCID_{50}$.

3.4.2. Blood sampling

Blood sampling was performed by retro-orbital puncture under isoflurane anesthesia. For final euthanasia EDTA-coated capillaries with a diameter of 1.3 mm (Sarstedt #19.447.001) were used. For regular bleeding (three-week break in between) sodium heparin-coated capillaries with a diameter 0.8 mm (minicaps® Hirschmann #9000205) were used and a maximum of 100 µL blood was drawn. Blood was collected in EDTA tubes for blood counts (Scil Vet ABC), in citrate or heparin tubes for platelet assays.

3.4.3. Bone marrow transplantation

Bone marrow transplantation (BMT) of transduced Lin marker-negative BM cells

Lin^- BM cells were isolated from BL/6J, Mpl-KO or mTmG reporter mice. Lin^- BM cells were 24 hours pre-stimulated / cultivated in SF StemSpan SFEM with 10 ng/mL mSCF, 20 ng/mL mTHPO, 20 ng/mL hIGF2, 10 ng/mL hFGF-1 (all PeproTech), 2 mM L-glutamine and 1% penicillin / streptomycin. Lin^- BM cells were transduced twice on the two following days with a defined multiplicity of infection (MOI) of the respective lentiviral vector (Table 1) on Retronectin® pre-coated wells (Takara, #T110A). Cell viability and transduction rates were determined by flow cytometry before transplantation. On day 4 after isolation, a minimum of $5x10^5$ cells/mouse were transplanted via tail vein injection (re-suspended in PBS, max. 150 µL) into lethally irradiated Mpl-KO CD45.1 mice (6 Gy, ^{137}Cs-γ rays, 0.036 γ/s., Gamma-Bestrahlungsanlage OB29/4, STS GmbH, Braunschweig) or BL/6J CD45.2 (7 Gy). $1x10^7$ fresh isolated whole BM cells were used for secondary transplantation of lethally irradiated Mpl-KO CD45.1 mice.

Bone marrow transplantation of FACsorted cells

MNCs isolated from BL/6J CD45.1 mice were stained for Lin markers and EPCR. 15,000 freshly FACsorted Lin^-EPCR^+ or $1.5x10^6$ Lin^-EPCR^- BM cells were transplanted via i.v. injection (re-suspended in PBS, max. 150 µL) without supporting bone marrow into lethally irradiated CD45.2/Ly5.2 (7 Gy) recipients. Whole BM cells from non-infected and IAV-infected ($1x10^4$ $TCID_{50}$ IAV PR8) where stained for Lin markers, c-Kit, CD150, CD34, CD48 and CD41. 1,500 FACsorted $CD41^+$ or $CD41^-$ $LKCD150^+CD34^-$ HSPCs from non-infected or IAV-infected mTmG reporter mice and $2.5x10^5$ supportive whole BM cells from BL/6J CD45.1 mice were transplanted via i.v. injection (re-suspended in PBS max. 150 µL) into lethally irradiated CD45.2/Ly5.2 (7 Gy) recipients. Transplanted mice were daily monitored for signs of adverse events for three weeks. Ciprofloxacin (20 mg/mL) was supplemented to the drinking water for two weeks. After three weeks, mice were monitored every 2 to 3 days and followed for at least 16 weeks post transplantation. Blood from transplanted mice was taken from the retro-orbital venous plexus. Blood counts were measured and the chimersim (either CD45.1, CD45.2 or dTomato expression) on leukocytes (white blood cells), lymphocytes (B and T cells), myeloid cells (granulocytes) and platelets (mTmG as donor) were analyzed (Table 9).

Table 9 | Antibodies used for analyzing the chimerism in the peripheral blood in transplanted recipient mice.

Antibodies / Reagent	Conjugate	Con.	Source	Identifier
anti-mouse CD11b (M1/70)	APC	1:100	BioLegend	Cat# 101212
anti-mouse Gr-1 (RB6-8C5)	eF450	1:100	eBioscience	Cat# 48-5931-82
anti-mouse CD3 (17A2)	eF450	1:100	eBioscience	Cat# 48-0032-82
anti-mouse B220 (RA3-6B2)	PerCP	1:100	BioLegend	Cat# 103234
anti-mouse CD45.1 (104)	BV605	1:100	BioLegend	Cat# 109841
anti-mouse CD41 (MWReg30)	FITC	1:1000	BioLegend	Cat# 133904

3.5. Analysis of primary murine cells from animal experiments

3.5.1. Bone marrow cells

From each mouse the BM cells were isolated from femora, tibia and coxae. For BM cell analysis of individual mice the cells were flushed with 1.5 mL SF Iscove's Modified Dulbecco's Medium (IMDM) without supplements using a 1 mL syringe fitted with a 23G cannula, centrifuged and the supernatant was frozen (-80°C) for cytokine determination (see 3.6). BM cell suspension was filtered through a 70 µm strainer (Corning or Miltenyi-Biotech) and erythrocytes were removed by red cell lysis (5 min, RT). BM cells were re-suspended in PBS EDTA with 2% FCS and cell numbers were determined with a hemocytometer with trypan blue staining. When applicable, the FC-receptor was blocked using an anti-mouse CD16/CD32 (1:100) unconjugated antibody prior surface staining.

Cell cycle analysis via Ki-67 and DNA amount

Cell cycle analysis was performed on BM cells freshly isolated from mice. BM cells were surface stained (Table 5) in PBS EDTA with 2% FCS, fixed (40 min, on ice; 1:4 dilution of the fixation/permeabilization concentrate (PFA based) in fixation/permeabilization diluent) and permeabilized (30 min, RT; 1x Permeabilization buffer (saponin based) in dH_20) using the Foxp3/transcription Factor Staining Buffer Set (eBioscience). Subsequently the proliferation marker Ki-67 (30 min, RT) and the amount of DNA (30 min, RT) were stained (Table 5). Cells were acquired with the Symphony A3 (BD Bioscience) flow cytometer.

3.5.2. Spleenocytes

Half of spleen was put through a 70 µm cell strainer and rinsed three times with PBS EDTA 2% FCS. Erythrocytes were removed (5 min, RT) by red cell lysis buffer. Spleenocytes isolated from transplanted mice (Publication 1) were stained for the presences of HSPCs (Table 10). Spleenocytes and BM cells from non-infected and IAV-infected mice (Publication 3) were stained for emerging IAV specific CD4 or CD8 T cells (Table 10). IAV specific T cells were identified by staining the surface presentation of the nucleoprotein (NP) of IAV on MHC class I CD4 and MHC class II CD8 by specific tetramers, following the manufactures' protocol (MBL).

Table 10 | Antibodies and reagents used to identify HSPCs and IAV specific T cells isolated from the spleen.

Antibodies / Reagent	Conjugate	Con.	Source	Identifier
Cells isolated from spleen from transplanted mice				
live / dead (DNA)	DAPI	1:1000	Sigma-Aldrich	Cat# D9542
Lineage marker panel anti-mouse TER-119 (Ter-119) anti-mouse CD11b (M1/70) anti-mouse Ly-6G/Ly-6C (RB6-8C5) anti-mouse CD3ε (17A2) anti-mouse CD45R/B220 (RA3-6B2)	Pacific Blue	1:10	BioLegend	Cat# 133310
anti-mouse c-Kit (2B8)	APC	1:100	eBioscience	Cat# 17-1171-83
anti-mouse Sca-1 (D7)	PerCP-Cy5.5	1:100	eBioscience	Cat# 45-5981-82
anti-mouse CD150 (TC15-12F12.2)	PE-Cy7	1:100	BioLegend	Cat# 115914
anti-mouse CD48 (HM48-1)	APC-Cy7	1:50	BioLegend	Cat# 103432
anti-mouse EPCR (eBio1560)	PE	1:100	eBioscience	Cat# 12-2012-82
IAV specific CD8 T cells				
anti-mouse CD3 (17A2)	eF450	1:100	eBioscience	Cat# 48-0032-82
anti-mouse CD8 (KT15)	FITC	1:100	Invitrogen	Cat# MA5-16759
H2Db Influenza NP Tetramer (ASNENMETM)	APC	1:20	MBL	Cat# TB-M508-2
IAV specific CD4 T cells				
anti-mouse CD3 (17A2)	eF450	1:100	eBioscience	Cat# 48-0032-82
anti-mouse CD4 (RM4-5)	APC	1:100	BioLegend	Cat# 100516
H2-IAb Influenza NP Tetramer (QVYSLIRPNENPAHK)	PE	1:10	MBL	Cat# TS-M716-1

3.5.3. Lung cells

Bronchoalveolar lavage

To study cells in the bronchiolar-alveolar space of non-infected and IAV-infected mice bronchoalveolar lavage was performed from sacrificed mice. A flexible 22G cannula (BD Insyte, #381223) was inserted into the trachea and fixed through strings. Cells from three lavages of one mouse were combined by injecting and aspirating 1 mL PBS-EDTA each round. Cells were washed and erythrocyte lysed (5 min, RT). Fc-receptor blocked cells were stained for platelet – leukocyte interaction (Table 11).

Table 11 | Antibodies used for detection of platelet-leukocyte interaction in the alveolar space.

Antibodies / Reagent	Conjugate	Con.	Source	Identifier
anti-mouse CD45 (30-F11)	FITC	1:100	BioLegend	Cat# 103108
anti-mouse CD41 (MWReg30)	PerCP-Cy5.5	1:100	BioLegend	Cat# 133918
anti-mouse F4/80 (BM8)	PE	1:100	BioLegend	Cat# 123110
anti-mouse CD11b (M1/70)	APC	1:100	BioLegend	Cat# 101212
anti-mouse Gr-1 (RB6-8C5)	eF450	1:100	eBioscience	Cat# 48-5931-82
anti-mouse MHCII (M5/11.4.15.2)	APC-Cy7	1:100	BioLegend	Cat# 107627
anti-mouse CD3 (145-2C11)	BV510	1:100	BD Bioscience	Cat# 563024
anti-mouse CD19 (6D5)	PE-Cy7	1:100	BioLegend	Cat# 115519

Digested lung samples

The whole lung was transferred into a cell culture dish and rinsed with PBS. The cleaned lung was cut into small pieces with a scissor in a 15 mL centrifugation tube with Hank's buffered saline supplemented with 4 mg/mL Dispase II (Sigma-Aldrich, # D4693). Lungs pieces were incubated for 1 hour at 37°C and regularly inverted. Lung tissue was disrupted by forced pipetting, homogenized by smashing on a 100 µm cell strainer with a syringe stamp. The strainer was rinsed with PBS EDTA with 2% FCS. Isolated cells were erythrocyte lysed and stained for HSPCs and megakaryocytic cells (Table 12).

Table 12 | Antibodies and reagents for identification of HSPCs and megakaryocytic cells in murine lung tissue.

Antibodies / Reagent	Conjugate	Con.	Source	Identifier
live / dead (DNA)	DAPI	1:1000	Sigma-Aldrich	Cat# D9542
anti-mouse CD45 (30-F11)	FITC	1:100	BioLegend	Cat# 103108
Lineage marker panel	Pacific Blue	1:20	BioLegend	Cat# 133310
anti-mouse c-Kit (2B8)	APC	1:100	eBioscience	Cat# 17-1171-83
anti-mouse Sca-1 (D7)	BV510	1:100	BioLegend	Cat# 108129
anti-mouse CD41 (MWReg30)	PerCP-Cy5.5	1:100	BioLegend	Cat# 133918
anti-mouse MHCII (M5/11.4.15.2)	APC-Cy7	1:100	BioLegend	Cat# 107627
anti-mouse Mpl (AMM2)	Biotin	1:100	IBL America	Cat# 10403
anti-mouse CD42b (Xia.G5)	PE	1:100	Emfret Analytics	Cat# M040-2
Streptavidin	PE-Cy7	1:100	BD Bioscience	Cat# 25-4317-82

3.5.4. Platelets

Activation Assay

100 µL blood was collected by retro-orbital bleeding from mice in 300 µL heparin in PBS (25 U/mL) or citrate tubes (Sarstedt). Blood cells were washed three-times and centrifuged in Tyrode's buffer (20x Tyrode's buffer, 1.0 mM $MgCl_2$, 0.1% glucose, 0.36% bovine serum albumin in dH_2O) without calcium. Equal amounts of washed platelets were treated for 10 min at 37°C and 10 min RT in Tyrode's buffer with calcium by adding either thrombin (0.01 U/mL, Sigma-Aldrich, #T4648), collagen-related peptide (CRP, 10 µg/mL, kindly provided by the Nieswandt Lab), ADP (10 µM, Sigma-Aldrich #A2754) or thromboxane analogue U46619 (3 µM, Tocris, #1932). Ice-cold 4% PFA in Tyrode's buffer without calcium was used to stop the activation. Platelet activation was determined by detecting P-selectin on the platelet cell surface via flow cytometry (Table 13).

Table 13 | Antibodies used to determine activation of platelets.

Antibodies / Reagent	Conjugate	Con.	Source	Identifier
anti-mouse CD41 (MWReg30)	PE	1:500	BioLegend	Cat# 133906
anti-mouse CD62P (Psel.KO2.3)	APC	1:500	eBioscience	Cat# 12-0626-82

Spreading Assay

The centers of the glass coverslips (13 mm diameter) were coated over night at 4°C with 100 µg/mL fibrinogen (VerSeal®, Grifols, PZN16528401) and blocked the next day for 1 hour at 37°C with PBS 1% BSA in a 24-well plate. From heparin-sampled blood washed platelets were isolated by centrifugation at room temperature at 150 x g for 10 to 15 min in Tyrode's buffer with calcium. Evaluation of washed platelet purity and number were determined via flow cytometry by staining with an anti-mouse CD41-PE antibody (1:1000; 15 min, RT). Washed platelets were used for the spreading assay when a purity of >98% was achieved. For one coverslip at least $5x10^6$ washed platelets were treated 10 min at 37°C with thrombin (0.01 U/mL) and incubated on the coated coverslips for different time points (5, 10 and 30 min). To remove non-spread/non-adherent platelets, the coverslips were directly washed three times with PBS and fixed with PBS 4% PFA (20 min, RT). To detect the spread platelets, platelets were stained with anti-mouse CD41-FITC antibodies (1:100, overnight, 4°C). Platelets were visualized and acquired using a 63x immersion oil objective and a confocal microscope (Leica SP8). Four to five images of one condition were analyzed for platelet spreading stages by two persons. Four spreading stages were defined by the morphological appearance of the platelet: stadium I = round resting, stadium II = filopodia, stadium III = mixture of filopodia and lamellipodia and stadium IV = lamellipodia (round flat).

Maturation, sialylation and viability

Platelets in EDTA-sampled blood were washed two times with Tyrode's buffer without calcium (800 x g, 5 min, RT). Equal amount of platelets were stained 30 min individually for platelet adhesive receptors (Table 14).

Table 14 | Antibodies used for staining platelet adherent receptors.

Antibodies / Reagent	Conjugate	Con.	Source	Identifier
anti-mouse CD41 (MWReg30)	PerCP Cy5.5	1:500	BioLegend	Cat# 133918
anti-mouse CD42a/GIX (Xia.B4)	FITC	1:100	Emfret Analytics	Cat# M051-1
anti-mouse CD42b/GPIbα (Xia.G5)	PE	1:100	Emfret Analytics	Cat# M040-2
anti-mouse CD42c/GPIbβ (Xia.C3)	FITC	1:100	Emfret Analytics	Cat# M050-1
anti-mouse CD42d/GPV (1C2)	APC	1:200	eBioscience	Cat# 17-0421-82
anti-mouse CD49b (DX5)	APC	1:200	eBioscience	Cat# 17-5971-63
Anti-mouse CD41/CD61 (Leo.F2)	PE	1:100	Emfret Analytics	Cat# M025-2

Platelet sialylation status was determined via the binding of Ricinus Communis agglutinin I (RCA I - FITC, 0.5 µg/mL, ThermoFisher #L32477, 20 min RT). Platelets treated with neuraminidase (NA, 0.3 U/mL, 30 min, RT) were used a positive control for RCA I binding. The metabolization of calcein-violet AM (100 nM, 30 min, 37°C, Biolegend, Cat#425203) was used as a viability marker for platelets.

3.6. Cytokine multiplex ELISA

Cytokine concentrations were determined in blood serum and bone marrow that was stored at -80°C. Preparation of the bone marrow supernatant is described in 3.5.1 in a maximum of 1.5 mL. Blood serum was generated by collecting blood in Z-serum tubes with clotting activators (Sarstedt, #41.1500.005) and harvested after centrifugation (13,000 x g, 4°C). The multiplex cytokine assay ProcartaPlex (Invitrogen, ThermoFisher) was custom made. The cytokines to be measured were selected based on cytokines identified and reported to activate HSCs, the experimental verification of the expression of the respective cytokine receptors or cytokines reported to be upregulated during IAV infection. 18 cytokines were analyzed (IFN-α, IFN-γ, IL-1α, IL-1β, IL-2, IL-3, IL-4, IL-5, IL-6, IL-7, IL-9, IL-10, IL-12p70, IL-13, IL-15, IL-17a, IP-10 and TNF-α) and the assay was performed according to the manufactures' protocol. The standard curve for each single cytokine was calculated by a four-fitting curve with the ProcartaPlex Analysis App. The THPO cytokine ELISA (R&D Systems, #MTP00) was performed from serum and bone marrow according the manufactures' protocol.

3.7. Histology

3.7.1. Paraffin-embedded sections

The organs of mice were fixed in 4% fresh buffered formalin (Sigma-Aldrich) or 4% fresh buffered paraformaldehyde (PFA, Carl Roth) for a minimum 24 hours at 4°C before paraffin embedding. The sternum was decalcified for 24 hours prior embedding. Dependent of the organ 1-to-2 µm sections were cut and hematoxylin / eosin stained for counting MKs in the BM and histopathological assessment. MKs in the BM were counted by two persons in minimum of 8 field of views using a light microscope and a 40x objective. Lung sections were subjected to histopathological analysis and were scored for pathologies from absent = 0, mild = 1, moderate = 2 and severe = 3. Following pathologies were assessed: inflammation, endothelial damage and structural damage (for details see Publication 3 Star Methods – Histology and electron microscopy'). Endothelial cells and platelets in lung paraffin sections were identified by a primary rabbit anti-human polyclonal antibody against von Willebrand factor (1:250, Agilent / Dako) and secondary polyclonal donkey anti-rabbit IgG HRP (1:1000, GE Healthcare). Von Willebrand factor positive (brown deposits) cells were visualized by the exposure of 3,3'-diaminobenzidin substrate (DAB, ThermoFisher). Lung sections were counter stained with hematoxylin and analyzed by two persons with a light microscope (Leica DM RBE).

3.7.2. Ultrathin sections for electron microscopy

Lung tissue of non-infected and IAV-infected mice were cut in ~1x1 cm small cubes and fixed in PBS 2.5% glutaraldehyde overnight at 4°C. Ultrathin sections were prepared according Publication 3 'Star Methods – Histology and electron microscopy'. Two to three ultrathin sections of two to three lung cubes were analyzed and imaged.

3.8. RNA-sequencing and gene expression analysis

RNA-sequencing (RNA-seq) was performed from FACsorted BM cells from non-infected (pooled from three mice / sample) and IAV-infected ($1x10^4$ $TCID_{50}$) C57BL/6J (one mouse / sample) mice. $CD41^+$ or $CD41^-$ LK $CD150^+CD34^-$ cells were directly sorted into 1.5 mL tubes with RNAzol and total RNA was purified with the Direct-zol RNA Microprep Kit (Zymo Research). The preparation of the RNA-Seq library was performed according a modified version of the NNSR priming method (Levin et al., 2010). The processing and bioinformatic analyses is described in detail in the Publication 3 'Star Methods' 'Next generation sequencing (RNA-sequencing)' and 'Bioinformatic analysis'. Gene expression data were analyzed with Microsoft Excel or gene enrichment analysis (GSEA) and visualized in Venn diagrams, volcano blots, or heatmaps using either BioVenn, GraphPad Prism or Morphosys. Gene ontology analysis was performed using ToppGene Suite-ToppFun.

3.9. Quantitative and statistical analysis

If not indicated otherwise data are represented as mean ± standard deviation (SD). Biological replicates ($n \geq 3$) and technical replicates are indicated in the respective figure legends of each publication. Flow cytometry data were analyzed with FlowJo (BD Bioscience). Statistical analysis was conducted using GraphPad Prism. Statistical testing between the mean of two groups, the two-tailed unpaired Student's t test with Welch correction, the comparison of the mean of three or more groups within an experimental group the one-way analysis of variation (ANOVA) with Dunnett's multiple comparison test and for comparison of the mean of three or more groups between the experimental groups two two-way ANOVA with Sidak's multiple comparison was used. Statistical significances are indicated in the respective figure and figure legends of each publication.

4. Results (publications)

Publication 1: Endothelial protein C receptor supports hematopoietic stem cell engraftment and expansion in Mpl-deficient mice

Kohlscheen S[1], Schenk F[1], **Rommel MGE**[1], Cullmann K[1] and Modlich U[1]

1 *Research Group Gene Modification in Stem Cells, Division of Veterinary Medicine, Paul-Ehrlich-Institute, Langen, Germany*

Journal: Blood

Date: 2019 Mar 28

Type: Research article

DOI: 10.1182/blood-2018-03-837344

PMID: 30683655

Original publication including the supplement see **Appendix 1**

Graphical Summary

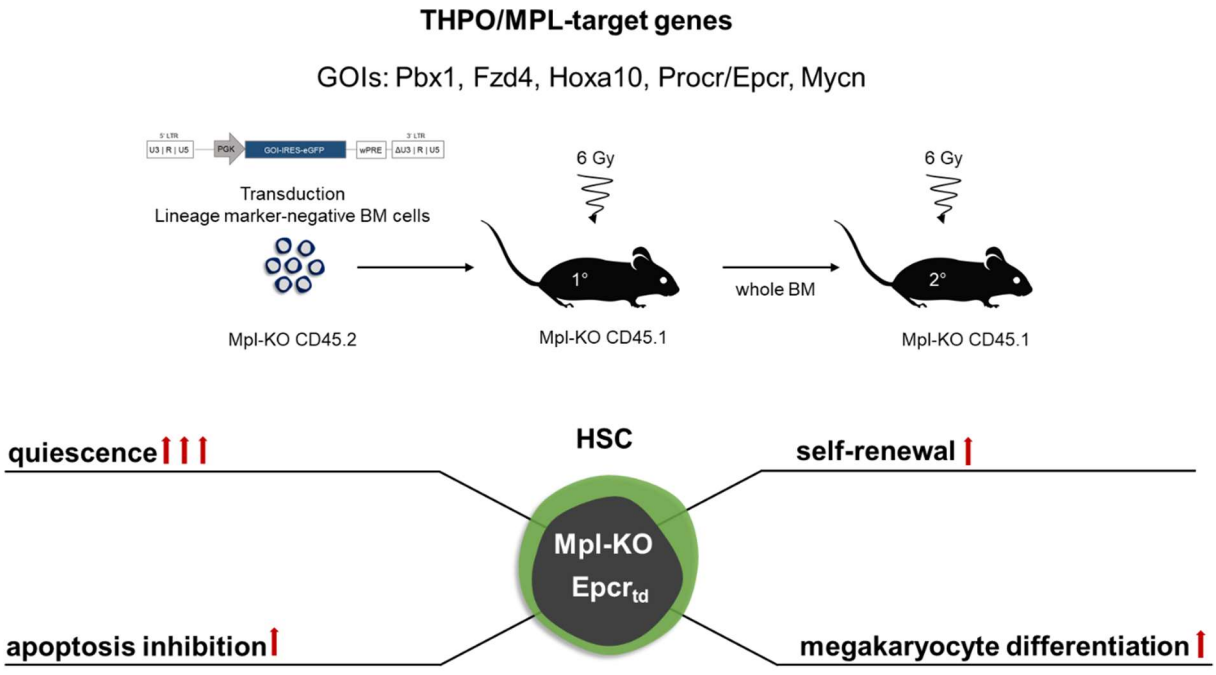

Figure 5 | Graphical summary publication 1.

Summary

Self-renewal and multipotency of HSCs are controlled by extrinsic and intrinsic factors. The thrombopoietin (THPO) receptor MPL is exclusively expressed on HSCs and the megakaryocytic/platelet lineage. THPO/MPL-signaling is essential for HSC quiescence during steady-state hematopoiesis as well as for expanding HSCs under stress conditions like serial transplantations. Furthermore, THPO/MPL-signaling is crucial for megakaryocyte lineage commitment. It remains elusive, how these opposing outcomes are controlled by the same cytokine/receptor signaling. In a previous study, our group identified Thpo target genes from DNA-microarray experiments in two models (1) Mpl-regenerated Mpl-deficient (Mpl-KO) HSCs and (2) wild-type HSCs inhibited for Mpl-signaling with a truncated dominant-negative MPL mutant. Amongst them the endothelial protein C receptor (*Procr*, EPCR/CD201), pre-B cell leukemia homeobox 1 (*Pbx1*), the Wnt receptor frizzled 5 (*Fzd4*), neuroblastoma-derived homolog Myc (*Mycn*) and homeobox A10 (*Hoxa10*) were found to upregulated in Mpl-regenerated Mpl-KO cells and downregulated in LSK cells from Mpl-KO or Thpo-deficient (Thpo-KO) mice, or mice with inhibited Mpl signaling compared to wild-type mice.

The five gene candidates were lentivirally overexpressed in Lin^- BM cells from Mpl-KO CD45.2 mice and transplanted into Mpl-KO CD45.1 recipient mice to rescue the Mpl-deficient phenotype. EPCR overexpression (Mpl-KO $Epcr_{td}$) expanded the number of phenotypic Mpl-KO LT-HSCs (9-fold, LSK $CD34^-CD135^-$ or 22-fold, LSK $CD150^+CD48^-$) compared to Mpl-KO cells overexpressing GFP, Pbx1, Fzd4, Hoxa10 or Mycn in primary recipients. This expansion rate was similar to wild-type (wt) Lin^- BM cells transplanted into Mpl-KO mice. Mpl-KO $EPCR_{td}$ HSC were able to engraft in secondary recipients and expanded phenotypic HSCs (4-fold, LSK $CD150^+CD48^-$). Phenotypic HSC expansion by EPCR correlated with upregulated expression of the anti-apoptotic gene Bcl-xL (3-fold) and a quiescent cell cycle profile. Mpl-KO $EPCR_{td}$ cells not only efficiently homed to the BM after 4 weeks post transplantation, they also established HSC (LSK $CD150^+CD48^-$) quiescence faster (Mpl-KO $EPCR_{td}$ G0 40%) compared to the negative control (Mpl-KO GFP_{td} G0 15%). In line with that, transplantation of FACsorted Lin^-EPCR^+ wt BM cells were superior in repopulation and engraftment potential in contrast to Lin^-EPCR^- wt BM cells. Besides restoring HSC functionality in Mpl-KO HSCs, EPCR overexpression in Mpl-KO cells rescued megakaryocyte numbers in the BM. However, this did not improve platelet counts in the peripheral blood. *In vitro* culture of FACsorted LSK cells with THPO maintained and supported the expression of EPCR, while in the absence of THPO EPCR-expression declined rapidly.

Author contributions

Saskia Kohlscheen constructed, produced and titrated lentiviral vectors; S.K. isolated and transduced Lin^- BM cells, performed the BM transplantation experiments and characterized the mice for chimerism and cellular composition in the peripheral blood, HSPCs and their cell cycle status in the BM and HSPCs in the spleen via flow cytometry; S.K. prepared and analyzed organs for histology; enumerated megakaryocytes in BM sections together with M.G.E.R.; S.K. FACsorted LSK cells, CMPs, GMPs and MEPs for RNA-isolation and qPCR; FACsorted Lin^- $EPCR^+$ and $EPCR^-$ BM cells for transplantation experiments and characterized mice chimerism and cellular composition in peripheral blood, HSPCs and their cell cycle status in the BM and HSPCs in the spleen via flow cytometry; S.K. FACsorted LSK cells for the *in vitro* stimulation experiments and analyzed EPCR expression via flow cytometry; S.K. analyzed and visualized data, and wrote the manuscript.

Franziska Schenk produced and titrated lentiviral vectors, contributed to the mouse transplantation experiments, and performed RNA-isolation and qPCR experiments.

Marcel G. E. Rommel produced and titrated lentiviral vectors, assisted in mouse transplantation experiments; M.G.E.R. assisted and performed a part of the characterization of transplanted mice for chimerism and cellular composition in the peripheral blood, HSPCs and their cell cycle status in the BM and HSPCs in the spleen via flow cytometry; M.G.E.R. FACsorted cells for transplantation and *in vitro* stimulation experiments and analyzed EPCR expression via flow cytometry; M.G.E.R. analyzed and visualized data, worte, proofread and discussed the manuscript

Katharina Cullmann isolated Lin^- BM cells and supported mouse transplantation experiments.

Ute Modlich developed the concept of the study, designed and supervised the experiments, critically evaluated data and wrote the manuscript

Contribution to Figures

Figure 1A S.K., 1B **M.G.E.R.**

Figure 2A S.K., 2B-C S.K. and **M.G.E.R.**

Figure 3A-G S.K.

Figure 4A-H S.K.

Figure 5A-C S.K., 5D-F S.K. and **M.G.E.R.**

Figure 6A-F S.K. and **M.G.E.R.**, 5G S.K.

Figure 7A-D S.K. and **M.G.E.R.**, 7E **M.G.E.R.**

Supplemental Data S.K.

Graphical Abstract **M.G.E.R.**

Publication 2: Signaling properties of murine MPL and MPL mutants after stimulation with thrombopoietin and romiplostim

Marcel G E Rommel[1], Keven Hoerster[1,2], Christian Milde[1], Franziska Schenk[1], Luise Roser[1], Saskia Kohlscheen[1,3], Niels Heinz[1,4] and Ute Modlich[1]

1 *Research Group Gene Modification in Stem Cells, Division of Veterinary Medicine, Paul-Ehrlich-Institute, Langen, Germany;*

2 *Institute for Transfusion Medicine, University Hospital Essen, University of Duisburg-Essen, Essen, Germany;*

3 *Current address: Department II of Internal Medicine, University Hospital of Schleswig-Holstein, Kiel, Germany;*

4 *Current address: BioNTech IMFS GmbH, Idar-Oberstein, Germany*

Journal: Experimental Hematology

Date: 2020 May

Type: Research article

DOI: 10.1016/j.exphem.2020.04.006

PMID: 32417303

Original publication including the supplement see **Appendix 2**

Graphical summary

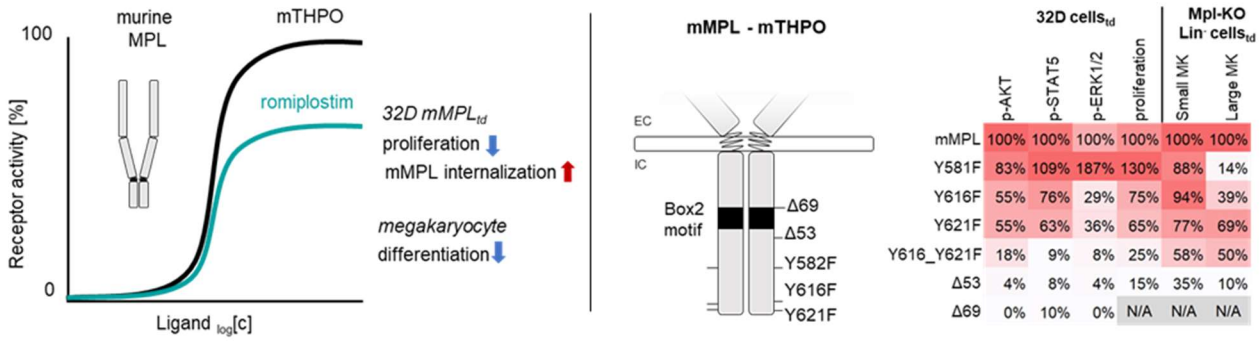

Figure 6 | Graphical summary publication 2.

Summary

The hematopoietic cytokine thrombopoietin (THPO) and its receptor myeloproliferative leukemia oncogene (MPL/THPO-R) are key regulators of HSC maintenance and megakaryocyte differentiation. THPO/MPL dysfunction contributes to hematological disorders in patients. Loss-of-function is associated with thrombocytopenias, bone marrow failure and aplastic anemias, while the gain-of-function causes myeloproliferative disorders. Treating thrombocytopenia with recombinant human (rh) THPO failed due to the development of rhTHPO specific antibodies and antibodies directed against the endogenous THPO. Modern human (h) THPO mimetics like the peptibody romiplostim or the small-molecule eltrombopag proved their efficacy in the treatment of immune thrombocytopenia. Romiplostim is further used in mouse models although it was specifically selected against the human MPL.

Signal transduction activity of romiplostim, murine (m) and hTHPO in the IL-3-dependent murine 32D cell line lentivirally overexpressing the mMPL or hMPL were conducted. Romiplostim induced mMPL activation leads to balanced phosphorylation of AKT, ERK1/2 and STAT5. However, phosphorylation intensity at high romiplostim concentrations was four- to five-fold reduced compared to phosphorylation after mTHPO-induced mMPL activation. In line with this, mMPL was faster internalized after binding romiplostim at high concentrations compared to mTHPO. Romiplostim was less potent in promoting murine megakaryocyte differentiation, proliferation and maturation compared to mTHPO. There was no difference in signaling capacity, internalization and proliferation rate after activation of the hMPL with romiplostim or hTHPO.

I mutated the intracellular domain of mMPL to determine whether different signaling pathways were linked to specific tyrosine residues. Lentiviral vectors expressing mMPL with tyrosine (Y) to phenylalanine (F) substitution at positions 582, 616 and 621, combined substations at positions 616 + 621, as well as truncated receptors lacking 53 and 69 amino acids from the C-terminal intracellular moiety were generated. Signal transduction of mMPL-mutants after activation with mTHPO and romiplostim was assessed in lentivirally transduced 32D cells. AKT and ERK1/2 phosphorylation was profoundly reduced in mMPL-Y616F and mMPL-Y621F expressing 32D cells after stimulation with mTHPO or romiplostim. Mutation at the position 582 increased in ERK1/2 phosphorylation upon activation and was accompanied by elevated base-line activation, resulting in THPO, romiplostim and IL-3-independent proliferation. Mpl-KO Lin^- BM cells transduced with mMPL-Y582F did not generate mature megakaryocytes, while mMPL-Y616F and mMPLY621F partly corrected megakaryopoiesis *in vitro*.

Author contributions

Marcel G. E. Rommel produced, titrated lentiviral vectors (murine Mpl and murine Mpl mutants) and transduced 32D cells; M.G.E.R. FACsorted lentivirally transduced 32D cells and performed signaling transduction assays via phosflow and Western blot; M.G.E.R. performed signaling transduction assays of transduced 32D cells with ERK, MEK, JAK2 and PI3K small molecule inhibitors via flow cytometry; M.G.E.R. performed receptor internalization, proliferation, viability and cell trace assays of transduced 32D cells; M.G.E.R. isolated, transduced Lin^- BM cells, differentiated megakaryocytes from Lin^- BM cells *in vitro* and analyzed morphology of *in vitro* MKs via cytospins and maturation markers and polyploidy via flow cytometry; M.G.E.R. analyzed and visualized data, and wrote the manuscript.

Keven Hörster constructed, produced and titrated lentiviral vectors (murine Mpl and murine Mpl mutants) and transduced 32D cells; K.H. performed initial signaling transduction assays via phosflow and Western blot analysis; K.H. isolated and transduced Lin^- BM cells and differentiated megakaryocytes from Lin^- BM cells *in vitro*; K.H. contributed morphological analysis from *in vitro* differentiated megakaryocytes via cytospins; K.H. analyzed and visualized data, proofread and discussed the manuscript.

Christian Milde produced, titrated lentiviral vectors (human Mpl), transduced 32D cells (human Mpl) and assisted M.G.E.R. in signaling transduction analysis via phosflow (human MPL studies).

Franziska Schenk produced, titrated lentiviral vectors (murine Mpl and Mpl mutants) and differentiated megakaryocytes Lin^- BM cells *in vitro*; F.S. contributed to cytopsins from *in vitro* differentiated megakaryocytes and characterized polyploidy of *in vitro* differentiated MKs via flow cytometry.

Luise Roser performed together with M.G.E.R. stimulation experiments of lentivirally transduced 32D for Western Blot analysis.

Saskia Kohlscheen supervised and assisted Keven Hörster in lentiviral vector construction and established phosflow protocol. S.K. designed and supervised the experiments, proofread and discussed the manuscript.

Niels Heinz designed, constructed lentiviral vectors for the expression of MPL mutants, and proofread and discussed the manuscript.

Ute Modlich developed the concept of the study, designed and supervised the experiments, critically evaluated data and wrote the manuscript.

Contribution to Figures

Figure 1 **M.G.E.R.**

Figure 2 **M.G.E.R.**

Figure 3 **M.G.E.R.**

Figure 4A-C **M.G.E.R.**, 4D L.R.

Figure 5A-D K.H. and **M.G.E.R.**

Figure 6 **M.G.E.R.**

Supplemental Data **M.G.E.R.**

Publication 3: Influenza A Virus Infection Instructs Hematopoiesis to Megakaryocyte-lineage Output

Marcel G. E. Rommel[1], Lisa Walz[2,10], Foteini Fotopoulou[3,4,5], Saskia Kohlscheen[1,11], Franziska Schenk[1], Csaba Miskey[6], Lacramioara Botezatu[6], Yvonne Krebs[2], Iris M. Voelker[7], Kevin Wittwer[2], Tim Holland-Letz[8], Zoltán Ivics[6], Veronika von Messling[2,12], Marieke A. G. Essers [4,9], Michael D. Milsom[3,4], Christian K. Pfaller[2] and Ute Modlich[1,13]

1 *Research Group Gene Modification in Stem Cells, Division of Veterinary Medicine, Paul-Ehrlich-Institute, 63225 Langen, Germany*

2 *Research Group Pathogenesis of Respiratory Viruses, Division Veterinary Medicine, Paul-Ehrlich-Institute, 63225 Langen, Germany*

3 *Division of Experimental Hematology, German Cancer Research Center (DKFZ), 69120 Heidelberg, Germany*

4 *Heidelberg Institute for Stem Cell Technology and Experimental Medicine (HI-STEM), 69120 Heidelberg, Germany*

5 *Faculty of Biosciences, University of Heidelberg, 69120 Heidelberg, Germany*

6 *Research Group Transposition and Genome Engineering, Division of Medical Biotechnology, Paul-Ehrlich-Institute, 63225 Langen, Germany*

7 *Molecular Biotechnology and Gene Therapy, Paul-Ehrlich-Institute, 63225 Langen, Germany*

8 *Division of Biostatistics, German Cancer Research Center (DKFZ), 69120 Heidelberg, Germany*

9 *Division of Inflammatory Stress in Stem Cells, German Cancer Research Center (DKFZ), 69120 Heidelberg, Germany*

10 *Current address: CureVac AG, 60325 Frankfurt am Main, Germany*

11 *Current address: Department II of Internal Medicine, University Hospital of Schleswig-Holstein, 24105 Kiel, Germany*

12 *Current address: Life Science Division, German Federal Ministry of Education and Research, 10117 Berlin, Germany*

13 *Faculty of Medicine, Goethe University Frankfurt am Main, 60590 Frankfurt am Main, Germany*

Journal: Cell Reports

Date: 2022 Oct 4

Type: Research article

DOI: 10.1016/j.celrep.2022.111447

PMID: 36198277

Original publication including the supplement see **Appendix 3**

Graphical Summary

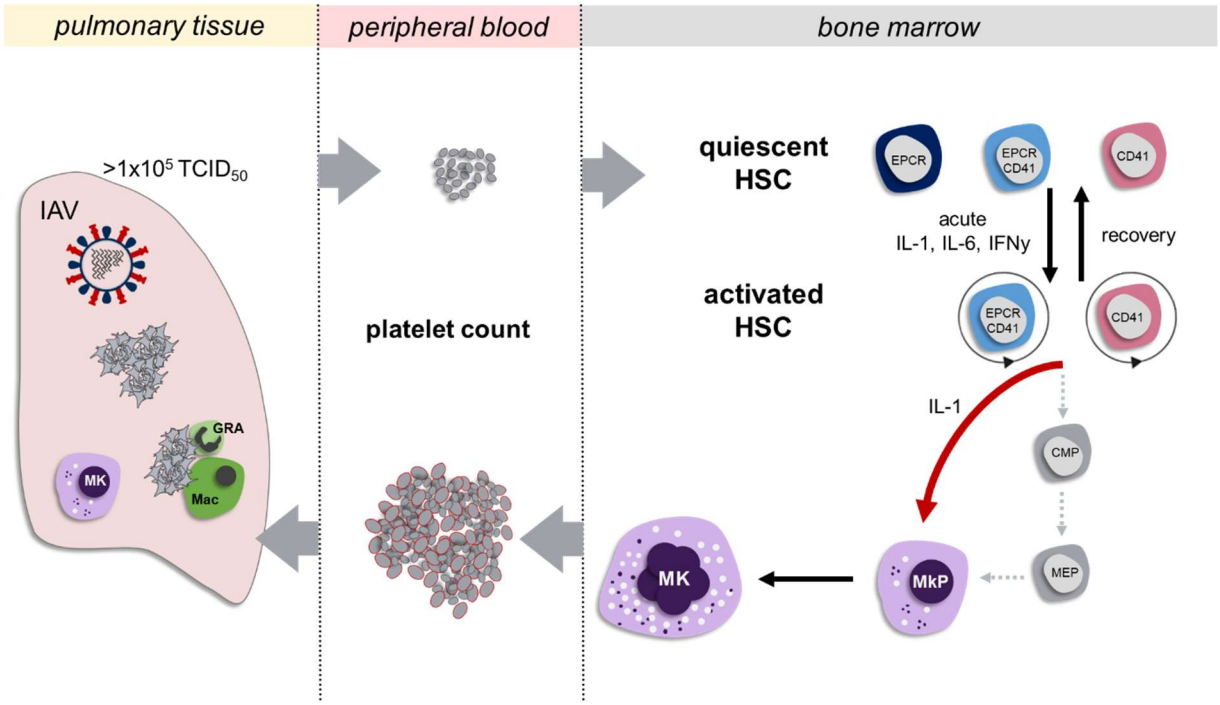

Figure 7 | Graphical summary publication 3.

Summary

Megakaryopoiesis describes the stepwise differentiation of megakaryocytes (MKs) from hematopoietic stem and progenitor cells (HSPCs) through discrete progenitor populations mostly guided by the THPO/MPL signaling axis. Rapid platelet production in response to thrombocytopenic events during inflammation implies MK generation via a different route, called emergency megakaryopoiesis. Heavily alternating platelet counts in patients are a predictive marker for severe respiratory infections, amongst them influenza.

I infected wild-type (wt) mice with increasing doses of influenza A virus (IAV) and observed similar to hospitalized patients, that platelets were promptly consumed, followed by a rapid and excessive rise of platelets (>1700x10^3/µl) with larger size. Simultaneously to platelet alternation in the blood, the number of mature MKs in the BM of IAV-infected mice was affected. Furthermore, von Willebrand factor positive deposits in the pulmonary capillaries of IAV-infected mice were identified, which were confirmed as accumulated and aggregated platelets in ultra-thin electron microscopic sections. Moreover, the presence of lung MKs amplified during IAV-infection. Platelet and MK recovery was preceded by cell cycle activation of $CD41^+$HSCs in IAV-infected mice, while $CD41^-EPCR^+$HSPCs kept quiescent. Neuraminidase inhibitor treatment with oseltamivir or immunization with a mismatch vaccine expressing the neuraminidase from a heterologous IAV H1N5 did not prevent platelet consumption and HSC activation after IAV infection. However, HSCs in vaccinated mice

reestablished quiescence faster. Loss of HSC quiescence negatively correlated with IAV titers determined in the lung tissue and at a viral threshold of $1x10^5$ $TCID_{50}$/g can be determined, irrespective of antiviral treatment, vaccination or initial IAV dose. Global bulk transcriptome analysis of $CD41^+$ HSPCs from IAV-infected mice exhibited a profile of favored megakaryocyte over erythroid development and positive enrichment for interleukin 1 receptor 1 (IL1R1) signaling. *In vitro* single-cell lineage tracing experiments proved that phenotypic $CD41^+$HSCs were the source of megakaryocytes. Transplantation of $CD41^+$HSPCs from infected wt mice established a high platelet chimerism and count in recipient mice faster in contrast to $CD41^+$HSPCs from non-infected mice. This proves the existence of emergency megakaryopoiesis during IAV infection. Platelets produced by emergency megakaryopoiesis 4 and 5 days post infection were hyper-reactive in activation and spreading assays, and exhibited an immature phenotype. Platelet consumption and fast reproduction were also observed in IAV-infected IL-6-KO and Mpl-KO mice. CD41 expression on HSPCs and MK progenitors rose rapidly in IAV-infected Mpl-KO and IL-6-KO mice, however, not in IAV-infected IL1R1-KO mice. In these mice, also thrombocytosis and hyper-reactive platelets were absent. In line with that, IAV-infected IL-1R1-KO mice exhibited a very weak correlation between viral load in the lung and loss of quiescence in CD41-expressing HSCs.

Author contribution

Marcel G. E. Rommel performed IAV infections, immunization and oseltamivir treatment of mice, blood sampling, bronchoalveolar lavage; M.G.E.R. performed mouse transplantation experiments, isolated BM cells and analyzed HSPC contribution, cell cycle, IAV specific T cells via flow cytometry; M.G.E.R. FACsorted HSPCs for mouse transplantation experiments and RNA-sequencing; M.G.E.R. FACsorted HSCs and MPPs for *in vitro* BrdU labeling and analyzed cell cycle and label incorporation via flow cytometry; isolated blood cells and analyzed chimerism via flow cytometry; M.G.E.R. performed colony forming unit assays from whole BM and analyzation of colonies together with L.B.; M.G.E.R. isolated spleenocytes and analyzed IAV specific T cells via flow cytometry; isolated lung cells from BAL and digested whole lungs and analyzed platelets, platelet-leukocyte interactions, lung megakaryocytes and HSPCs via flow cytometry and cytospins; M.G.E.R. isolated platelets for *in vitro* platelet assays (platelet activation, viability, sialyation [all analyzed via flow cytometry] and spreading assays [analyzed via confocal imaging]); assisted F.F in preparation of Lin^- BM cells for single-cell FACsort (INDEX-sort) and flow cytometric analysis of colonies from the *in vitro* lineage tracing; M.G.E.R. characterized cell morphology of colonies from the *in vitro* lineage tracing via cytospins; M.G.E.R. analyzed the processed RNA-seq data from Csaba Miskey by GSEA, differential gene expression and gene ontology, and visualized results in volcano blots, heat maps and Venn diagrams; M.G.E.R. performed and analyzed results from cytokine multiplex

and THPO ELISA; M.G.E.R. prepared organs for histology together with F.S and S.K., analyzed histology of paraffin (light-microscope) and ultra-thin (electron microscope) sections together with U.M and I.M.V; enumerated MKs in BM sections together with I.M.V. and S.K.; M.G.E.R. assisted L.W., Y.K. or K.W. in titration of lung and tracheal tissues from infected mice; analyzed and visualized data, and wrote the manuscript.

Lisa Walz produced and titrated IAV PR8 stocks; designed and propagated VSV*ΔG replicon particles for immunization of mice; performed IAV infections and immunizations of mice, and titrated IAV in lung and tracheal tissues from infected mice.

Foteini Fotopoulou performed BM cell preparation, isolated Lin^- BM cells, single-cell FACsorted (INDEX-Sort) and cultivated LT-HSCs in the *in vitro* lineage trace assay; F.F. characterized the generated colonies by enumeration and flow cytometric analysis; F.F. performed the classification and analysis of the differentiation potential of LT-HSC with the R-script based on the flow cytometric data.

Saskia Kohlscheen contributed to mouse infection experiments, blood sampling, and isolation of BM cells, flow cytometric analysis (HSPC composition and cell cycle analysis), histology and enumeration of MKs in BM sections together with M.G.E.R.

Franziska Schenk performed IAV infections, blood sampling, assisted in bronchoalveolar lavage; F.S. performed isolation, transduction and transplantation of Lin^- BM cells; F.S. isolated BM cells, isolated RNA from liver samples for Thpo qPCR (acquisition and analysis), assisted M.G.E.R. in *in vitro* platelet activation, viability, sialyation and spreading assays. She analyzed the platelet spreading assay together with Marcel Rommel.

Csaba Miskey performed RNA isolation for next generation sequencing, next generation sequencing, processed raw RNA-seq data and differential gene expression analysis.

Lacramioara Botezatu performed transplantation of FACsorted HSPCs in mice, assessed and analyzed colonies from the CFU assay together with M.G.E.R., and proofread the manuscript.

Yvonne Krebs performed IAV infections, immunization and oseltamivir treatment in mice and titrated IAV in lung and tracheal tissues from infected mice.

Iris M. Voelker performed histo-pathological evaluation of paraffin-embedded sections from IAV-infected lungs and enumerated together with M.G.E.R. MKs in BM sections.

Kevin Wittwer produced and titrated IAV PR8 stocks, performed IAV infections and titrated IAV in lung and tracheal tissues from infected mice.

Tim Holland-Letz wrote the R-script for analyzing the flow cytometric colony readout of the *in vitro* lineage tracing experiment.

Zoltán Ivics provided the RNA-sequencing platform, proofread and discussed the manuscript

Veronika von Messling designed, developed and discussed results from the infection mouse model (lethal dose, antiviral treatment and immunization), provided IAV PR8, and proofread and discussed the manuscript.

Marieke A. G. Essers provided and discussed results from the *in vitro* lineage tracing assay, proofread and discussed the manuscript.

Michael D. Milsom designed, provided and discussed results from the *in vitro* lineage tracing assay, proofread and discussed the manuscript.

Christian K. Pfaller designed and discussed results from the infection mouse model (sub-lethal dose), discussed RNA-sequencing results, proofread and discussed the manuscript.

Ute Modlich developed the overall concept of the study, designed and supervised the experiments, critically evaluated data and wrote the manuscript.

Contribution to Figures

Figure 1A, C-J, L **M.G.E.R.**; 1B L.W., Y.K., K.W. and **M.G.E.R.**, 1K **M.G.E.R.** and F.S.
Figure 2 **M.G.E.R.** and S.K.
Figure 3 **M.G.E.R.**
Figure 4A-J **M.G.E.R.**, 4K **M.G.E.R.** and L.B., 4L-P **M.G.E.R.** and F.F.
Figure 5A and F and **M.G.E.R.**, 5B-E and G-J C.M. and **M.G.E.R.**
Figure 6 **M.G.E.R.**
Figure 7A-C, E-H, J-L **M.G.E.R.**, 7D Y.K., K.W. and **M.G.E.R.**, 7I F.S. and **M.G.E.R.**

Supplemental Figure 1A-B, E-H **M.G.E.R.**, 1C-D **M.G.E.R.,** I.M.V. and U.M., 1H-J **M.G.E.R** and U.M.
Supplemental Figure 2 **M.G.E.R.**
Supplemental Figure 3A-B, D-E **M.G.E.R.**, 3C **M.G.E.R.**, S.K. and I.M.V.
Supplemental Figure 4A-B **M.G.E.R.**, 4C **M.G.E.R.** and L.B., 4D-E F.F. and **M.G.E.R.**
Supplemental Figure 5A and I C.M., 5B-C and H C.M. and **M.G.E.R.**, 5E-G **M.G.E.R.**
Supplemental Figure 6 and 7 **M.G.E.R.**

Graphical Abstract **M.G.E.R**

.

Publication 4: Endothelial-platelet interactions in influenza-induced pneumonia: A potential therapeutic target

Rommel MGE[1], Milde C[1], Eberle R[2], Schulze H[3] and Modlich U[1]

1 Research Group Gene Modification in Stem Cells, Division of Veterinary Medicine, Paul-Ehrlich-Institute, Langen, Germany

2 Morphology, Division of Immunology, Paul-Ehrlich-Institute, Langen, Germany

3 Institute of Experimental Biomedicine, Chair I, University Hospital Würzburg, Germany

Journal: Anatomia, Histologia, Embryologia

Date: 2020 Sep

Type: Review article

DOI: 10.1111/ahe.12521

PMID: 31793053

Original publication see **Appendix 4**

Summary

Respiratory virus infections spread around the world during the cold-seasons, infecting humans and animals. Pneumonia is frequently observed during influenza virus infections. The epithelial-endothelial, more precisely the alveolar-capillary barrier, plays an essential functional but also protective role. Severe cases of influenza are associated with alveolar-capillary dysfunction and damage, leading to acute lung injury (ALI) and high morbidity rates. Even in patients, surviving ALI the long-term quality of life is adversely affected. Stressed and damaged endothelial cells secrete massive amounts of pro-inflammatory cytokines and present danger molecules on the surface creating a pro-thrombotic milieu in pulmonary capillaries. In this milieu platelets tend to accumulate and aggregate. Vaccination can protect from IAV pathogenesis, however, treatment of ALI is limited to antiviral drugs inhibiting influenza virus replication, anti-inflammatory drugs or active ventilation and oxygen support. Until now, no influenza treatments are developed against platelet-endothelial interaction or damage. This review article recapitulates influenza virus-induced pathology, discusses research animal models and compares those to the human pathology. Besides, own histopathological analysis of the IAV infection mouse model are presented. Molecular and cellular platelet-endothelial-epithelial interaction mechanisms are discussed in the light of potential novel therapeutic approaches.

Author contributions

Marcel G. E. Rommel wrote the subsections 'Abstract', '1. Impact of influenza on human health', '2. Influenza virus structure', '6. The role of the endothelium in IAV-induced pneumonia', '7. Platelets in Influenza-induced pneumonia', '8. Potential therapeutic target or treatments in acute respiratory lung injury' and '9. Conclusion'; M.G.E.R. acquired and analyzed lung histology from paraffin-embedded (light-microscope) and ultra-thin (electron microscope) sections together with U.M. and C.M.

Christian Milde wrote the subsections '3. Clinical symptoms in human patients' and '4. Histopathology of influenza infection'. C.M. analyzed lung histology from paraffin-embedded (light-microscope) and ultra-thin (electron microscope) sections.

Regina Eberle prepared the lung ultra-thin sections for electron microscopy and assisted during image acquisition.

Harald Schulze assessed and analyzed histology of IAV-infected lungs from electron microscopic images. H.S. discussed and commented on the manuscript.

Ute Modlich wrote the subsection '5. Animal models for influenza research' and constructively revised the other subsections; acquired and analyzed lung histology from paraffin (light-microscope) and ultra-thin (electron microscope) sections; developed and outlined the scope of the review.

Figure contribution

Figure 1A-F **M.G.E.R.**; G-H **M.G.E.R.** and C.M.

Figure 2 **M.G.E.R.** and U.M.

Figure 3 **M.G.E.R.** and U.M.

5. Discussion

5.1. Publication 1: Endothelial protein C receptor supports hematopoietic stem cell engraftment and expansion in Mpl-deficient mice

5.1.1. Downstream target genes of THPO/MPL signaling

THPO/MPL-signaling is essential for postnatal steady-state HSC maintenance, reflected by the Mpl-KO mouse with an 80-90% reduced HSC pool with impaired self-renewal and multipotency and more importantly in CAMT patients. MPL downstream target genes potentially regulating HSC function or megakaryopoiesis were selected based on the overlap of downregulated genes from induced bone marrow failure in steady-state hematopoiesis by a truncated dominant-negative THPO receptor (Kohlscheen et al., 2015) and upregulated genes in Mpl-regenerated Mpl-KO hematopoiesis (Heckl et al., 2011).

Among five tested genes, I found Lin^- Mpl-KO BM cells transduced with Epcr to enrich phenotypic LT-HSCs (LSK $CD34^-Flt3^-$ or LSK $CD150^+CD48^-$) in frequency and number, and enable secondary transplantation in Mpl-KO mice. EPCR is described as one of the immuno-phenotypic cell surface markers for identification of wt murine dormant HSCs in the BM with superior reconstitution potential in transplantation experiments (Balazs et al., 2006; Kent et al., 2009). Single-cell transplantation of EPCR expressing SLAM HSCs (ESALM) from wt mice resulted in 500- to 1,800-fold expansion in wt recipient mice confirming that EPCR expression is linked to HSC self-renewal (Benz et al., 2012). This is reflected in the improved expansion (self-renewal) of MPL-KO $EPCR_{td}$ cells in the aplastic mouse model. It is remarkable, that EPCR transduction rates of 10 to 30% in Lin^- BM cells from Mpl-KO were sufficient to restore self-renewal upon transplantation, since LT-HSCs faction is 90% reduced in Mpl-KO mice. Interestingly, cell expansion was restricted to LT-HSCs, while progenitors including ST-HSCs (LSK $CD34^+Flt3^-$), MPPs (LSK $CD34^+Flt3^+$) and myeloid progenitors remained at the level of control transduced Mpl-KO GFP cells. This led to the conclusion that EPCR expressing HSCs favor self-renewal over differentiation. Although targeted HSC gene expression by lineage-specific promotors was not the aim, transgene expression and co-expressed GFP by the PGK promotor in Mpl-KO $EPCR_{td}$ cells was the highest in LT-HSCs and 1/3 reduced in LSK cells. This result mirrors the EPCR distribution in wt LT-HSCs and LSK cells. Co-expressed GFP was nearly absent or not detectable in other BM cells or in the peripheral blood. In contrast, positive (wt) and negative (Mpl-KO) GFP transduced controls exhibited GFP expression in all lineages and cell populations in the BM and peripheral blood. Vector integration site analysis in peripheral blood and BM cells of Mpl-KO mice transplanted with Mpl-KO $EPCR_{td}$ cells would identify the clonal diversity (number and abundance) of all engrafted HSC clones and could

confirm that transgene expression was limited to the HSC pool. On the other hand, one alternative explanation would be that Mpl-KO $EPCR_{td}$ HSC expand without the production of any downstream cells. It would be interesting to compare lentiviral overexpression of endothelial cell-selective adhesion molecule 1 (ESAM-1) to overexpression of EPCR in Mpl-KO cells in the aplastic Mpl-KO mouse model. ESAM-1 is also initially described as an endothelial cell specific marker, however, is selectively expressed on murine and human HSCs (Forsberg et al., 2005; Yokota et al., 2009).

The molecular function of EPCR is so far described in endothelial cells and the coagulation pathway. Signaling from EPCR itself is unlikely, since the cytoplasmic moiety consists of only 6 aa (Oganesyan et al., 2002). EPCR shares significant structural homology with the major histocompatibility complex class I (MHC) family proteins and is the receptor for protein C (PC), which plays an important role in the PC anticoagulation pathway (Fukudome and Esmon, 1994). EPCR facilitates the generation of activated PC (aPC) by presenting PC to the thrombin-thrombomodulin complex. aPC binding to EPCR promotes endocytosis of EPCR (Nayak et al., 2009). As an anticoagulant enzyme, aPC proteolytically inactivates the coagulation factors Va and VIIIa. In damaged endothelial cells aPC also accounts for cytoprotective effects, by non-canonical cleavage of protease activated receptor 1 (PAR-1) and the recruitment of beta-arrestin-2 and activation of PI3K/AKT and the GTPase Ras-related C3 botulinum toxin substrate 1 (Rac1) signaling, leading to cell survival und suppression of inflammatory pathways (Riewald et al., 2002; Mosnier and Griffin, 2003). Direct localization of HSCs in the perivascular niche in the BM provides endothelial-derived aPC for non-canonical PAR-1 cleavage and cytoprotective signaling on HSCs. Non-canonical PAR-1 cleavage on HSCs is associated with BM retention by nitric oxide restriction, low level of cell division control protein (Cdc) 42 and Ras Homolog Family Member A (RhoA) activity and elevated very late activation protein 4 receptor (VLA-4, integrin subunit alpha 4) and 5 expression (Gur-Cohen et al., 2015). Canonical PAR-1 cleavage by thrombin drives the generation of nitric oxide production, leads to TACE-mediated EPCR shedding, increases Cdc42 and RhoA activity, reduces CXCL12 production in stromal cells and therefore increases HSPC mobilization into the peripheral blood. EPCR overexpression in Mpl-KO HSCs leads to an advantage in homing in the best possible BM niche. In this BM niche self-renewal is preferred compared to differentiation. A quasi-cell autonomous aPC generation by PC, EPCR and thrombomodulin action and aPC cleavage of PAR-1 signaling in HSCs is also conceivable, since thrombomodulin is expressed on murine HSCs and MPPs (Basu et al., 2020). However, hematopoietic thrombomodulin deletion had only minor effects on steady-state hematopoiesis and HSC function. This favors the hypothesis that aPC is provided by endothelial cells either local in the BM niche or systemically to induce cytoprotection. The aPC/EPCR/PAR-1 axis keeps fetal liver HSCs in a

slow cycling state in the perisinusoidal niche and prevents apoptosis (Iwasaki et al., 2010). aPC/EPCR/PAR-1 signaling requires the co-localization in caveolin-1 (Cav-1)-enriched lipid rafts (Bae et al., 2007; 2008). The absence of Cav-1 in HSCs disrupted quiescence with reduced ability of HSC self-renewal *in vitro* and *in vivo* assays (Bai et al., 2014). Functional lipid raft structures on the surface of the cell membrane are essential for Rho GTPases (Rac-1 and RhoH) and the lipid raft-associated surface receptors CXCR4, VLA-4 and c-Kit, which regulates migration, mobilization and homing of HSCs (Jahn et al., 2007; Bonig and Papayannopoulou, 2013). Mpl-KO $EPCR_{td}$ cells proofed to have a superior homing and engraftment potential in the BM early post transplantation in Mpl-KO mice. One explanation is that the positive regulation of Rac-1 and VLA-4 activity by aPC/EPCR/PAR-1 signaling in lipid rafts in the transduced Mpl-KO cells enhance chemotaxis and adhesion to BM niche cells (Yamazaki et al., 2006; Chae et al., 2008). One concludes that the superior homing of Mpl-KO $EPCR_{td}$ cells correlates with the establishment with a quiescent HSC pool after transplantation, which is more likely if they reside in their respective BM niche. Further studies should investigate the localization of Mpl-KO $EPCR_{td}$ in situ. Alternatively, one might use transient overexpression of EPCR in cultivated HSC-enriched cell populations to improve HSCs homing and engraftment of ex vivo gene therapy.

EPCR is used for isolation of fetal and adult HSCs in mice. In humans, this was recently shown for HSCs isolated from cord blood (Anjos-Afonso et al., 2022). Own data indicated a lack of EPCR expression on HSCs from mobilized patients, which is in accordance with the idea that EPCR is shed and not detectable with commercially available antibodies, or even downregulated. The small molecule UM171 induced the expression of EPCR on human cord blood-derived HSCs *in vitro* and was linked to higher engraftment potential in xenotransplantation experiments compared to EPCR-negative HSCs (Fares et al., 2017). UM171 supplementation to the cell culture medium inhibits histone demethylation and de-acetylation to preserve stem cell gene expression responsible for self-renewal (Chagraoui et al., 2021). Cultivation of murine HSCs with UM171 or other pyrimidoindole derivatives did not result in expansion and better engraftment potential, however, EPCR distribution on the transplanted cells was not shown (Fares et al., 2014). It would be highly interesting to identify small molecules, which induce the expression of EPCR on cultivated HSCs to maintain the superior engraftment potential in culture. Murine LSK cell stimulation with SCF, FLT3L and THPO in my experiments maintained the expression of EPCR compared to cultivation with SCF and FLT3L. This suggests that THPO does not transcriptionally regulate EPCR expression, but rather reduces the shedding of EPCR in culture. EPCR also marked the engrafting HSC population in long-term culture of murine HSCs (28 days) with SCF and THPO (Wilkinson et al., 2019), bolstering the beneficial effect of THPO on EPCR expression (Che et

al., 2022). In addition, EPCR maintenance should be tested in cytokine cocktails without the supplementation of THPO that are known to expand or maintain murine HSCs *in vitro* e.g. SCF, FLT3L, IL-3 and IL-11 (Li et al., 2003), to determine whether THPO is indeed the key factor. EPCR is shed by a variety of mediators including inflammatory cytokines (IL-1 or TNFα) or thrombin by the activation of TACE. Adding a TACE-inhibitor during HSC cultivation would represent an interesting approach to preserve cytoprotective EPCR signaling during ex vivo HSC manipulation in murine and human gene therapies models.

5.1.2. EPCR expression rescues megakaryopoiesis with deficient thrombopoiesis in Mpl-KO mice

The second manifestation of Mpl deficiency is reduced and impaired megakaryopoiesis and thrombopoiesis. Strikingly, Mpl-KO $EPCR_{td}$ cells improved the generation of large MKs in the BM of Mpl-KO mice, without altering myeloid or lymphoid progenitor lineages. This strongly highlights the positive correlation of the HSC population and the generation and levels of MKs (Figure 8).

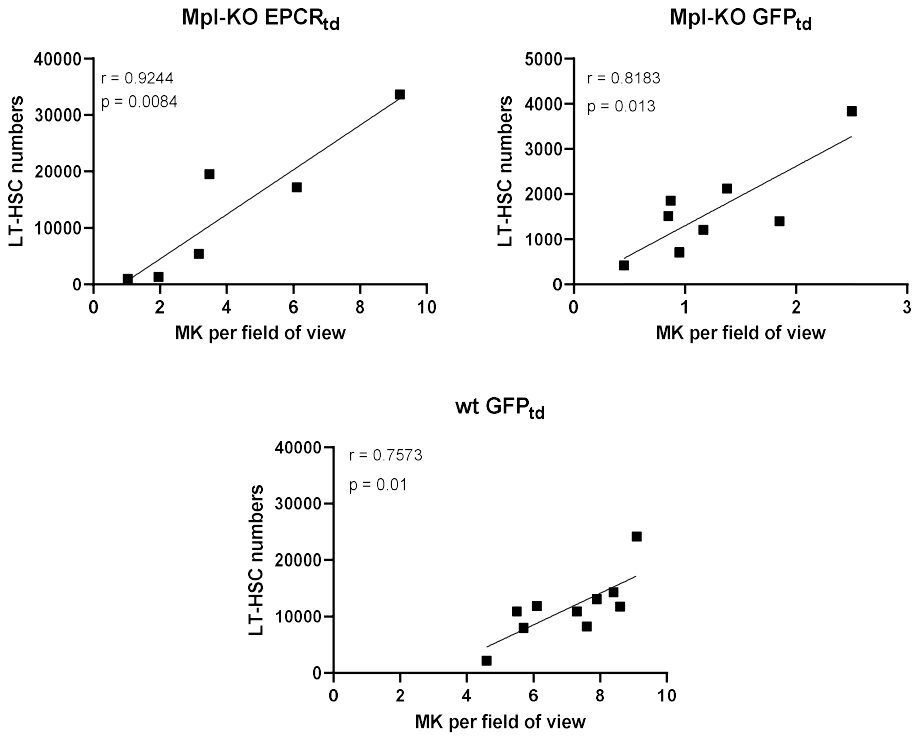

Figure 8 | Numbers of LT-HSCs and megakaryocytes in the BM postivlty correlate. Pearson correlation and linear regression of LT-HSC numbers in Mpl-KO mice transplanted with Mpl-KO $EPCR_{td}$, Mpl-KO GFP_{td} and wt GFP_{td} Lin^- BM cells determined using flow cytometry and number of MKs per field of view (40x magnification). Prepared from using data from own results (Kohlscheen et al., 2019).

Furthermore, this underlines the hypothesis that MKs are directly branched from HSCs and only a small fraction of MKs are generated by phenotypically defined MPP, CMP and MEPs

(Yamamoto et al., 2013; Rodriguez-Fraticelli et al., 2018). To test this hypothesis in the mouse I used, lentiviral integration site analysis should be performed in MKPs and MKs and compared to myeloid and lymphoid progenitors. Remarkably, megakaryopoiesis in mice transplanted with Mpl-KO $EPCR_{td}$ has to be independent of THPO/MPL signaling. In one study using megakaryocytic specific deletion of Mpl ($Mpl^{PF4cre/PF4cre}$ mouse) the authors showed, that THPO signaling via MPL is not required in MK expansion, maturation or platelet production (Ng et al., 2014).

The aPC/EPCR/PAR-1 signaling upregulates the expression of VLA-4. Adhesive interaction between endothelial cells and MKs through the VLA-4/VCAM-1 axis is associated with the maturation of MKs (Avraham et al., 1993). In BM sections large mature MKs in Mpl-KO $Epcr_{td}$ transplanted mice were enumerated, however, determining the number, chimerism and polyploidy of MK progenitor cells and MKs using flow cytometry would help to strengthen the observation. Despite the restoration of megakaryopoiesis in Mpl-KO cells overexpressing EPCR, the corresponding increase in peripheral platelet counts in primary and secondary transplanted mice was not detected. MKs in the BM of Mpl-KO $Epcr_{td}$ appeared to be large in size and polyploid, however, high polyploidy is not necessarily correlated with the development of demarcation membranes needed for sufficient platelet production (Zimmet et al., 1997). Analysis of the demarcation membrane system in Mpl-KO $Epcr_{td}$-derived cells would be of interest to understand why platelet formation was not improved. EPCR overexpression in Mpl-KO cells upregulated the expression of the pro-survival gene Bcl-xL, which was shown to inhibit caspase activation and platelet generation in cultured MKs (Kaluzhny et al., 2002). Proplatelet formation in mature MKs was shown to be dependent on apoptosis by caspase-3 and -9 signaling (Botton et al., 2002; Josefsson et al., 2020). Mouse models carrying mutations that impair apoptosis by overexpression anti-apoptotic Bcl-2 (Ogilvy et al., 1999) or deletion of the pro-apoptotic Bim (Bouillet et al., 1999) exhibited also reduced platelet counts. Therefore, it is likely that EPCR mediated signaling actively inhibits proplatelets formation by antagonizing apoptosis. Furthermore, PAR-1 signaling controls the activity of the Rho GTPases Cdc42, RhoA and Rac1. Canonical thrombin/PAR-1 activity leads to high RhoA and Cdc42 activity, however, is suppressed by non-canonical aPC/EPCR/PAR-1 signaling. RhoA and Cdc42 activity is essential for the accurate MK localization in the BM sinusoids and for the formation of proplatelets, however, is indispensable for MK endomitosis (Dütting et al., 2017; Heib et al., 2021). This is in line, with my observations, that rescued megakaryopoiesis by EPCR overexpression in Mpl-KO HSCs generate MKs with normal polyploidy, but lack thrombopoiesis. Although murine MKPs and MKs normally do not express EPCR, it is likely the transgene expression is passed to Mpl-KO $Epcr_{td}$-derived MKs in this study, which would actively inhibit canonical thrombin/PAR-1 activity needed for correct proplatelet formation.

5.2. Publication 2: Signaling properties of murine MPL and MPL mutants after stimulation with thrombopoietin and romiplostim

5.2.1. Reduced murine MPL-signaling after romiplostim stimulation

The cytokine dependent 32D cells transduced with mMPL, hMPL and mMPL mutants were utilized as test model to assess MPL signaling by phosflow analysis, which represents an excellent tool to measure multiple conditions at single-cell level with good quantification. mMpl-32D cells were transduced with a low MOI (0.1) to ensure a low vector copy number per cell, which could reassemble a physiological receptor expression for signaling assessment. High expression levels of MPL on the cell surface tend to signal in the absence of the ligand THPO and could altered signaling output (Whitty and Borysenko, 1999). The peptide THPO analogue romiplostim activated the mMPL-32D cells without signaling preference for phosphorylated (p)-AKT, p-ERK1/2 and p-STAT5 nor differential activation in the presence of JAK, PI3K, ERK1/2 or MEK small-molecule inhibitors. Although these three signaling pathways are key players in early or late signal transduction, it would be feasible and important to analyze the phosphorylation states of other STAT family proteins like STAT1/3, MAP kinase family proteins like p38 or eukaryotic initiation factor 4F (eIF4F), PI3K family proteins like ribosomal protein S6 (RSP6) or ribosomal kinase 1 (RSK1) to gain a detailed overview of MPL signaling activated by romiplostim. To complement the signaling analysis in 32D cells lentivirally transduced with mMPL or hMPL, activation and signaling analysis of romiplostim in primary murine and human HSCs, MK progenitor cells or MKs should be performed. Besides the phosphorylation of signal proteins, the expression of self-renewal (e.g. c-Myc or Fos) or prosurvival genes after MPL activation with romiplostim could alter the cell proliferation. I tested the ability of romiplostim to induced megakaryopoiesis from Lin^- BM cells from wt mice and detected reduced numbers of mature and polyploid MKs in culture. Reduced polyploidy in human cord blood-derived MKs differentiated with high concentration of romiplostim was reported (Currao et al., 2013). Romiplostim favored cell proliferation of immature progenitor cells over MK maturation in this study. As a next step, it would be possible to test the ability of romiplostim to favor the expansion of murine or human HSCs over MK development *in vitro* in colony forming unit assays or by analyzing the maintenance of HSC surface marker expression. Recently it was shown that hMPL activation with surrogate proteins ligands, so-called ‘diabodies’, induced opposing HSC fate decisions (Cui et al., 2021). Similar to observations in this study after stimulation of mMPL with romiplostim, they reported that the tested diabodies had a balanced signaling pathway activation in a cell culture model overexpressing human MPL and observed reduced MPL signaling capacity at higher concentrations. The reduced, but balanced intensity of MPL activation by the diabodies preserved stem-like properties of cultured human HSCs and lacked MK differentiation. They suggested that the different HSC fate decisions are linked

to altered MPL orientations and geometries through diabody binding at non-canonical binding sites.

In the literature, two mechanisms of MPL activation by THPO are under debate (1) THPO-induced conformational changes in pre-existing dimers or (2) THPO-induced MPL-homodimer formation. Most of cytokine class I receptors including MPL are proposed to exist as pre-formed dimers in the plasma membrane (Syed et al., 1998; Livnah et al., 1999) and THPO binding induces conformational changes in the dimer to facilitate the activation through the plasma membrane to JAK2. Single-molecule imaging of MPL-THPO interactions strongly supports the hypothesis that MPL, when expressed at physiological amounts, is present as a monomer either in a free form non-dimerized and a small fraction is bound to THPO (concentration of THPO $[c]^1$, Figure 7A) in a non-signaling competent state (Sakamoto et al., 2016; Wilmes et al., 2020).

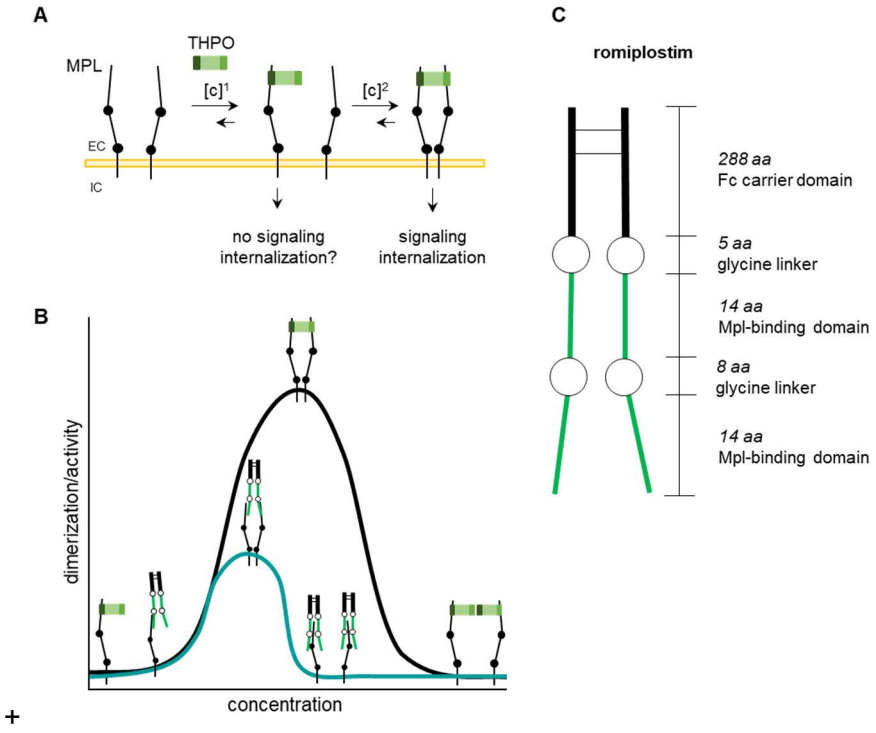

Figure 9 | MPL dimerization upon THPO or romiplostim binding. (A and B) THPO-induced MPL-homodimerization. At low levels of THPO (below $[c]^1$) most MPL-monomers at the cell surface membrane are not bound to THPO and inactive, while a small fraction of MPL-monomers are bound to one THPO. Increasing the level of THPO, increases the proportion of THPO-MPL monomers and rises the probability of the formation of THPO-MPL homodimers (1:2 stoichiometry). Homodimer formation is then controlled by the availability of MPL-monomers $[c]^2$ at the cell surface. The maximum in dimerization and signaling activity is reached at the point when the concentration of THPO is equal to $[c]^1$. High THPO concentration leads to the saturation of the MPL-monomers unable to dimerize. The two binding sites of THPO are indicated in high (dark green) and low affinity (light green). EC = extracellular and IC = intracellular space. **(C)** Representative scheme of the peptide THPO analogue 'romiplostim' (Nplate®, Amgen), indicated in green are the 14 aa (IEGPTLRGWLAARA) Mpl-binding domain and the circles represent the 5 and 8 aa glycine linker/spacer between Mpl-binding domains and the fusion to the human IgG Fc-fragment. Inspired from Wilmes et al., 2020.

With increasing THPO concentration more MPL-monomers with bound THPO are present at the cell surface and the probability that the low affinity binding site of THPO will bind a second MPL monomer rises (concentration of MPL-monomers $[c]^2$; Figure 7A and B). For functional dimerization one THPO and two MPL-monomers (1:2 THPO/MPL stoichiometry) are necessary (Wilmes et al., 2020). The maximum of signaling occurs at the THPO concentration $[c]^1$, when 50% of the MPL-monomers bound one THPO molecule and have the possibility to form a homodimer with another MPL-monomer. At very high concentrations all MPL-monomers are saturated with one THPO (1:1 stoichiometry) and are unable to form a homodimer for signal transduction (Figure 7B), something which was observed already in early MPL signaling studies, however, left undiscussed (Cwirla et al., 1997; Drachman and Kaushansky, 1997; Cui et al., 2021). The phosphorylation intensity of STAT, AKT and ERK1/2 was four- to five-fold reduced at high romiplostim concentration compared to activation after mTHPO. Romiplostim exhibits four MPL binding-sites extremely flexible linked by glycine spacer residues (Figure 7C). Romiplostim has intrinsically more possibilities to bind at one MPL monomer. It is even thinkable, that one romiplostim could bind more than two MPL-monomers at the same time, thereby reducing the right stoichiometry and following concentration $[c]^2$ of available MPL-monomers for dimerization (Figure 7B). Therefore, the saturation of MPL-molecules could be observed at lower romiplostim concentrations limiting signaling capacity. One could argue, that the larger three-dimensional structure of romiplostim alter the mMPL-homodimer geometry needed for fully functional signaling, which could further explain reduced mMPL-signaling after romiplostim activation at high concentrations. Similar to the study which used ‘diabodies’, romiplostim competes with THPO for the MPL binding site, following the binding position should be in the same region of THPO, however, the exact binding positions for both are yet not reported. Identification of the romiplostim binding site would further strengthen the hypothesis that an alternative binding site could induced a non-canonical MPL geometry to induce reduced signaling, which is linked to opposing outputs. Proliferation of mMpl-32D cells after activation with increasing dose of romiplostim was reduced compared to mTHPO. This was accompanied with faster internalization of mMpl after stimulation with romiplostim at high concentration compared to mTHPO. The MPL concentration on the cell surface controls and fine-tunes signaling capacity and duration (Hitchcock et al., 2008), next to negative regulators of intracellular signaling (e.g. SOCS, LYN or LNK). Internalization via clathrin-mediated receptor endocytosis needs adaptor protein 2 (AP2), which associates with the activated MPL cytoplasmic domain at the tyrosine residue 626 (hMPL) and the Box2 domain (Dahlen et al., 2003; Hitchcock et al., 2008). Reduced proliferation of mMPL-32D cells could be due altered mMPL recycling to the cell surface or increased proteasomal degradation after stimulation with romiplostim.

Differences in signaling intensity or internalization of human MPL stimulated with romiplostim were not observed. This is in line with the therapeutic usage of romiplostim in patients with thrombocytopenia to boost platelet production, or aplastic anemia to target HSC self-renewal to generate blood cells. Although the murine and human MPL have a protein sequence identity of 81.6% and similarity of 85%, the biggest differences are found in the predicted THPO-binding region 90 to 240 aa of the CRM1 domain with an identity of 69% respectively. Suboptimal interspecies cross-reactivity of THPO and MPL is observed in insufficient engraftment of human HSCs in xenogenic mouse models (Rongvaux et al., 2011). Since romiplostim is especially selected against the human THPO-binding domain in the extracellular part of MPL, the reduced signaling intensity could be indeed related to an alternative binding site of romiplostim at mMPL inducing non-canonical mMPL geometry for signal transduction. Taken together, the therapeutic approach of targeting MPL selectively for either platelet production or HSC maintenance and expansion is feasible. This aim appears to be achievable via alternatively induced MPL geometry and reduced yet balanced signaling intensity rather than by selectively activating one particular signaling pathway.

5.2.2. Recapitulating human MPL mutations and functionality in murine MPL mutants equivalents

The aim was to determine whether signaling pathways were specifically initiated by certain tyrosine residues in the intracellular part of mMPL. To address that, lentiviral vectors expressing mMpl with tyrosine (Y) to phenylalanine (F) substitution at positions Y582F, Y616F and Y621F, combined substitutions at positions Y616F_Y621F, as well as truncated receptors lacking 53 and 69 aa were created. The mutated tyrosine position Y582F was identified as a gain-of-function mutation with increased ERK1/2 and normal AKT and STAT5 phosphorylation in 32D cells, which leads to increased proliferation of Y582F-32D cells stimulated with mTHPO or romiplostim. ERK1/2 activation by mMPL is important for cell proliferation, since selective inhibition of the MEK pathway in mMPL Ba/F3 cells from other studies showed reduced proliferation. Furthermore, the murine Y581F reflects the studies performed with the human equivalent Y591F mutation by increased ERK1/2 signaling and proliferation in Ba/F3 cells (Sangkhae et al., 2014). The phosphorylated human tyrosine Y591 position provides a docking site for SH2-containing proteins such as SYK and negatively regulates Ras signaling after hMPL stimulation. Mutation in the tyrosine position 591, which was recently found in a patient with essential thrombocythemia, is also associated with constitutive ERK1/2 and STAT3 signaling linked by either increased receptor trafficking to the cell-surface or reduced receptor internalization (Cabagnols et al., 2016). This is mirrored in the generated Y582F mMPL mutant by constitutive ERK1/2 signaling in the murine background. Additionally, Mpl-KO Lin^- BM cells transduced with Y582F-MPL could not rescue the megakaryopoiesis *in vitro* assays after

stimulation with mTHPO, although activation of Ras and ERK1/2 signaling is associated with differentiation and maturation in megakaryocytic cell lines (UT7, K562 or CMK cells), murine and human MKs (Melemed et al., 1997; Rouyez et al., 1997; Whalen et al., 1997; Herrera et al., 1998; Rojnuckarin et al., 1999). However, MAP-kinase hyper-activation abolishes proplatelet formation in mature MKs (Bluteau et al., 2014). This suggests that balanced signaling from MPL is more important for MK differentiation than favoring on particular signaling pathway. *In vitro* MK differentiation after hMPL activation by the aforementioned diabodies was related to balanced activation of all pathways (Cui et al., 2021).

To note, all MK differentiation studies by MPL activation were performed in cell culture models. Interestingly, transgenic knock-in mice expressing the truncated MPL version lacking 60 C-terminal aa (Δ60) exhibited physiological numbers of peripheral platelets and MKs, either in the BM or spleen with unaltered polyploidy. This indicates, that activation of signaling pathways related to the C-terminal half of the receptor is not essential for MK differentiation or platelet production. THPO signaling in platelets isolated from Δ60 mice revealed complete absence of AKT and MAPK activation, but are able to activate the JAK-STAT3 pathway (Luoh et al., 2000). These results are partially mimicked by Y616F and Y621F mMPL mutant variants, exhibiting unaltered STAT5 signaling, yet reduced ERK and AKT signaling in 32D cells, however, rescued Mpl-deficient in Mpl-KO transduced Lin^- BM cells. HSCs from these mice exhibited normal engraftment potential in primary and secondary recipients and moderately reduced engraftment in tertiary and quaternary recipients, linking THPO signaling for HSC maintenance and self-renewal to JAK2-mediated signaling only (Tong et al., 2007). In contrast, in MPNs with W515L MPL, JAK2 Y617F or calreticulin mutations in patients or in generated mouse models, all signaling pathways are constitutively active and result in elevated numbers of erythrocytes often combined with granulocytes and platelets (polycythemia vera) or specifically the megakaryocytic-lineage (essential thrombocythemia). It was shown that the additional mutation at the position Y625F and the double mutation Y625F_Y630F in combination with the MPN-inducing W515L mutation in hMPL were able to reverse the myeloproliferative phenotype in mice transplanted with wt Lin^- BM cells retrovirally overexpressing the respective mutant, which was not seen for W515L Y630F hMPL in this model. Deleting the Box2 motif from the intracellular part of mMPL (Δ69) resulted in complete loss of signaling and proliferation. This is consistent with previous studies of truncated mMPL versions variants at position Δ68, Δ93 and Δ109 in transfected Ba/F3 cells (Drachman and Kaushansky, 1997) or by deleting the aa from 576 to 599 in the cytoplasmic moiety using UT7 cells (Porteu et al., 1996). Box2 is absolutely required for JAK2 binding and activation for downstream signaling. Transplantation of wt Lin^- BM cells transduced with a truncated dominant-negative Mpl (Δ109) induces thrombocytopenia and reduced HSC numbers in primary recipients (Kohlscheen et al., 2015). Based on my data,

I emphasize the predictive role of the murine model in investigation of the signaling of MPL. This study highlights that murine amino acid equivalent MPL mutations detected in the human MPL found in MPN patients reassemble the same phenotype and functionality in cell culture models. As a next step, the generation of respective mouse models would be a promising tool to characterize MPN pathology as well as to develop and test therapeutic strategies, which can be translated for clinical application.

5.3. Publication 3: Influenza A Virus Infection Instructs Hematopoiesis to Megakaryocyte-lineage Output

5.3.1. Respiratory IAV infection as a model to study stress hematopoiesis

Blood loss, infection with pathogens or administration of cytotoxic or inflammatory agents (cytokines, polyI:C or LPS) can lead to stress hematopoiesis. Most inflammatory stress hematopoiesis models use a systemic administration or spread of pathogens. In this sense, the used non-systemic respiratory IAV infection mouse model is different from other established stress hematopoiesis models. The model used in my experiments takes advantage of the natural route of IAV infection and the fact that most influenza strains can replicate exclusively in epithelial cells of the respiratory tract. IAV does not have the potential to lead to viremia or systemic infection in mice (Hermesh et al., 2010) compared to other respiratory viruses like vesicular stomatitis virus (VSV; Roberts et al., 1999), middle east respiratory syndrome coronavirus (MERS-CoV; Cockrell et al., 2016) or severe acute respiratory syndrome corona virus (SARS-CoV; Subbarao and Roberts, 2006). To note SARS-CoV-2 was unidentified at the time point when the study was started, although reported pathologies in SARS-CoV-2-infected patients like pneumonia, microthrombosis and cytokine storm are similar to influenza. However, SARS-CoV-2 infections spread systemically in patients and in mice expressing human angiotensin converting enzyme 2 (Winkler et al., 2020), which would represent a systemic stress hematopoiesis model. Wt BL6 mice often do not express the entry receptor for respiratory viruses and transgenic mice with the human entry receptor have to be generated. Furthermore, in some cases viral infection studies have to be conducted in mice deficient in inflammatory cytokine signaling e.g. IFNAR-KO or defective in innate immune sensing, generating an incomplete immune response to allow virus replication. Viral infection in these models result in high morbidity and lethality within few days. Finding from these models might be predictive for immunocompromised patients, but may not for the majority of the population. My infection model in immunocompetent wt BL6 mice with a clinically relevant IAV is different. Observed bronchial-, interstitial- and vascular inflammation, endothelial- and structural damage, lymphopenia and alternating platelet counts reflected human IAV-induced pulmonary pathologies in many aspects. The moderate pathology score and alternating peripheral blood counts even in sub-lethal infected mice, which represents a more likely initial

dose of infection in humans, revealed that my reported results not only account for severe IAV infections. Several stress hematopoiesis studies in mice using viral or bacterial pathogens, often do not provide histological or blood count analysis and thus have limited comparability to pathologies observed in infected humans (Baldridge et al., 2010; Bruin et al., 2013; Matatall et al., 2014; 2016; Hirche et al., 2017). For us, histo-pathological analysis was particularly useful at time points IAV was not detectable by titration in the lungs of infected mice (>12 days post infection) to assess severity of IAV infection.

Lymphopenia and alternating platelet counts in IAV-infected wt mice reassemble blood count data from hospitalized patients infected with IAV. Both thrombocytopenia and thrombocytosis are reported from humans with IAV-infection (Tran et al., 2004; Jain et al., 2009; Kim et al., 2016). However, the time point of infection in human is unknown and therefore the correct time point of blood count analysis post infection. From the used IAV-infection model I may predict that thrombocytopenia in humans occurs at an early time point after infection and thrombocytosis is associated with IAV progression or recovery. To note, I analyzed individual mice every day and did not follow one mouse over time. It is remarkable that the alternating platelet count is robustly observed in IAV-infected mice independent of the initial viral load. Kinetics of platelet loss and increase in mice treated with the RNA virus-mimicking agent polyI:C followed similar kinetics seen in my IAV-infected mice. However, the excessive rise in platelets above physiological levels is less pronounced or absent in the polyI:C model compared to the IAV infection in mice (Haas et al., 2015; Bogeska et al., 2022). This is presumable due to a persistent pro-thrombotic milieu in the IAV-infected lung. Damaged endothelial cells activate platelets and consciously sequesters platelets from the peripheral blood into the pulmonary capillaries. This amplifies platelet production by emergency megakaryopoiesis.

Mouse models are successfully used in pre-clinical influenza vaccine or antiviral drug development. Mismatch vaccination with an experimental VSV-based vaccine or antiviral treatment with the neuraminidase inhibitor oseltamivir was utilized to protect the mice from IAV-induced morbidity. In addition, predicting the influenza strains circulating each year is difficult, causing potential virus lineage-mismatch in vaccination and thus less protection for the population (Lee et al., 2021). The used IAV-infection mouse model reflects that aspect as well. Conducting IAV infection with different initial IAV doses, vaccinated and or antiviral treated mice allowed us to correlate the lung and tracheal tissue titers with various parameter. Viral titers above $1x10^5$ $TCID_{50}$/g in the respiratory tract positively correlated with HSC activation and elevated inflammatory cytokines in the BM. It is concerning that, IAV infections may activate HSCs even with doses below the sub-lethal dose, if virus replication exceeds the determined threshold. Faster recovery of HSC quiescence in mismatch vaccinated mice was

clearly linked to enhanced viral clearance and a less diverse and pronounced cytokine profile in the BM. One might speculate that virus lineage-matched vaccination in combination with the same or lower initial IAV dose would fully protect HSCs from activation. Repeated proliferation of HSC could causes permanent defects, which are linked to HSC exhaustion and clonal hematopoiesis during aging. This would further highlight the importance of IAV vaccination, as it could additionally protect and preserve HSC functionality during life.

5.3.2. IAV-induced activation of HSCs by acute inflammatory insult

Hallmarks of IAV infection are excessive production of inflammatory cytokines and chemokines, and the recruitment of immune cells into the infected lung. The central orchestrator for amplifying inflammatory cytokines and potentially causing a cytokine storm are pulmonary endothelial cells and not the IAV-infected epithelium (Teijaro et al., 2011). IFNα, IFNγ, TNFα, IL-1α and IL-6 are the earliest produced cytokines in the lung 24 hours post infection (Moltedo et al., 2009; Teijaro et al., 2011). Although the level of cytokines in the bronchoalveolar lavage in the IAV-infected mice were not measured and cytokines in blood sera were below level of detection, IFNγ, TNFα, IL-1α and IL-6 were detected to be significantly elevated in the BM two and four days post infection. To note, these cytokines were also found in nasal fluids from humans two days post infection with IAV (intranasal) (Fritz et al., 1999; Kaiser et al., 2001). Even though cytokine stimulation of FACsorted HSCs *in vitro* pointed out that, IL-1 and IL-6 enhance HSC proliferation *in vitro*, stimulation of HSCs in the MNCs bulk with IL-1, IL-6, TNFα or IFNγ resulted in accelerated HSC cell cycling for all tested cytokines. The possibility that IFNγ or TNFα in combination with other pro-inflammatory cytokines have synergistic effects on HSC activation. This reflects the complex interaction of HSCs with the hematopoietic BM niche cells more closely and demonstrates that hematopoietic cells produce further cytokines in the response to the tested inflammatory cytokines (Zhao et al., 2014). Abrogating IL-6 and IL1 cytokine signaling *in vivo* did not completely reduce HSC activation during IAV infection. This highlights the complex signaling pathways of inflammatory cytokines in stress hematopoiesis, but also suggests the presence of an even larger inflammatory cytokine network *in vivo*. Since IAV infection in cytokine- or cytokine receptor-knockout mice likely results in an altered initial cytokine response in pulmonary tissue the cytokines found in the BM of these mice may differ in composition and level compared to wt-infected mice. Therefore, generation of BM chimeras in wt mice with BM/HSCs from one or more cytokine receptor knockouts (e.g. IL1R1-, IFNAR-, IFNGR- and TNFR-KO) would represent an improved model to study IAV-induced stress hematopoiesis. As an alternative, to knockout mouse models or BM chimeras, the usage of anti-inflammatory antibodies, e.g. anakinra (IL-1), etanercept (TNFα), tocilizumab (IL-6) or anifrolumab (IFNα) in wt mice are an option to investigate the role of each cytokine and the influence in HSC activation and fate. Both

approaches were recently used by the Essers group in bacterial mimicking LPS-induced stress hematopoiesis in quadruple BM chimera wt mice or immunomodulatory treated wt mice. This study reports that multiple cytokines in combination activated HSCs (LSK $CD150^{+}CD48^{-}CD34^{-}$), and anti-inflammatory antibodies reduced, however, did not prevent HSC activation (Demel et al., 2022). One concludes from their study and my IAV infection study that inflammatory cytokines have a key role in HSC activation, however, cannot overall explain HSC proliferation. Although cytokines reported in the literature to be originally identified and produced in the lung were upregulated in the BM, one cannot exclude the possibility that non-hematopoietic or hematopoietic BM niche cells produced these cytokines locally. Furthermore, activation of HSCs may be related to insufficient support from the BM niche cells, which provide fewer factors required to maintain and retain HSCs in their niche during inflammation (Mitroulis et al., 2020). Analyzing changes in non-hematopoietic BM niche cells, e.g. MSCs or ECs, or cytokine-producing monocytes or macrophages in the BM would be a promising strategy to understand the cause of HSC activation. It may also answer the question, whether HSC activation depends solely on the presence of pro-inflammatory cytokines and their site of production. Since IAV PR8 does not spread systemically (Hermesh et al., 2010) and IAV RNAs in our sorted HSPC populations were not detected, HSC activation by direct IAV recognition in the BM can be excluded. The study focused on HSCs in the BM, whether IAV infection has an influence on HSC migration and extramedullary hematopoiesis e.g. in the spleen were not investigated, although inflammatory cytokines are known to have an effect on that.

Acute or chronic HSC activation has been associated with DNA-damage, increased mutational burden and permanent defects with increasing the risk of hematopoietic malignancies (Kristinsson et al., 2011; Walter et al., 2015). Reduced HSPC engraftment potential during an acute IAV infection was observed, but HSPCs functionality after recovery was not evaluated. Transplantation of IAV-recovered HSCs may shed light on whether respiratory infection could alter hematopoiesis long-term. The HSPC engraftment potential of IAV-infected IL-6 or IL1R1-KO mice were not investigated, since HSCs from these mice might exhibit already intrinsic difference in functionality in transplantations assays. Therefore, it would be relevant whether immunomodulatory treatment in wt mice could rescue HSC functionality during the acute phase of infection. Since immunomodulatory treatments like anakinra or toclizumab are under evaluation in severe respiratory infections of humans (Alijotas-Reig et al., 2020; Mehta et al., 2020; Ryabkova et al., 2021), the treatment would have a beneficial impact on preserving HSC quiescence and function.

5.3.3. Phenotypic and cell cycle state characterization of HSCs during IAV-induced inflammation

In steady-state hematopoiesis, the cell surface marker Sca-1 is expressed on HSCs and MPPs and absent on myeloid progenitors like CMPs, GMPs and MEPs. Inflammation in the BM upregulates Sca-1 expression on all BM cells (Malek et al., 1989). Especially Sca-1-negative myeloid progenitors strongly upregulate the expression of Sca-1, thereby phenotypically appear in the HSC-enriched LSK population (Essers et al., 2009; Pietras et al., 2014). It is remarkable, that a local IAV-infection causes inflammation in the distant BM seen by mild Sca-1 upregulation. This sets my study apart from systemically administered cytokines mimicking viral (polyI:C) or bacterial (LPS) infection and replicating pathogens like bacteria, viruses or protozoa. In these models Sca-1 upregulation is dramatically elevated and overwhelming cytokine levels are observed quickly after administration (Essers et al., 2009; Pietras et al., 2014; 2016; Hirche et al., 2017). In consequence, the Sca-1 marker was excluded to avoid contamination in the HSC characterization during IAV-infection. Recently the surface marker CD86 (B-lymphocyte activation antigen B7-2) was suggested as an alternative marker for Sca-1 for HSC characterization (Kanayama et al., 2020). CD86 can be used to identify HSCs in steady-state and inflammation to reduce misinterpretation of stress hematopoiesis. Including CD86 in the HSC characterization during IAV-infection would help to distinguish HSCs and myeloid progenitors cell even more precisely.

HSCs characterized as Lin^{-}c-$Kit^{+}CD150^{+}CD34^{-}CD48^{-}$ in my study were transiently activated measured by elevated Ki-67 levels during the acute phase of infection (<8 dpi) and regained quiescence in the recovery phase (>8 dpi). It is noteworthy that loss of quiescence in my non-systemic IAV infection was equal to the HSC activation reported in systemic infection models using the exact same HSC definition and cell cycle analysis (Haas et al., 2015; Hirche et al., 2017). These findings support that HSC activation is not only observed after severe or chronic systemic virus infection (Hirche et al., 2017), but alarmingly also at low dose non-systemic respiratory IAV infection. Although Ki-67 is used for the state-of-the-art analysis to identify quiescent HSCs, Ki-67 is gradually expressed in the S-phase and gradually degraded after cell division. Thus, HSCs that re-enter quiescence still express Ki-67, and the fraction of cycling HSCs in G1-phase can be overestimated (Miller et al., 2018). Besides analyzing HSC cycle state, specific upregulated surface markers upon inflammation are discussed. The bone marrow stromal cell antigen 2 (*Bst2*/CD317) and CD69 (*Clec2c*) are rapidly and dose-dependently elevated on HSCs ($L^{-}S^{+}K^{+}CD150^{+}CD48^{+}$) after polyI:C or LPS challenge in mice and the expression of these markers positively correlates with loss of HSC quiescence (Bujanover et al., 2018; Thapa et al., 2022). Including these markers in my HSC characterization would be a great advantage because cell cycle activation and surface marker

expression could be correlated without analyzing the cell cycle state through intracellular staining, which do not allow further functional analysis like colony forming unit-, *in vitro* lineage trace- or transplantation assays. This approach would be essential during the acute phase of IAV infection. With the cell cycle analysis approach used in this study, the cell cycle state was only assessed at the time point of analysis. However, HSCs that have undergone one or more divisions during the acute phase but regain quiescence again during the recovery phase were not traced. DNA labeling of HSCs with BrdU or EdU in combination of Ki-67 and the amount of DNA during IAV infection would allow tracing of HSCs. However, since it is necessary to fixate the cells to detect BrdU incorporated into the DNA, one would be unable to examine functional HSC activity by transplantation at the same time. To address this issue, one could perform the IAV challenge in transgenic mice that specifically label HSPCs by the doxycycline-dependent expression of the fusion protein histone H2B-GFP (Scl-tTA;H2B-GFP mice). By infecting these mice, one could determine in the recovery phase whether in HSCs actively divided (loss of GFP marking) in the acute phase. As a next step divided and quiescent HSCs and non-dividing and dormant HSCs can be challenged in reconstitution assays to evaluate differences in functionality and fate.

A comprehensive comparison between studies of stress hematopoiesis can be rather difficult, since different HSC characterizations were used over the past 15 years: $L^-S^+K^+CD150^+$ (Baldridge et al., 2010), $L^-S^+K^+CD150^+CD34^-$ (Essers et al., 2009), SP-LSK (Sato et al., 2009), $L^-S^+K^+Flt3^-CD48^-CD150^+$ (Pietras et al., 2014), $L^-K^+CD150^+CD48^-CD34^-$ (Haas et al., 2015; Hirche et al., 2017), or $L^-K^+CD150^+CD48^-EPCR^+$ (Matatall et al., 2016). Furthermore, the purity and functionality of the defined HSCs in steady-state and especially during inflammation is questionable and the characterization needs surface markers which are unaltered in both conditions. In my own study (Publication 1) EPCR was identified not only a surface marker that enriches HSCs, but is also essential for quiescence in wt HSCs and Mpl-KO HSCs overexpressing EPCR. Including EPCR in my HSC characterization, $EPCR^+$ $CD41^-$ HSC ($L^-K^+CD150^+CD34^-CD48^-$) were quiescent and did not change in cell numbers during the acute phase of IAV infection. A similar observation was reported by Rabe et al., showing that chronic IL-1 exposure (each day for 20 days) in wt mice did not alter the quiescence and number of $EPCR^+CD34^-$ HSCs ($L^-S^+K^+Flt3^-CD48^-CD150^+$) and exhibited unchanged functionality with superior multi-lineage and BM engraftment potential in primary and secondary transplantations (Rabe et al., 2020). Multi-lineage colony forming potential in my study was linked to the phenotype $EPCR^+CD41^-$ HSCs ($L^-K^+CD150^+CD34^-CD48^-$), irrespective whether isolated from IAV-infected mice or non-infected mice. This proofs that EPCR expression immune-phenotypically defines quiescent HSC and that these cells also exist during IAV infection. One could hypothesize that non-canonical aPC/EPCR/PAR-1-induced signaling in HSCs is

cytoprotective and induces an anti-inflammatory state, which acts as a threshold regulator for activation by balancing pro-inflammatory signals. Furthermore, EPCR positively influence VLA-4 expression and Rac1 activity, which retain HSCs in the most supportive BM niche even during inflammation. This raises the question of whether HSCs defined by EPCR expression would be quiescent and exhibited steady-state functionality in reported stress hematopoiesis studies. Therefore, further studies on stress hematopoiesis need to include EPCR in their HSC characterization.

5.3.4. Emergency megakaryopoiesis and the bypass differentiation into megakaryocytic lineage

I proved existence of the emergency megakaryopoiesis during IAV infection. $CD41^+EPCR^-$ and $CD41^+EPCR^+$ HSCs ($L^-K^+CD150^+CD34^-CD48^-$) are subpopulations in the immune-phenotypic defined HSCs and are quiescent during steady-state, but efficiently activated during inflammation. This is in line with the observation of Haas et al., reporting that stem cell-like megakaryocyte-committed progenitors (SL-MkPs, $CD41^{high}L^-K^+CD150^+CD34^-CD48^-$; Haas et al., 2018) were rapidly activated after polyI:C injection in wt mice, which represents the HSC sub-population performing emergency megakaryopoiesis. To note, in this study the $CD41^{low/medium}$ HSCs are also not activated nor altered in numbers, similar to $EPCR^+CD41^-$ HSCs in my study. This bolsters the fact that a HSC population exists, phenotypically characterized by EPCR expression, which is not altered in quiescence and functionality during inflammation. Defined $CD41^+EPCR^{+/-}$ HSCs in my study, represent a quiescent subpopulation of the identified platelet-biased, yet multipotent vWF-positive HSCs ($L^-S^+K^+CD150^+CD48^-CD34^-$) in steady-state hematopoiesis (Sanjuan-Pla et al., 2013; Shin et al., 2014). However, $CD41^+EPCR^{+/-}$ HSCs share also similarity with recently identified proliferating megakaryocyte progenitors (pMKPs, $EPCR^-CD41^{med/+}$ $L^-K^+Sca\text{-}1^{-/low/mid}CD45^+CD150^+CD48^-Mpl^+CD9^+$; Prins et al., 2020). Unexpectedly, pronounced platelet-biased reconstitution from transplanted $CD41^+$ HSPCs from IAV-infected mice was observed for 10 to 12 weeks after transplantation. This is different for transplanted $CD41^+$ LSKs, pMKPs or SL-MkPs which exhibit short-term platelet reconstitution for maximum 2 weeks after transplantation (Haas et al., 2015; Nishikii et al., 2015; Prins et al., 2020). Therefore, IAV infection may alter the epigenetic landscape of HSPCs thereby keeping MK-biased differentiation memorized for a certain amount of time. As next step, the DNA methylation and chromatin accessibility of HSPCs from non-infected and IAV-infected mice should be assessed to determine whether open megakaryocyte enhancer regions are the cause of prolonged MK potential. Since HSC, MKPs and MKs exhibit a strong overlapping open chromatin signature minor changes would be of relevance (Heuston et al., 2018). I was surprised that $CD41^+$ HSPCs from IAV-infected mice exhibited multi-lineage and BM engraftment. This is again in contrast to transplanted $CD41^+$ LSK, pMKPs or SL-MkPs,

which are unipotent for the megakaryocyte lineage and do not engraft long-term in recipient mice. Lineage restricted and mutli-lineage HSCs in my experiments would have been identified by transplanting the different HSC subpopulations of $CD41^{+/-}$ $EPCR^{+/-}$ and/or using cell numbers lower than 100 HPSCs compared to 1,500 HSPCs used in the transplantation assays. However, it is possible to provide evidence that transplanted $CD41^{+}$ HSPCs generated $CD41^{-}$ HSCs ($L^{-}S^{+}K^{+}CD150^{+}CD48^{-}CD34^{-}$) and vice versa, revealing that both populations are highly dynamic *in vivo* and there is no unidirectional fate. Therefore, one can hypothesize that, $CD41^{+}EPCR^{-}$ HSCs represents the earliest stage of MKP development with uni-lineage potential *in vivo*, while $CD41^{+}EPCR^{+}$ HSCs harbor platelet-biased yet multi-lineage engraftment potential.

Activation of $CD41^{+}$ HSCs and emergency megakaryopoiesis were absent in IAV-infected IL1R1-KO mice. Furthermore, thrombocytopenia and thrombocytosis in IAV-infected IL-1R1-KO mice was not detected. It was shown that solely platelet depletion by anti-platelet antibodies does not trigger $CD41^{+}$HSC activation and emergency megakaryopoiesis (Haas et al., 2015; Ramasz et al., 2019). Therefore, IAV-induced emergency megakaryopoiesis is more likely dependent on inflammatory IL-1 signaling. Although CD41 upregulation was observed by systemic administration of LPS or TNFα in wt mice, platelet counts in treated mice or HSC reconstitution potential were not reported and therefore direct evidence for emergency megakaryopoiesis induced by these cytokines is not provided (Haas et al., 2015; Yamashita and Passegué, 2019). I and others (Rabe et al., 2020) identified that IL1R1 expression on HSCs correlates with the co-expression of CD41, making them responsive for IL-1 during IAV-induced inflammation. Furthermore, the absence of IL-1 signaling has been shown to significantly reduce the expansion of the $EPCR^{+}CD41^{+}$ HSC population ($L^{-}S^{+}K^{+}CD34^{-}Flt3^{-}CD48^{-}CD150^{+}$) during lifetime in mice. This HSC population is associated with elevated platelet counts and myeloid-biased differentiation in transplantation assays in aged mice (Kovtonyuk et al., 2022 and own data). Interestingly, the phenotypic appearance of HSCs three weeks after IAV infection, was shifted to co-expression of EPCR and CD41, which reassembles the HSC contribution found in 2 year old wt mice (Kovtonyuk et al., 2022). Data from mouse models and the clinic highlight that inflammatory conditions positively correlate with the formation of clonal hematopoiesis in the aged population (Mann et al., 2018; Zhang et al., 2019; Sezaki et al., 2020). This raises the question whether viral respiratory infections during life contribute to the phenomenon of HSC inflamm-aging. HSPCs self-renewal and engraftment potential, irrespective of the CD41-expression, was reduced during the acute phase of infection. However, HSC functionality and transcriptomic profiling after recovery from IAV infection should be conducted to shed light on whether phenotypically aged HSC were also aged in functionality after a single respiratory infection.

Contrary to inflamm-aging, IL-1 has been identified to be essential in the induction of innate immune training, also known as 'trained immunity' (Mitroulis et al., 2018; Moorlag et al., 2020). Thereby modulating the epigenetic landscape of HSPCs to induce a heritable, yet time restricted, effect on the myeloid lineage to be adapted for imminent infections (Kaufmann et al., 2018). Epigenetic changes by histone modification remodeling in HSPCs after the exposure of LPS or beta-glucan were memorized for over 6 months and passed on to myeloid progenies (Laval et al., 2020). These HSCs keep the accessibility of genes to favor myeloid commitment to protect the host from further pathogens. Therefore, examination of trained immunity induced in HSPCs and mature myeloid cells and platelets recovered from IAV-infection would stress the idea that HSPCs are immune cells. Furthermore, this would provide a new approach for targeting immune memory, e.g., against pathogens, at the top of the hematopoietic hierarchy.

Although granulocytes are one of the first infiltrating innate immune cells into the IAV-infected lung attracted by inflammatory cytokines, I did not detect an amplified myeloid-biased output in infected animals. A reduced myeloid reconstitution in recipient mice transplanted with $CD41^+$ HSPCs was observed. This sets my study apart from stress hematopoiesis observed in LPS or bacterial challenged mice, with predominant emergency granulopoiesis (Manz and Boettcher, 2014). Important to note, the majority of congenic transplantations performed in other stress hematopoiesis studies identified the chimerism based on the CD45.1 and CD45.2 isoforms, which is unsuitable to detect platelet chimerism, since CD45 is not expressed on murine platelets. Consequently, only the myeloid compartment was analyzed, and it is unknown whether inflammation in these studies has an influence on MK/platelet-biased differentiation and reconstitution. This highlights the importance of membrane tagged fluorescence reporter mice as the tool for platelet analysis in transplantation experiments. Interestingly, the number of CMPs ($L^-K^+S^-CD34^+CD16/CD32^-$) dropped massively between 4 to 8 dpi during IAV infection. This reflects the time with highest neutrophil infiltration into the IAV-infected lung (Hermesh et al., 2010), supporting the hypothesis that granulocytes are produced from MPPs and especially the CMP pool rather than directly from the HSCs. This was elegantly shown by Morcos et al. during steady-state hematopoiesis, using computationally integrating experimental approaches for fate mapping, mitotic tracking, and single-cell RNA-sequencing. This study revealed that the differentiation from CMPs to myeloid and erythroid lineages is much more pronounced than to the generation of the megakaryocytic-lineage. This interpretation is supported by the relationship between myelopoiesis and megakaryopoiesis / thrombopoiesis observed in Mpl-KO mice hematopoiesis. Myeloid progenitor numbers (CMPs, GMPs and MEPs), including mature granulocytes in the peripheral blood, are less altered, while the numbers of HSCs, MKs and platelets are vastly reduced (own

data, Ng et al., 2014). CD41 upregulation was pronounced on HSCs, MPPs and MKPs, however, absent on CMPs, GMPs or MEPs during IAV infection in wt and Mpl-KO mice, strengthen the existence of the short cut pathway from HSPCs to the megakaryocytic lineage, which is extensively used during acute demand. Strikingly, THPO/MPL-independent thrombopoiesis in IAV-infected Mpl-KO mice were detected, which followed similar platelet count kinetic found in IAV-infected wt mice. This raises the question, whether Mpl-KO mice generate their MKs and platelets by using the short-cut pathway and not through defined progenitor cells or whether the short-cut pathway is the only existing mechanism in general. Two studies recently confirmed that HSCs directly contribute to MKPs in the absence of any intermediate in the MPP or CMP compartment during unperturbed steady-state hematopoiesis by transposon tagged cell tracing or RNA-sequencing, fate mapping and mitotic tracking (Rodriguez-Fraticelli et al., 2018; Morcos et al., 2022). One can hypothesize that, applying these described methodologies in the Mpl-deficient background would ultimately answer the question whether MKs are directly produced by HSCs or both pathways are used, however, during different demands.

5.3.5. Platelet function during IAV infection – hemostasis or innate immunity?

In addition to their role in hemostasis and maintaining blood vessel integrity, platelets have attributed functions in the innate immune response (Yeaman, 2014; Zufferey et al., 2017). IAV-induced emergency megakaryopoiesis enhanced MKP replenishment and endomitosis of existing MKPs and MKs in the BM. The newly generated MKPs or MKs produced platelets with larger in size, immature phenotype, and hyper-reactivity during the acute phase of IAV infection in wt mice. Hyper-reactive and immature platelets are reported in respiratory infections of IAV and SARS-CoV-2 in patients (Rondina et al., 2012; Fan et al., 2020; Manne et al., 2020). However, my model links the observation of altered platelet functionality and appearance with emergency megakaryopoiesis. The pro-coagulant platelets will have contributed to the IAV pathology with accumulated and aggregated platelets, which were located in pulmonary capillaries (Lê et al., 2015). IAV-damaged capillaries in the lung additionally contribute to the platelet activation. However, in IAV-infected IL1R1-KO mice, where emergency megakaryopoiesis was absent, only a mild change in platelet activation was observed. This bolsters that inflammatory-induced emergency megakaryopoiesis during IAV infection directly influences platelet functionality.

The presence of hyper-reactive platelets was recently linked to aging-associated inflammation induced by elevated levels of TNFα. In this scenario platelet-biased HSCs were increased and MK polyploidy higher and platelets had elevated mitochondrial mass and oxidative metabolism (Davizon-Castillo et al., 2019). Since increased TNFα levels and $CD41^+$ HSCs in the BM of IAV-infected mice were detected, emergency megakaryopoiesis-produced platelets may have

also higher mitochondrial mass with amplified metabolic activity. Elevated platelet metabolic activity via calcein AM as a measurement of platelet viability were detected, however, calcein AM is metabolized by unspecific esterases and does not correlate with the amount of mitochondria. Presumably, higher metabolic activity is related to the increased platelet size. Since transplanted CD41$^+$ HSPCs from IAV-infected mice memorized emergency megakaryopoiesis by enhanced platelet-biased reconstitution, it would be interesting to examine platelet functionality in recipient mice at different time points post transplantation. This would shed light on whether the pro-coagulant platelet functionality is related to platelet production / generation or that emergency megakaryopoiesis-produced MKs exhibited an altered gene expression equipping platelets with an enhanced functionality. Recent studies characterized MKs isolated by their ploidy states from 2n to 32n from the BM. This study performed single-cell transcriptome analysis and found distinct cellular heterogeneity (Sun et al., 2021). This group suggests a function-based classification of three MK subtypes (1) platelet generating aryl hydrocarbon receptor nuclear translocator like 1 (ARNTL$^+$) MKs (8n-32n), (2) HSC-niche supporting myosin light chain 4 (MYL4$^+$) MKs (8n-32n) and (3) immune tetraspanin-25 (CD53$^+$) and lymphocyte specific protein 1 (LSP1$^+$) MKs (2n-8n). Since rapid platelet replenishment was detected, IAV-induced emergency megakaryopoiesis would have replenished primarily platelet generating MKs. However, more precise characterization of MKs could elucidate whether emergency-produced MKs differ from steady-state produced MKs. Pro-inflammatory cytokines are able to change the global transcriptome of MKs towards antiviral and biological active genes, which are consequently passed on platelets, in RNA-transcripts or proteins, in the process of platelet formation. These antiviral equipped platelets may have a role in innate immunity next to hemostasis. Platelet transcriptomes from septic (Middleton et al., 2019), SARS-CoV-2 (Manne et al., 2020) and IAV H1N1 2009 (Campbell et al., 2019) patients showed alternation towards mitochondrial dysfunction, immune regulation and antigen presentation. This underlines the fast dynamic adaption of thrombopoiesis, that platelets can be reprogrammed to enhance hemostasis or gain immune cells functions in acute demands. Since inflammation is the driver of emergency megakaryopoiesis in IAV-infected mice and of CD41$^+$ HSPCs revealed positive correlation of innate immune response and antiviral genes in global transcriptome analysis, it is possible that emergency megakaryopoiesis-produced platelets exhibited immune functions. Investigating the transcriptome and proteome of MKPs and platelets could shed light on the question whether the fast platelet production is beneficial (immune effector function) or fueling the IAV-induced pathology (pro-thrombotic).

References

Acar, M., Kocherlakota, K.S., Murphy, M.M., Peyer, J.G., Oguro, H., Inra, C.N., Jaiyeola, C., Zhao, Z., Luby-Phelps, K., and Morrison, S.J. (2015). Deep imaging of bone marrow shows non-dividing stem cells are mainly perisinusoidal. Nature *526*, 126-130.

Adolfsson, J., Borge, O.J., Bryder, D., Theilgaard-Mönch, K., Astrand-Grundström, I., Sitnicka, E., Sasaki, Y., and Jacobsen, S.E. (2001). Upregulation of Flt3 expression within the bone marrow Lin(-)Sca1(+)c-kit(+) stem cell compartment is accompanied by loss of self-renewal capacity. Immunity *15*, 659-669.

Adolfsson, J., Månsson, R., Buza-Vidas, N., Hultquist, A., Liuba, K., Jensen, C.T., Bryder, D., Yang, L., Borge, O.-J., and Thoren, L.A.M., et al. (2005). Identification of Flt3+ lympho-myeloid stem cells lacking erythro-megakaryocytic potential a revised road map for adult blood lineage commitment. Cell *121*, 295-306.

Akashi, K., Traver, D., Miyamoto, T., and Weissman, I.L. (2000). A clonogenic common myeloid progenitor that gives rise to all myeloid lineages. Nature *404*, 193-197.

Alexander, W.S., Roberts, A.W., Nicola, N.A., Li, R., and Metcalf, D. (1996). Deficiencies in progenitor cells of multiple hematopoietic lineages and defective megakaryocytopoiesis in mice lacking the thrombopoietic receptor c-Mpl. Blood *87*, 2162-2170.

Alijotas-Reig, J., Esteve-Valverde, E., Belizna, C., Selva-O'Callaghan, A., Pardos-Gea, J., Quintana, A., Mekinian, A., Anunciacion-Llunell, A., and Miró-Mur, F. (2020). Immunomodulatory therapy for the management of severe COVID-19. Beyond the anti-viral therapy: A comprehensive review. Autoimmunity reviews *19*, 102569.

Anjos-Afonso, F., Buettner, F., Mian, S.A., Rhys, H., Perez-Lloret, J., Garcia-Albornoz, M., Rastogi, N., Ariza-McNaughton, L., and Bonnet, D. (2022). Single cell analyses identify a highly regenerative and homogenous human CD34+ hematopoietic stem cell population. Nature communications *13*, 2048.

Arai, F., Hirao, A., Ohmura, M., Sato, H., Matsuoka, S., Takubo, K., Ito, K., Koh, G.Y., and Suda, T. (2004). Tie2/angiopoietin-1 signaling regulates hematopoietic stem cell quiescence in the bone marrow niche. Cell *118*, 149-161.

Archimbaud, E., Ottmann, O.G., Yin, J.A., Lechner, K., Dombret, H., Sanz, M.A., Heil, G., Fenaux, P., Brugger, W., and Barge, A., et al. (1999). A randomized, double-blind, placebo-controlled study with pegylated recombinant human megakaryocyte growth and development factor (PEG-rHuMGDF) as an adjunct to chemotherapy for adults with de novo acute myeloid leukemia. Blood *94*, 3694-3701.

Asada, N., Kunisaki, Y., Pierce, H., Wang, Z., Fernandez, N.F., Birbrair, A., Ma'ayan, A., and Frenette, P.S. (2017). Differential cytokine contributions of perivascular haematopoietic stem cell niches. Nature cell biology *19*, 214-223.

Assinger, A. (2014). Platelets and infection - an emerging role of platelets in viral infection. Frontiers in immunology *5*, 649.

Athanasiou, M., Mavrothalassitis, G., Sun-Hoffman, L., and Blair, D.G. (2000). FLI-1 is a suppressor of erythroid differentiation in human hematopoietic cells. Leukemia *14*, 439-445.

Avraham, H., Cowley, S., Chi, S.Y., Jiang, S., and Groopman, J.E. (1993). Characterization of adhesive interactions between human endothelial cells and megakaryocytes. The Journal of clinical investigation *91*, 2378-2384.

Bae, J.-S., Yang, L., and Rezaie, A.R. (2007). Receptors of the protein C activation and activated protein C signaling pathways are colocalized in lipid rafts of endothelial cells. Proceedings of the National Academy of Sciences of the United States of America *104*, 2867-2872.

Bae, J.-S., Yang, L., and Rezaie, A.R. (2008). Lipid raft localization regulates the cleavage specificity of protease activated receptor 1 in endothelial cells. Journal of thrombosis and haemostasis : JTH *6*, 954-961.

Bai, L., Shi, G., Zhang, L., Guan, F., Ma, Y., Li, Q., and Cong, Y.-S. (2014). Cav-1 deletion impaired hematopoietic stem cell function. Cell death & disease *5*, e1140.

Balazs, A.B., Fabian, A.J., Esmon, C.T., and Mulligan, R.C. (2006). Endothelial protein C receptor (CD201) explicitly identifies hematopoietic stem cells in murine bone marrow. Blood *107*, 2317-2321.

Baldridge, M.T., King, K.Y., Boles, N.C., Weksberg, D.C., and Goodell, M.A. (2010). Quiescent haematopoietic stem cells are activated by IFN-gamma in response to chronic infection. Nature *465*, 793-797.

Ballmaier, M., Germeshausen, M., Schulze, H., Cherkaoui, K., Lang, S., Gaudig, A., Krukemeier, S., Eilers, M., Strauss, G., and Welte, K. (2001). c-mpl mutations are the cause of congenital amegakaryocytic thrombocytopenia. Blood *97*, 139-146.

Bastian, L.S., Kwiatkowski, B.A., Breininger, J., Danner, S., and Roth, G. (1999). Regulation of the megakaryocytic glycoprotein IX promoter by the oncogenic Ets transcription factor Fli-1. Blood *93*, 2637-2644.

Basu, S., Liang, H.P.H., Hernandez, I., Zogg, M., Fields, B., May, J., Ogoti, Y., Wyseure, T., Mosnier, L.O., and Burns, R.T., et al. (2020). Role of thrombomodulin expression on hematopoietic stem cells. Journal of thrombosis and haemostasis : JTH *18*, 123-135.

Beck, D., Thoms, J.A.I., Perera, D., Schütte, J., Unnikrishnan, A., Knezevic, K., Kinston, S.J., Wilson, N.K., O'Brien, T.A., and Göttgens, B., et al. (2013). Genome-wide analysis of transcriptional regulators in human HSPCs reveals a densely interconnected network of coding and noncoding genes. Blood *122*, e12-22.

Behrens, K., and Alexander, W.S. (2018). Cytokine control of megakaryopoiesis. Growth factors (Chur, Switzerland) *36*, 89-103.

Benveniste, P., Frelin, C., Janmohamed, S., Barbara, M., Herrington, R., Hyam, D., and Iscove, N.N. (2010). Intermediate-term hematopoietic stem cells with extended but time-limited reconstitution potential. Cell stem cell *6*, 48-58.

Benz, C., Copley, M.R., Kent, D.G., Wohrer, S., Cortes, A., Aghaeepour, N., Ma, E., Mader, H., Rowe, K., and Day, C., et al. (2012). Hematopoietic stem cell subtypes expand differentially during development and display distinct lymphopoietic programs. Cell stem cell *10*, 273-283.

Berenson, R.J., Andrews, R.G., Bensinger, W.I., Kalamasz, D., Knitter, G., Buckner, C.D., and Bernstein, I.D. (1988). Antigen CD34+ marrow cells engraft lethally irradiated baboons. The Journal of clinical investigation *81*, 951-955.

Bernitz, J.M., Kim, H.S., MacArthur, B., Sieburg, H., and Moore, K. (2016). Hematopoietic Stem Cells Count and Remember Self-Renewal Divisions. Cell *167*, 1296-1309.e10.

Besancenot, R., Chaligné, R., Tonetti, C., Pasquier, F., Marty, C., Lécluse, Y., Vainchenker, W., Constantinescu, S.N., and Giraudier, S. (2010). A senescence-like cell-cycle arrest occurs during megakaryocytic maturation: implications for physiological and pathological megakaryocytic proliferation. PLoS biology *8*.

Besancenot, R., Roos-Weil, D., Tonetti, C., Abdelouahab, H., Lacout, C., Pasquier, F., Willekens, C., Rameau, P., Lecluse, Y., and Micol, J.-B., et al. (2014). JAK2 and MPL protein levels determine TPO-induced megakaryocyte proliferation vs differentiation. Blood *124*, 2104-2115.

Bluteau, D., Balduini, A., Balayn, N., Currao, M., Nurden, P., Deswarte, C., Leverger, G., Noris, P., Perrotta, S., and Solary, E., et al. (2014). Thrombocytopenia-associated mutations in the ANKRD26 regulatory region induce MAPK hyperactivation. The Journal of clinical investigation *124*, 580-591.

Bogeska, R., Mikecin, A.-M., Kaschutnig, P., Fawaz, M., Büchler-Schäff, M., Le, D., Ganuza, M., Vollmer, A., Paffenholz, S.V., and Asada, N., et al. (2022). Inflammatory exposure drives long-lived impairment of hematopoietic stem cell self-renewal activity and accelerated aging. Cell stem cell *29*, 1273-1284.e8.

Bonig, H., and Papayannopoulou, T. (2013). Hematopoietic stem cell mobilization: updated conceptual renditions. Leukemia *27*, 24-31.

Botton, S. de, Sabri, S., Daugas, E., Zermati, Y., Guidotti, J.E., Hermine, O., Kroemer, G., Vainchenker, W., and Debili, N. (2002). Platelet formation is the consequence of caspase activation within megakaryocytes. Blood *100*, 1310-1317.

Bouillet, P., Metcalf, D., Huang, D.C., Tarlinton, D.M., Kay, T.W., Köntgen, F., Adams, J.M., and Strasser, A. (1999). Proapoptotic Bcl-2 relative Bim required for certain apoptotic responses, leukocyte homeostasis, and to preclude autoimmunity. Science (New York, N.Y.) *286*, 1735-1738.

Bouilloux, F., Juban, G., Cohet, N., Buet, D., Guyot, B., Vainchenker, W., Louache, F., and Morlé, F. (2008). EKLF restricts megakaryocytic differentiation at the benefit of erythrocytic differentiation. Blood *112*, 576-584.

Bradford, G.B., Williams, B., Rossi, R., and Bertoncello, I. (1997). Quiescence, cycling, and turnover in the primitive hematopoietic stem cell compartment. Experimental hematology *25*, 445-453.

Brecher, G., and Cronkite, E.P. (1951). Post-radiation parabiosis and survival in rats. Proceedings of the Society for Experimental Biology and Medicine. Society for Experimental Biology and Medicine (New York, N.Y.) *77*, 292-294.

Bresnick, E.H., Lee, H.-Y., Fujiwara, T., Johnson, K.D., and Keles, S. (2010). GATA switches as developmental drivers. The Journal of biological chemistry *285*, 31087-31093.

Brown, E., Carlin, L.M., Nerlov, C., Lo Celso, C., and Poole, A.W. (2018). Multiple membrane extrusion sites drive megakaryocyte migration into bone marrow blood vessels. Life science alliance *1*.

Broxmeyer, H.E., Orschell, C.M., Clapp, D.W., Hangoc, G., Cooper, S., Plett, P.A., Liles, W.C., Li, X., Graham-Evans, B., and Campbell, T.B., et al. (2005). Rapid mobilization of murine and human hematopoietic stem and progenitor cells with AMD3100, a CXCR4 antagonist. The Journal of experimental medicine *201*, 1307-1318.

Broxmeyer, H.E., Williams, D.E., Lu, L., Cooper, S., Anderson, S.L., Beyer, G.S., Hoffman, R., and Rubin, B.Y. (1986). The suppressive influences of human tumor necrosis factors on bone marrow hematopoietic progenitor cells from normal donors and patients with leukemia: synergism of tumor necrosis factor and interferon-gamma. Journal of immunology (Baltimore, Md. : 1950) *136*, 4487-4495.

Bruin, A.M. de, Demirel, Ö., Hooibrink, B., Brandts, C.H., and Nolte, M.A. (2013). Interferon-γ impairs proliferation of hematopoietic stem cells in mice. Blood *121*, 3578-3585.

Bryder, D., Ramsfjell, V., Dybedal, I., Theilgaard-Mönch, K., Högerkorp, C.M., Adolfsson, J., Borge, O.J., and Jacobsen, S.E. (2001). Self-renewal of multipotent long-term repopulating hematopoietic stem cells is negatively regulated by Fas and tumor necrosis factor receptor activation. The Journal of experimental medicine *194*, 941-952.

Bujanover, N., Goldstein, O., Greenshpan, Y., Turgeman, H., Klainberger, A., Scharff, Y., and Gazit, R. (2018). Identification of immune-activated hematopoietic stem cells. Leukemia *32*, 2016-2020.

Burstein, S.A., Mei, R.L., Henthorn, J., Friese, P., and Turner, K. (1992). Leukemia inhibitory factor and interleukin-11 promote maturation of murine and human megakaryocytes in vitro. Journal of cellular physiology *153*, 305-312.

Cabagnols, X., Favale, F., Pasquier, F., Messaoudi, K., Defour, J.P., Ianotto, J.C., Marzac, C., Le Couédic, J.P., Droin, N., and Chachoua, I., et al. (2016). Presence of atypical thrombopoietin receptor (MPL) mutations in triple-negative essential thrombocythemia patients. Blood *127*, 333-342.

Cabezas-Wallscheid, N., Klimmeck, D., Hansson, J., Lipka, D.B., Reyes, A., Wang, Q., Weichenhan, D., Lier, A., Paleske, L. von, and Renders, S., et al. (2014). Identification of regulatory networks in HSCs and their immediate progeny via integrated proteome, transcriptome, and DNA methylome analysis. Cell stem cell *15*, 507-522.

Calvi, L.M., Adams, G.B., Weibrecht, K.W., Weber, J.M., Olson, D.P., Knight, M.C., Martin, R.P., Schipani, E., Divieti, P., and Bringhurst, F.R., et al. (2003). Osteoblastic cells regulate the haematopoietic stem cell niche. Nature *425*, 841-846.

Campbell, R.A., Schwertz, H., Hottz, E.D., Rowley, J.W., Manne, B.K., Washington, A.V., Hunter-Mellado, R., Tolley, N.D., Christensen, M., and Eustes, A.S., et al. (2019). Human megakaryocytes possess intrinsic antiviral immunity through regulated induction of IFITM3. Blood *133*, 2013-2026.

Cantor, A.B., and Orkin, S.H. (2002). Transcriptional regulation of erythropoiesis: an affair involving multiple partners. Oncogene *21*, 3368-3376.

Chae, H.-D., Lee, K.E., Williams, D.A., and Gu, Y. (2008). Cross-talk between RhoH and Rac1 in regulation of actin cytoskeleton and chemotaxis of hematopoietic progenitor cells. Blood *111*, 2597-2605.

Chagraoui, J., Girard, S., Spinella, J.-F., Simon, L., Bonneil, E., Mayotte, N., MacRae, T., Coulombe-Huntington, J., Bertomeu, T., and Moison, C., et al. (2021). UM171 Preserves Epigenetic Marks that Are Reduced in Ex Vivo Culture of Human HSCs via Potentiation of the CLR3-KBTBD4 Complex. Cell stem cell *28*, 48-62.e6.

Challen, G.A., Boles, N.C., Chambers, S.M., and Goodell, M.A. (2010). Distinct hematopoietic stem cell subtypes are differentially regulated by TGF-beta1. Cell stem cell *6*, 265-278.

Che, J.L.C., Bode, D., Kucinski, I., Cull, A.H., Bain, F., Becker, H.J., Jassinskaja, M., Barile, M., Boyd, G., and Belmonte, M., et al. (2022). Identification and characterization of in vitro expanded hematopoietic stem cells. EMBO reports *23*, e55502.

Chen, S., Hu, M., Shen, M., Wang, S., Wang, C., Chen, F., Tang, Y., Wang, X., Zeng, H., and Chen, M., et al. (2018). IGF-1 facilitates thrombopoiesis primarily through Akt activation. Blood *132*, 210-222.

Chen, W.-M., Yu, B., Zhang, Q., and Xu, P. (2010). Identification of the residues in the extracellular domain of thrombopoietin receptor involved in the binding of thrombopoietin and a nuclear distribution protein (human NUDC). The Journal of biological chemistry *285*, 26697-26709.

Cheshier, S.H., Morrison, S.J., Liao, X., and Weissman, I.L. (1999). In vivo proliferation and cell cycle kinetics of long-term self-renewing hematopoietic stem cells. Proceedings of the National Academy of Sciences of the United States of America *96*, 3120-3125.

Cheshier, S.H., Prohaska, S.S., and Weissman, I.L. (2007). The effect of bleeding on hematopoietic stem cell cycling and self-renewal. Stem cells and development *16*, 707-717.

Christensen, J.L., and Weissman, I.L. (2001). Flk-2 is a marker in hematopoietic stem cell differentiation: a simple method to isolate long-term stem cells. Proceedings of the National Academy of Sciences of the United States of America *98*, 14541-14546.

Cockrell, A.S., Yount, B.L., Scobey, T., Jensen, K., Douglas, M., Beall, A., Tang, X.-C., Marasco, W.A., Heise, M.T., and Baric, R.S. (2016). A mouse model for MERS coronavirus-induced acute respiratory distress syndrome. Nature microbiology *2*, 16226.

Comazzetto, S., Murphy, M.M., Berto, S., Jeffery, E., Zhao, Z., and Morrison, S.J. (2019). Restricted Hematopoietic Progenitors and Erythropoiesis Require SCF from Leptin Receptor+ Niche Cells in the Bone Marrow. Cell stem cell *24*, 477-486.e6.

Cui, L., Moraga, I., Lerbs, T., van Neste, C., Wilmes, S., Tsutsumi, N., Trotman-Grant, A.C., Gakovic, M., Andrews, S., and Gotlib, J., et al. (2021). Tuning MPL signaling to influence hematopoietic stem cell differentiation and inhibit essential thrombocythemia progenitors. Proc. Natl. Acad. Sci. U.S.A. *118*.

Currao, M., Balduini, C.L., and Balduini, A. (2013). High doses of romiplostim induce proliferation and reduce proplatelet formation by human megakaryocytes. PloS one *8*, e54723.

Cwirla, S.E., Balasubramanian, P., Duffin, D.J., Wagstrom, C.R., Gates, C.M., Singer, S.C., Davis, A.M., Tansik, R.L., Mattheakis, L.C., and Boytos, C.M., et al. (1997). Peptide agonist of the thrombopoietin receptor as potent as the natural cytokine. Science (New York, N.Y.) *276*, 1696-1699.

Dahlen, D.D., Broudy, V.C., and Drachman, J.G. (2003). Internalization of the thrombopoietin receptor is regulated by 2 cytoplasmic motifs. Blood *102*, 102-108.

Damia, G., Komschlies, K.L., Futami, H., Back, T., Gruys, M.E., Longo, D.L., Keller, J.R., Ruscetti, F.W., and Wiltrout, R.H. (1992). Prevention of acute chemotherapy-induced death in mice by recombinant human interleukin 1: protection from hematological and nonhematological toxicities. Cancer research *52*, 4082-4089.

Davizon-Castillo, P., McMahon, B., Aguila, S., Bark, D., Ashworth, K., Allawzi, A., Campbell, R.A., Montenont, E., Nemkov, T., and D'Alessandro, A., et al. (2019). TNF-α-driven inflammation and mitochondrial dysfunction define the platelet hyperreactivity of aging. Blood *134*, 727-740.

Decker, M., Leslie, J., Liu, Q., and Ding, L. (2018). Hepatic thrombopoietin is required for bone marrow hematopoietic stem cell maintenance. Science (New York, N.Y.) *360*, 106-110.

Decker, T., Müller, M., and Stockinger, S. (2005). The yin and yang of type I interferon activity in bacterial infection. Nature reviews. Immunology *5*, 675-687.

Demel, U.M., Lutz, R., Sujer, S., Demerdash, Y., Sood, S., Grünschläger, F., Kuck, A., Werner, P., Blaszkiewicz, S., and Uckelmann, H.J., et al. (2022). A complex proinflammatory cascade mediates the activation of HSCs upon LPS exposure in vivo. Blood advances *6*, 3513-3528.

Deutsch, V.R., and Tomer, A. (2006). Megakaryocyte development and platelet production. British journal of haematology *134*, 453-466.

Ding, L., and Morrison, S.J. (2013). Haematopoietic stem cells and early lymphoid progenitors occupy distinct bone marrow niches. Nature *495*, 231-235.

Ding, L., Saunders, T.L., Enikolopov, G., and Morrison, S.J. (2012). Endothelial and perivascular cells maintain haematopoietic stem cells. Nature *481*, 457-462.

Doré, L.C., and Crispino, J.D. (2011). Transcription factor networks in erythroid cell and megakaryocyte development. Blood *118*, 231-239.

Doulatov, S., Notta, F., Eppert, K., Nguyen, L.T., Ohashi, P.S., and Dick, J.E. (2010). Revised map of the human progenitor hierarchy shows the origin of macrophages and dendritic cells in early lymphoid development. Nature immunology *11*, 585-593.

Drachman, J.G., and Kaushansky, K. (1997). Dissecting the thrombopoietin receptor: functional elements of the Mpl cytoplasmic domain. Proc. Natl. Acad. Sci. U.S.A. *94*, 2350-2355.

Drachman, J.G., Millett, K.M., and Kaushansky, K. (1999). Thrombopoietin signal transduction requires functional JAK2, not TYK2. The Journal of biological chemistry *274*, 13480-13484.

Dubois, C.M., Ruscetti, F.W., Stankova, J., and Keller, J.R. (1994). Transforming growth factor-beta regulates c-kit message stability and cell-surface protein expression in hematopoietic progenitors. Blood *83*, 3138-3145.

Dütting, S., Gaits-Iacovoni, F., Stegner, D., Popp, M., Antkowiak, A., van Eeuwijk, J.M.M., Nurden, P., Stritt, S., Heib, T., and Aurbach, K., et al. (2017). A Cdc42/RhoA regulatory circuit downstream of glycoprotein Ib guides transendothelial platelet biogenesis. Nature communications *8*, 15838.

Dykstra, B., Kent, D., Bowie, M., McCaffrey, L., Hamilton, M., Lyons, K., Lee, S.-J., Brinkman, R., and Eaves, C. (2007). Long-term propagation of distinct hematopoietic differentiation programs in vivo. Cell stem cell *1*, 218-229.

Eckly, A., Heijnen, H., Pertuy, F., Geerts, W., Proamer, F., Rinckel, J.-Y., Léon, C., Lanza, F., and Gachet, C. (2014). Biogenesis of the demarcation membrane system (DMS) in megakaryocytes. Blood *123*, 921-930.

Edginton-White, B., and Bonifer, C. (2022). The transcriptional regulation of normal and malignant blood cell development. The FEBS journal *289*, 1240-1255.

Esplin, B.L., Shimazu, T., Welner, R.S., Garrett, K.P., Nie, L., Zhang, Q., Humphrey, M.B., Yang, Q., Borghesi, L.A., and Kincade, P.W. (2011). Chronic exposure to a TLR ligand injures hematopoietic stem cells. Journal of immunology (Baltimore, Md. : 1950) *186*, 5367-5375.

Essers, M.A.G., Offner, S., Blanco-Bose, W.E., Waibler, Z., Kalinke, U., Duchosal, M.A., and Trumpp, A. (2009). IFNalpha activates dormant haematopoietic stem cells in vivo. Nature *458*, 904-908.

Ezumi, Y., Takayama, H., and Okuma, M. (1995). Thrombopoietin, c-Mpl ligand, induces tyrosine phosphorylation of Tyk2, JAK2, and STAT3, and enhances agonists-induced aggregation in platelets in vitro. FEBS letters *374*, 48-52.

Fan, B.E., Chong, V.C.L., Chan, S.S.W., Lim, G.H., Lim, K.G.E., Tan, G.B., Mucheli, S.S., Kuperan, P., and Ong, K.H. (2020). Hematologic parameters in patients with COVID-19 infection. American journal of hematology *95*, E131-E134.

Fares, I., Chagraoui, J., Gareau, Y., Gingras, S., Ruel, R., Mayotte, N., Csaszar, E., Knapp, D.J.H.F., Miller, P., and Ngom, M., et al. (2014). Cord blood expansion. Pyrimidoindole derivatives are agonists of human hematopoietic stem cell self-renewal. Science (New York, N.Y.) *345*, 1509-1512.

Fares, I., Chagraoui, J., Lehnertz, B., MacRae, T., Mayotte, N., Tomellini, E., Aubert, L., Roux, P.P., and Sauvageau, G. (2017). EPCR expression marks UM171-expanded CD34+ cord blood stem cells. Blood *129*, 3344-3351.

Feese, M.D., Tamada, T., Kato, Y., Maeda, Y., Hirose, M., Matsukura, Y., Shigematsu, H., Muto, T., Matsumoto, A., and Watarai, H., et al. (2004). Structure of the receptor-binding domain of human thrombopoietin determined by complexation with a neutralizing antibody fragment. Proceedings of the National Academy of Sciences of the United States of America *101*, 1816-1821.

Fielder, P.J., Gurney, A.L., Stefanich, E., Marian, M., Moore, M.W., Carver-Moore, K., and Sauvage, F.J. de (1996). Regulation of thrombopoietin levels by c-mpl-mediated binding to platelets. Blood *87*, 2154-2161.

Forsberg, E.C., Prohaska, S.S., Katzman, S., Heffner, G.C., Stuart, J.M., and Weissman, I.L. (2005). Differential expression of novel potential regulators in hematopoietic stem cells. PLoS genetics *1*, e28.

Foudi, A., Hochedlinger, K., van Buren, D., Schindler, J.W., Jaenisch, R., Carey, V., and Hock, H. (2009). Analysis of histone 2B-GFP retention reveals slowly cycling hematopoietic stem cells. Nature biotechnology *27*, 84-90.

Fox, J.G., Barthold, S.W., Davisson, M.T., Newcomer, C.E., Quimby, F.W., and Smith, A.L. (2007). The mouse in biomedical research (Amsterdam: Elsevier).

Fritz, R.S., Hayden, F.G., Calfee, D.P., Cass, L.M., Peng, A.W., Alvord, W.G., Strober, W., and Straus, S.E. (1999). Nasal cytokine and chemokine responses in experimental influenza A virus infection: results of a placebo-controlled trial of intravenous zanamivir treatment. The Journal of infectious diseases *180*, 586-593.

Fröbel, J., Landspersky, T., Percin, G., Schreck, C., Rahmig, S., Ori, A., Nowak, D., Essers, M., Waskow, C., and Oostendorp, R.A.J. (2021). The Hematopoietic Bone Marrow Niche Ecosystem. Frontiers in cell and developmental biology *9*, 705410.

Fukudome, K., and Esmon, C.T. (1994). Identification, cloning, and regulation of a novel endothelial cell protein C/activated protein C receptor. The Journal of biological chemistry *269*, 26486-26491.

Gainsford, T., Nandurkar, H., Metcalf, D., Robb, L., Begley, C.G., and Alexander, W.S. (2000). The residual megakaryocyte and platelet production in c-mpl-deficient mice is not dependent on the actions of interleukin-6, interleukin-11, or leukemia inhibitory factor. Blood *95*, 528-534.

Galloway, J.L., Wingert, R.A., Thisse, C., Thisse, B., and Zon, L.I. (2005). Loss of gata1 but not gata2 converts erythropoiesis to myelopoiesis in zebrafish embryos. Developmental cell *8*, 109-116.

Gatti, R.A., Meuwissen, H.J., Allen, H.D., Hong, R., and Good, R.A. (1968). Immunological reconstitution of sex-linked lymphopenic immunological deficiency. Lancet (London, England) *2*, 1366-1369.

Gazit, R., Mandal, P.K., Ebina, W., Ben-Zvi, A., Nombela-Arrieta, C., Silberstein, L.E., and Rossi, D.J. (2014). Fgd5 identifies hematopoietic stem cells in the murine bone marrow. The Journal of experimental medicine *211*, 1315-1331.

Geddis, A.E., Fox, N.E., and Kaushansky, K. (2001). Phosphatidylinositol 3-kinase is necessary but not sufficient for thrombopoietin-induced proliferation in engineered Mpl-bearing cell lines as well as in primary megakaryocytic progenitors. The Journal of biological chemistry *276*, 34473-34479.

Gekas, C., and Graf, T. (2013). CD41 expression marks myeloid-biased adult hematopoietic stem cells and increases with age. Blood *121*, 4463-4472.

Ghanima, W., Cooper, N., Rodeghiero, F., Godeau, B., and Bussel, J.B. (2019). Thrombopoietin receptor agonists: ten years later. Haematologica *104*, 1112-1123.

Ghilardi, N., Wiestner, A., and Skoda, R.C. (1998). Thrombopoietin production is inhibited by a translational mechanism. Blood *92*, 4023-4030.

Gill, H., Leung, G.M.K., Lopes, D., and Kwong, Y.-L. (2017). The thrombopoietin mimetics eltrombopag and romiplostim in the treatment of refractory aplastic anaemia. British journal of haematology *176*, 991-994.

Glaccum, M.B., Stocking, K.L., Charrier, K., Smith, J.L., Willis, C.R., Maliszewski, C., Livingston, D.J., Peschon, J.J., and Morrissey, P.J. (1997). Phenotypic and functional characterization of mice that lack the type I receptor for IL-1. Journal of immunology (Baltimore, Md. : 1950) *159*, 3364-3371.

Graham, F.L., Smiley, J., Russell, W.C., and Nairn, R. (1977). Characteristics of a human cell line transformed by DNA from human adenovirus type 5. The Journal of general virology *36*, 59-74.

Greenberger, J.S., Sakakeeny, M.A., Humphries, R.K., Eaves, C.J., and Eckner, R.J. (1983). Demonstration of permanent factor-dependent multipotential (erythroid/neutrophil/basophil) hematopoietic progenitor cell lines. Proceedings of the National Academy of Sciences of the United States of America *80*, 2931-2935.

Grinenko, T., Arndt, K., Portz, M., Mende, N., Günther, M., Cosgun, K.N., Alexopoulou, D., Lakshmanaperumal, N., Henry, I., and Dahl, A., et al. (2014). Clonal expansion capacity defines two consecutive developmental stages of long-term hematopoietic stem cells. The Journal of experimental medicine *211*, 209-215.

Grover, A., Sanjuan-Pla, A., Thongjuea, S., Carrelha, J., Giustacchini, A., Gambardella, A., Macaulay, I., Mancini, E., Luis, T.C., and Mead, A., et al. (2016). Single-cell RNA sequencing reveals molecular and functional platelet bias of aged haematopoietic stem cells. Nature communications *7*, 11075.

Grozovsky, R., Begonja, A.J., Liu, K., Visner, G., Hartwig, J.H., Falet, H., and Hoffmeister, K.M. (2015). The Ashwell-Morell receptor regulates hepatic thrombopoietin production via JAK2-STAT3 signaling. Nature medicine *21*, 47-54.

Gur-Cohen, S., Itkin, T., Chakrabarty, S., Graf, C., Kollet, O., Ludin, A., Golan, K., Kalinkovich, A., Ledergor, G., and Wong, E., et al. (2015). PAR1 signaling regulates the retention and recruitment of EPCR-expressing bone marrow hematopoietic stem cells. Nature medicine *21*, 1307-1317.

Gurney, A.L., Carver-Moore, K., Sauvage, F.J. de, and Moore, M.W. (1994). Thrombocytopenia in c-mpl-deficient mice. Science (New York, N.Y.) *265*, 1445-1447.

Haas, S., Hansson, J., Klimmeck, D., Loeffler, D., Velten, L., Uckelmann, H., Wurzer, S., Prendergast, Á.M., Schnell, A., and Hexel, K., et al. (2015). Inflammation-Induced Emergency Megakaryopoiesis Driven by Hematopoietic Stem Cell-like Megakaryocyte Progenitors. Cell stem cell *17*, 422-434.

Haas, S., Trumpp, A., and Milsom, M.D. (2018). Causes and Consequences of Hematopoietic Stem Cell Heterogeneity. Cell stem cell *22*, 627-638.

Haltalli, M.L.R., Watcham, S., Wilson, N.K., Eilers, K., Lipien, A., Ang, H., Birch, F., Anton, S.G., Pirillo, C., and Ruivo, N., et al. (2020). Manipulating niche composition limits damage to haematopoietic stem cells during Plasmodium infection. Nature cell biology *22*, 1399-1410.

Hanika, A., Larisch, B., Steinmann, E., Schwegmann-Weßels, C., Herrler, G., and Zimmer, G. (2005). Use of influenza C virus glycoprotein HEF for generation of vesicular stomatitis virus pseudotypes. The Journal of general virology *86*, 1455-1465.

Harker, L.A., Roskos, L.K., Marzec, U.M., Carter, R.A., Cherry, J.K., Sundell, B., Cheung, E.N., Terry, D., and Sheridan, W. (2000). Effects of megakaryocyte growth and development factor on platelet production, platelet life span, and platelet function in healthy human volunteers. Blood *95*, 2514-2522.

Hartley, J.W., and Rowe, W.P. (1975). Clonal cells lines from a feral mouse embryo which lack host-range restrictions for murine leukemia viruses. Virology *65*, 128-134.

Heckl, D., Wicke, D.C., Brugman, M.H., Meyer, J., Schambach, A., Büsche, G., Ballmaier, M., Baum, C., and Modlich, U. (2011). Lentiviral gene transfer regenerates hematopoietic stem cells in a mouse model for Mpl-deficient aplastic anemia. Blood *117*, 3737-3747.

Heib, T., Hermanns, H.M., Manukjan, G., Englert, M., Kusch, C., Becker, I.C., Gerber, A., Wackerbarth, L.M., Burkard, P., and Dandekar, T., et al. (2021). RhoA/Cdc42 signaling drives cytoplasmic maturation but not endomitosis in megakaryocytes. Cell reports *35*, 109102.

Hermesh, T., Moltedo, B., Moran, T.M., and López, C.B. (2010). Antiviral instruction of bone marrow leukocytes during respiratory viral infections. Cell host & microbe *7*, 343-353.

Herrera, R., Hubbell, S., Decker, S., and Petruzzelli, L. (1998). A role for the MEK/MAPK pathway in PMA-induced cell cycle arrest: modulation of megakaryocytic differentiation of K562 cells. Experimental cell research *238*, 407-414.

Heuston, E.F., Keller, C.A., Lichtenberg, J., Giardine, B., Anderson, S.M., Hardison, R.C., and Bodine, D.M. (2018). Establishment of regulatory elements during erythro-megakaryopoiesis identifies hematopoietic lineage-commitment points. Epigenetics & chromatin *11*, 22.

Hidalgo San Jose, L., Sunshine, M.J., Dillingham, C.H., Chua, B.A., Kruta, M., Hong, Y., Hatters, D.M., and Signer, R.A.J. (2020). Modest Declines in Proteome Quality Impair Hematopoietic Stem Cell Self-Renewal. Cell reports *30*, 69-80.e6.

Hirche, C., Frenz, T., Haas, S.F., Döring, M., Borst, K., Tegtmeyer, P.-K., Brizic, I., Jordan, S., Keyser, K., and Chhatbar, C., et al. (2017). Systemic Virus Infections Differentially Modulate Cell Cycle State and Functionality of Long-Term Hematopoietic Stem Cells In Vivo. Cell reports *19*, 2345-2356.

Hitchcock, I.S., Chen, M.M., King, J.R., and Kaushansky, K. (2008). YRRL motifs in the cytoplasmic domain of the thrombopoietin receptor regulate receptor internalization and degradation. Blood *112*, 2222-2231.

Ho, T.T., Warr, M.R., Adelman, E.R., Lansinger, O.M., Flach, J., Verovskaya, E.V., Figueroa, M.E., and Passegué, E. (2017). Autophagy maintains the metabolism and function of young and old stem cells. Nature *543*, 205-210.

Huang, H., and Cantor, A.B. (2009). Common features of megakaryocytes and hematopoietic stem cells: what's the connection? Journal of cellular biochemistry *107*, 857-864.

Ihara, K., Ishii, E., Eguchi, M., Takada, H., Suminoe, A., Good, R.A., and Hara, T. (1999). Identification of mutations in the c-mpl gene in congenital amegakaryocytic thrombocytopenia. Proceedings of the National Academy of Sciences of the United States of America *96*, 3132-3136.

Ikonomi, P., Noguchi, C.T., Miller, W., Kassahun, H., Hardison, R., and Schechter, A.N. (2000a). Levels of GATA-1/GATA-2 transcription factors modulate expression of embryonic and fetal hemoglobins. Gene *261*, 277-287.

Ikonomi, P., Rivera, C.E., Riordan, M., Washington, G., Schechter, A.N., and Noguchi, C.T. (2000b). Overexpression of GATA-2 inhibits erythroid and promotes megakaryocyte differentiation. Experimental hematology *28*, 1423-1431.

Ikuta, K., Ingolia, D.E., Friedman, J., Heimfeld, S., and Weissman, I.L. (1991). Mouse hematopoietic stem cells and the interaction of c-kit receptor and steel factor. International journal of cell cloning *9*, 451-460.

Ikuta, K., and Weissman, I.L. (1992). Evidence that hematopoietic stem cells express mouse c-kit but do not depend on steel factor for their generation. Proceedings of the National Academy of Sciences of the United States of America *89*, 1502-1506.

Inra, C.N., Zhou, B.O., Acar, M., Murphy, M.M., Richardson, J., Zhao, Z., and Morrison, S.J. (2015). A perisinusoidal niche for extramedullary haematopoiesis in the spleen. Nature *527*, 466-471.

Ishibashi, T., Kimura, H., Uchida, T., Kariyone, S., Friese, P., and Burstein, S.A. (1989). Human interleukin 6 is a direct promoter of maturation of megakaryocytes in vitro. Proceedings of the National Academy of Sciences of the United States of America *86*, 5953-5957.

Italiano, J.E., Patel-Hett, S., and Hartwig, J.H. (2007). Mechanics of proplatelet elaboration. Journal of thrombosis and haemostasis : JTH *5 Suppl 1*, 18-23.

Ito, K., Turcotte, R., Cui, J., Zimmerman, S.E., Pinho, S., Mizoguchi, T., Arai, F., Runnels, J.M., Alt, C., and Teruya-Feldstein, J., et al. (2016). Self-renewal of a purified Tie2+ hematopoietic stem cell population relies on mitochondrial clearance. Science (New York, N.Y.) *354*, 1156-1160.

Iwasaki, H., Arai, F., Kubota, Y., Dahl, M., and Suda, T. (2010). Endothelial protein C receptor-expressing hematopoietic stem cells reside in the perisinusoidal niche in fetal liver. Blood *116*, 544-553.

Jacobson, L.O., Simmons, E.L., Marks, E.K., and Eldredge, J.H. (1951). Recovery from radiation injury. Science (New York, N.Y.) *113*, 510-511.

Jagerschmidt, A., Fleury, V., Anger-Leroy, M., Thomas, C., Agnel, M., and O'brien, D.P. (1998). Human thrombopoietin structure-function relationships: identification of functionally important residues. The Biochemical journal *333 (Pt 3)*, 729-734.

Jahn, T., Leifheit, E., Gooch, S., Sindhu, S., and Weinberg, K. (2007). Lipid rafts are required for Kit survival and proliferation signals. Blood *110*, 1739-1747.

Jain, S., Kamimoto, L., Bramley, A.M., Schmitz, A.M., Benoit, S.R., Louie, J., Sugerman, D.E., Druckenmiller, J.K., Ritger, K.A., and Chugh, R., et al. (2009). Hospitalized patients with 2009 H1N1 influenza in the United States, April-June 2009. The New England journal of medicine *361*, 1935-1944.

Josefsson, E.C., Vainchenker, W., and James, C. (2020). Regulation of Platelet Production and Life Span: Role of Bcl-xL and Potential Implications for Human Platelet Diseases. International journal of molecular sciences *21*.

Junt, T., Schulze, H., Chen, Z., Massberg, S., Goerge, T., Krueger, A., Wagner, D.D., Graf, T., Italiano, J.E., and Shivdasani, R.A., et al. (2007). Dynamic visualization of thrombopoiesis within bone marrow. Science (New York, N.Y.) *317*, 1767-1770.

Kaiser, L., Fritz, R.S., Straus, S.E., Gubareva, L., and Hayden, F.G. (2001). Symptom pathogenesis during acute influenza: interleukin-6 and other cytokine responses. Journal of medical virology *64*, 262-268.

Kaluzhny, Y., Yu, G., Sun, S., Toselli, P.A., Nieswandt, B., Jackson, C.W., and Ravid, K. (2002). BclxL overexpression in megakaryocytes leads to impaired platelet fragmentation. Blood *100*, 1670-1678.

Kanayama, M., Izumi, Y., Yamauchi, Y., Kuroda, S., Shin, T., Ishikawa, S., Sato, T., Kajita, M., and Ohteki, T. (2020). CD86-based analysis enables observation of bona fide hematopoietic responses. Blood *136*, 1144-1154.

Kaser, A., Brandacher, G., Steurer, W., Kaser, S., Offner, F.A., Zoller, H., Theurl, I., Widder, W., Molnar, C., and Ludwiczek, O., et al. (2001). Interleukin-6 stimulates thrombopoiesis through thrombopoietin: role in inflammatory thrombocytosis. Blood *98*, 2720-2725.

Kaufmann, E., Sanz, J., Dunn, J.L., Khan, N., Mendonça, L.E., Pacis, A., Tzelepis, F., Pernet, E., Dumaine, A., and Grenier, J.-C., et al. (2018). BCG Educates Hematopoietic Stem Cells to Generate Protective Innate Immunity against Tuberculosis. Cell *172*, 176-190.e19.

Kaushansky, K. (2005). The molecular mechanisms that control thrombopoiesis. The Journal of clinical investigation *115*, 3339-3347.

Kaushansky, K., Lok, S., Holly, R.D., Broudy, V.C., Lin, N., Bailey, M.C., Forstrom, J.W., Buddle, M.M., Oort, P.J., and Hagen, F.S. (1994). Promotion of megakaryocyte progenitor expansion and differentiation by the c-Mpl ligand thrombopoietin. Nature *369*, 568-571.

Kent, D.G., Copley, M.R., Benz, C., Wöhrer, S., Dykstra, B.J., Ma, E., Cheyne, J., Zhao, Y., Bowie, M.B., and Zhao, Y., et al. (2009). Prospective isolation and molecular characterization of hematopoietic stem cells with durable self-renewal potential. Blood *113*, 6342-6350.

Kiel, M.J., Yilmaz, O.H., Iwashita, T., Yilmaz, O.H., Terhorst, C., and Morrison, S.J. (2005). SLAM family receptors distinguish hematopoietic stem and progenitor cells and reveal endothelial niches for stem cells. Cell *121*, 1109-1121.

Kim, J.K., Jeon, J.-S., Kim, J.W., and Kim, G.-Y. (2016). Correlation Between Abnormal Platelet Count and Respiratory Viral Infection in Patients From Cheonan, Korea. Journal of clinical laboratory analysis *30*, 185-189.

Kimura, H., Ishibashi, T., Shikama, Y., Okano, A., Akiyama, Y., Uchida, T., and Maruyama, Y. (1990). Interleukin-1 beta (IL-1 beta) induces thrombocytosis in mice: possible implication of IL-6. Blood *76*, 2493-2500.

King, K.Y., and Goodell, M.A. (2011). Inflammatory modulation of HSCs: viewing the HSC as a foundation for the immune response. Nature reviews. Immunology *11*, 685-692.

Kohlscheen, S., Schenk, F., Rommel, M.G.E., Cullmann, K., and Modlich, U. (2019). Endothelial protein C receptor supports hematopoietic stem cell engraftment and expansion in Mpl-deficient mice. Blood *133*, 1465-1478.

Kohlscheen, S., Wintterle, S., Schwarzer, A., Kamp, C., Brugman, M.H., Breuer, D.C., Büsche, G., Baum, C., and Modlich, U. (2015). Inhibition of Thrombopoietin/Mpl Signaling in Adult Hematopoiesis Identifies New Candidates for Hematopoietic Stem Cell Maintenance. PloS one *10*, e0131866.

Kondo, M., Weissman, I.L., and Akashi, K. (1997). Identification of clonogenic common lymphoid progenitors in mouse bone marrow. Cell *91*, 661-672.

Kopf, M., Baumann, H., Freer, G., Freudenberg, M., Lamers, M., Kishimoto, T., Zinkernagel, R., Bluethmann, H., and Köhler, G. (1994). Impaired immune and acute-phase responses in interleukin-6-deficient mice. Nature *368*, 339-342.

Koseoglu, S., and Flaumenhaft, R. (2013). Advances in platelet granule biology. Current opinion in hematology *20*, 464-471.

Kovtonyuk, L.V., Caiado, F., Garcia-Martin, S., Manz, E.-M., Helbling, P., Takizawa, H., Boettcher, S., Al-Shahrour, F., Nombela-Arrieta, C., and Slack, E., et al. (2022). IL-1 mediates microbiome-induced inflammaging of hematopoietic stem cells in mice. Blood *139*, 44-58.

Kristinsson, S.Y., Björkholm, M., Hultcrantz, M., Derolf, Å.R., Landgren, O., and Goldin, L.R. (2011). Chronic immune stimulation might act as a trigger for the development of acute myeloid leukemia or myelodysplastic syndromes. Journal of clinical oncology : official journal of the American Society of Clinical Oncology *29*, 2897-2903.

Ku, H., Yonemura, Y., Kaushansky, K., and Ogawa, M. (1996). Thrombopoietin, the ligand for the Mpl receptor, synergizes with steel factor and other early acting cytokines in supporting proliferation of primitive hematopoietic progenitors of mice. Blood *87*, 4544-4551.

Kuter, D.J. (2002). Whatever happened to thrombopoietin? Transfusion *42*, 279-283.

Kuter, D.J. (2013). The biology of thrombopoietin and thrombopoietin receptor agonists. International journal of hematology *98*, 10-23.

Kuter, D.J., Goodnough, L.T., Romo, J., DiPersio, J., Peterson, R., Tomita, D., Sheridan, W., and McCullough, J. (2001). Thrombopoietin therapy increases platelet yields in healthy platelet donors. Blood *98*, 1339-1345.

Kuter, D.J., Mufti, G.J., Bain, B.J., Hasserjian, R.P., Davis, W., and Rutstein, M. (2009). Evaluation of bone marrow reticulin formation in chronic immune thrombocytopenia patients treated with romiplostim. Blood *114*, 3748-3756.

Kuter, D.J., and Rosenberg, R.D. (1995). The reciprocal relationship of thrombopoietin (c-Mpl ligand) to changes in the platelet mass during busulfan-induced thrombocytopenia in the rabbit. Blood *85*, 2720-2730.

Kuvardina, O.N., Herglotz, J., Kolodziej, S., Kohrs, N., Herkt, S., Wojcik, B., Oellerich, T., Corso, J., Behrens, K., and Kumar, A., et al. (2015). RUNX1 represses the erythroid gene expression program during megakaryocytic differentiation. Blood *125*, 3570-3579.

Kwiatkowski, B.A., Bastian, L.S., Bauer, T.R., Tsai, S., Zielinska-Kwiatkowska, A.G., and Hickstein, D.D. (1998). The ets family member Tel binds to the Fli-1 oncoprotein and inhibits its transcriptional activity. The Journal of biological chemistry *273*, 17525-17530.

Laurenti, E., and Göttgens, B. (2018). From haematopoietic stem cells to complex differentiation landscapes. Nature *553*, 418-426.

Laval, B. de, Maurizio, J., Kandalla, P.K., Brisou, G., Simonnet, L., Huber, C., Gimenez, G., Matcovitch-Natan, O., Reinhardt, S., and David, E., et al. (2020). C/EBPβ-Dependent Epigenetic Memory Induces Trained Immunity in Hematopoietic Stem Cells. Cell stem cell *26*, 657-674.e8.

Lê, V.B., Schneider, J.G., Boergeling, Y., Berri, F., Ducatez, M., Guerin, J.-L., Adrian, I., Errazuriz-Cerda, E., Frasquilho, S., and Antunes, L., et al. (2015). Platelet activation and aggregation promote lung inflammation and influenza virus pathogenesis. American journal of respiratory and critical care medicine *191*, 804-819.

Lee, J.K.H., Lam, G.K.L., Shin, T., Samson, S.I., Greenberg, D.P., and Chit, A. (2021). Efficacy and effectiveness of high-dose influenza vaccine in older adults by circulating strain and antigenic match: An updated systematic review and meta-analysis. Vaccine *39 Suppl 1*, A24-A35.

Lee, J.W., Lee, S.-E., Jung, C.W., Park, S., Keta, H., Park, S.K., Kim, J.-A., Oh, I.-H., and Jang, J.H. (2019). Romiplostim in patients with refractory aplastic anaemia previously treated with immunosuppressive therapy: a dose-finding and long-term treatment phase 2 trial. The Lancet. Haematology *6*, e562-e572.

Lefrançais, E., Ortiz-Muñoz, G., Caudrillier, A., Mallavia, B., Liu, F., Sayah, D.M., Thornton, E.E., Headley, M.B., David, T., and Coughlin, S.R., et al. (2017). The lung is a site of platelet biogenesis and a reservoir for haematopoietic progenitors. Nature *544*, 105-109.

Lemischka, I.R., Raulet, D.H., and Mulligan, R.C. (1986). Developmental potential and dynamic behavior of hematopoietic stem cells. Cell *45*, 917-927.

Levin, J., Peng, J.P., Baker, G.R., Villeval, J.L., Lecine, P., Burstein, S.A., and Shivdasani, R.A. (1999). Pathophysiology of thrombocytopenia and anemia in mice lacking transcription factor NF-E2. Blood *94*, 3037-3047.

Levin, J.Z., Yassour, M., Adiconis, X., Nusbaum, C., Thompson, D.A., Friedman, N., Gnirke, A., and Regev, A. (2010). Comprehensive comparative analysis of strand-specific RNA sequencing methods. Nature methods *7*, 709-715.

Li, J., Yang, C., Xia, Y., Bertino, A., Glaspy, J., Roberts, M., and Kuter, D.J. (2001). Thrombocytopenia caused by the development of antibodies to thrombopoietin. Blood *98*, 3241-3248.

Li, Z., Schwieger, M., Lange, C., Kraunus, J., Sun, H., van den Akker, E., Modlich, U., Serinsöz, E., Will, E., and Laer, D. von, et al. (2003). Predictable and efficient retroviral gene transfer into murine bone marrow repopulating cells using a defined vector dose. Experimental hematology *31*, 1206-1214.

Lin, J.-X., and Leonard, W.J. (2019). Fine-Tuning Cytokine Signals. Annual review of immunology *37*, 295-324.

Linden, H.M., and Kaushansky, K. (2000). The glycan domain of thrombopoietin enhances its secretion. Biochemistry *39*, 3044-3051.

Linden, H.M., and Kaushansky, K. (2002). The glycan domain of thrombopoietin (TPO) acts in trans to enhance secretion of the hormone and other cytokines. The Journal of biological chemistry *277*, 35240-35247.

Livnah, O., Stura, E.A., Middleton, S.A., Johnson, D.L., Jolliffe, L.K., and Wilson, I.A. (1999). Crystallographic evidence for preformed dimers of erythropoietin receptor before ligand activation. Science (New York, N.Y.) *283*, 987-990.

Long, M.W., Heffner, C.H., Williams, J.L., Peters, C., and Prochownik, E.V. (1990). Regulation of megakaryocyte phenotype in human erythroleukemia cells. The Journal of clinical investigation *85*, 1072-1084.

Lord, B.I., Testa, N.G., and Hendry, J.H. (1975). The relative spatial distributions of CFUs and CFUc in the normal mouse femur. Blood *46*, 65-72.

Luoh, S.M., Stefanich, E., Solar, G., Steinmetz, H., Lipari, T., Pestina, T.I., Jackson, C.W., and Sauvage, F.J. de (2000). Role of the distal half of the c-Mpl intracellular domain in control of platelet production by thrombopoietin in vivo. Molecular and cellular biology *20*, 507-515.

Macpherson, I., and Stoker, M. (1962). Polyoma transformation of hamster cell clones--an investigation of genetic factors affecting cell competence. Virology *16*, 147-151.

Madin, S.H., and Darby, N.B. (1958). Established kidney cell lines of normal adult bovine and ovine origin. Proceedings of the Society for Experimental Biology and Medicine. Society for Experimental Biology and Medicine (New York, N.Y.) *98*, 574-576.

Malek, T.R., Danis, K.M., and Codias, E.K. (1989). Tumor necrosis factor synergistically acts with IFN-gamma to regulate Ly-6A/E expression in T lymphocytes, thymocytes and bone marrow cells. Journal of immunology (Baltimore, Md. : 1950) *142*, 1929-1936.

Mann, M., Mehta, A., Boer, C.G. de, Kowalczyk, M.S., Lee, K., Haldeman, P., Rogel, N., Knecht, A.R., Farouq, D., and Regev, A., et al. (2018). Heterogeneous Responses of Hematopoietic Stem Cells to Inflammatory Stimuli Are Altered with Age. Cell reports *25*, 2992-3005.e5.

Manne, B.K., Denorme, F., Middleton, E.A., Portier, I., Rowley, J.W., Stubben, C., Petrey, A.C., Tolley, N.D., Guo, L., and Cody, M., et al. (2020). Platelet gene expression and function in patients with COVID-19. Blood *136*, 1317-1329.

Månsson, R., Hultquist, A., Luc, S., Yang, L., Anderson, K., Kharazi, S., Al-Hashmi, S., Liuba, K., Thorén, L., and Adolfsson, J., et al. (2007). Molecular evidence for hierarchical transcriptional lineage priming in fetal and adult stem cells and multipotent progenitors. Immunity *26*, 407-419.

Manz, M.G., and Boettcher, S. (2014). Emergency granulopoiesis. Nature reviews. Immunology *14*, 302-314.

Marshall-Clarke, S., Downes, J.E., Haga, I.R., Bowie, A.G., Borrow, P., Pennock, J.L., Grencis, R.K., and Rothwell, P. (2007). Polyinosinic acid is a ligand for toll-like receptor 3. The Journal of biological chemistry *282*, 24759-24766.

Martin, F., Prandini, M.H., Thevenon, D., Marguerie, G., and Uzan, G. (1993). The transcription factor GATA-1 regulates the promoter activity of the platelet glycoprotein IIb gene. The Journal of biological chemistry *268*, 21606-21612.

Martin, P., and Papayannopoulou, T. (1982). HEL cells: a new human erythroleukemia cell line with spontaneous and induced globin expression. Science (New York, N.Y.) *216*, 1233-1235.

Matatall, K.A., Jeong, M., Chen, S., Sun, D., Chen, F., Mo, Q., Kimmel, M., and King, K.Y. (2016). Chronic Infection Depletes Hematopoietic Stem Cells through Stress-Induced Terminal Differentiation. Cell reports *17*, 2584-2595.

Matatall, K.A., Shen, C.-C., Challen, G.A., and King, K.Y. (2014). Type II interferon promotes differentiation of myeloid-biased hematopoietic stem cells. Stem cells (Dayton, Ohio) *32*, 3023-3030.

Mathé, G., Amiel, J.L., Schwarzenberg, L., Cattan, A., and Schneider, M. (1965). Adoptive immunotherapy of acute leukemia: experimental and clinical results. Cancer research *25*, 1525-1531.

Matsumura, I. (1999). Transcriptional regulation of the cyclin D1 promoter by STAT5: its involvement in cytokine-dependent growth of hematopoietic cells. The EMBO journal *18*, 1367-1377.

Matthews, E.E., Thévenin, D., Rogers, J.M., Gotow, L., Lira, P.D., Reiter, L.A., Brissette, W.H., and Engelman, D.M. (2011). Thrombopoietin receptor activation: transmembrane helix dimerization, rotation, and allosteric modulation. FASEB journal : official publication of the Federation of American Societies for Experimental Biology *25*, 2234-2244.

McKinstry, W.J., Li, C.L., Rasko, J.E., Nicola, N.A., Johnson, G.R., and Metcalf, D. (1997). Cytokine receptor expression on hematopoietic stem and progenitor cells. Blood *89*, 65-71.

Medzhitov, R. (2008). Origin and physiological roles of inflammation. Nature *454*, 428-435.

Megías, J., Yáñez, A., Moriano, S., O'Connor, J.-E., Gozalbo, D., and Gil, M.-L. (2012). Direct Toll-like receptor-mediated stimulation of hematopoietic stem and progenitor cells occurs in vivo and promotes differentiation toward macrophages. Stem cells (Dayton, Ohio) *30*, 1486-1495.

Mehta, P., McAuley, D.F., Brown, M., Sanchez, E., Tattersall, R.S., and Manson, J.J. (2020). COVID-19: consider cytokine storm syndromes and immunosuppression. Lancet (London, England) *395*, 1033-1034.

Melemed, A.S., Ryder, J.W., and Vik, T.A. (1997). Activation of the mitogen-activated protein kinase pathway is involved in and sufficient for megakaryocytic differentiation of CMK cells. Blood *90*, 3462-3470.

Méndez-Ferrer, S., Lucas, D., Battista, M., and Frenette, P.S. (2008). Haematopoietic stem cell release is regulated by circadian oscillations. Nature *452*, 442-447.

Méndez-Ferrer, S., Michurina, T.V., Ferraro, F., Mazloom, A.R., Macarthur, B.D., Lira, S.A., Scadden, D.T., Ma'ayan, A., Enikolopov, G.N., and Frenette, P.S. (2010). Mesenchymal and haematopoietic stem cells form a unique bone marrow niche. Nature *466*, 829-834.

Middleton, E.A., Rowley, J.W., Campbell, R.A., Grissom, C.K., Brown, S.M., Beesley, S.J., Schwertz, H., Kosaka, Y., Manne, B.K., and Krauel, K., et al. (2019). Sepsis alters the transcriptional and translational landscape of human and murine platelets. Blood *134*, 911-923.

Miller, I., Min, M., Yang, C., Tian, C., Gookin, S., Carter, D., and Spencer, S.L. (2018). Ki67 is a Graded Rather than a Binary Marker of Proliferation versus Quiescence. Cell reports *24*, 1105-1112.e5.

Mitroulis, I., Kalafati, L., Bornhäuser, M., Hajishengallis, G., and Chavakis, T. (2020). Regulation of the Bone Marrow Niche by Inflammation. Frontiers in immunology *11*, 1540.

Mitroulis, I., Ruppova, K., Wang, B., Chen, L.-S., Grzybek, M., Grinenko, T., Eugster, A., Troullinaki, M., Palladini, A., and Kourtzelis, I., et al. (2018). Modulation of Myelopoiesis Progenitors Is an Integral Component of Trained Immunity. Cell *172*, 147-161.e12.

Moltedo, B., López, C.B., Pazos, M., Becker, M.I., Hermesh, T., and Moran, T.M. (2009). Cutting edge: stealth influenza virus replication precedes the initiation of adaptive immunity. Journal of immunology (Baltimore, Md. : 1950) *183*, 3569-3573.

Moorlag, S.J.C.F.M., Khan, N., Novakovic, B., Kaufmann, E., Jansen, T., van Crevel, R., Divangahi, M., and Netea, M.G. (2020). β-Glucan Induces Protective Trained Immunity against Mycobacterium tuberculosis Infection: A Key Role for IL-1. Cell reports *31*, 107634.

Morcos, M.N.F., Li, C., Munz, C.M., Greco, A., Dressel, N., Reinhardt, S., Sameith, K., Dahl, A., Becker, N.B., and Roers, A., et al. (2022). Fate mapping of hematopoietic stem cells reveals two pathways of native thrombopoiesis. Nature communications *13*, 4504.

Morrison, S.J., and Scadden, D.T. (2014). The bone marrow niche for haematopoietic stem cells. Nature *505*, 327-334.

Morrison, S.J., Wandycz, A.M., Hemmati, H.D., Wright, D.E., and Weissman, I.L. (1997a). Identification of a lineage of multipotent hematopoietic progenitors. Development (Cambridge, England) *124*, 1929-1939.

Morrison, S.J., Wright, D.E., and Weissman, I.L. (1997b). Cyclophosphamide/granulocyte colony-stimulating factor induces hematopoietic stem cells to proliferate prior to mobilization. Proceedings of the National Academy of Sciences of the United States of America *94*, 1908-1913.

Morrissey, P., Charrier, K., Bressler, L., and Alpert, A. (1988). The influence of IL-1 treatment on the reconstitution of the hemopoietic and immune systems after sublethal radiation. Journal of immunology (Baltimore, Md. : 1950) *140*, 4204-4210.

Mosnier, L.O., and Griffin, J.H. (2003). Inhibition of staurosporine-induced apoptosis of endothelial cells by activated protein C requires protease-activated receptor-1 and endothelial cell protein C receptor. The Biochemical journal *373*, 65-70.

Müller-Sieburg, C.E., Cho, R.H., Karlsson, L., Huang, J.-F., and Sieburg, H.B. (2004). Myeloid-biased hematopoietic stem cells have extensive self-renewal capacity but generate diminished lymphoid progeny with impaired IL-7 responsiveness. Blood *103*, 4111-4118.

Müller-Sieburg, C.E., Cho, R.H., Thoman, M., Adkins, B., and Sieburg, H.B. (2002). Deterministic regulation of hematopoietic stem cell self-renewal and differentiation. Blood *100*, 1302-1309.

Müller-Sieburg, C.E., Townsend, K., Weissman, I.L., and Rennick, D. (1988). Proliferation and differentiation of highly enriched mouse hematopoietic stem cells and progenitor cells in response to defined growth factors. The Journal of experimental medicine *167*, 1825-1840.

Müller-Sieburg, C.E., Whitlock, C.A., and Weissman, I.L. (1986). Isolation of two early B lymphocyte progenitors from mouse marrow: a committed pre-pre-B cell and a clonogenic Thy-1-lo hematopoietic stem cell. Cell *44*, 653-662.

Muzumdar, M.D., Tasic, B., Miyamichi, K., Li, L., and Luo, L. (2007). A global double-fluorescent Cre reporter mouse. Genesis (New York, N.Y. : 2000) *45*, 593-605.

Nagai, Y., Garrett, K.P., Ohta, S., Bahrun, U., Kouro, T., Akira, S., Takatsu, K., and Kincade, P.W. (2006). Toll-like receptors on hematopoietic progenitor cells stimulate innate immune system replenishment. Immunity *24*, 801-812.

Naudé, P.J.W., Boer, J.A. den, Luiten, P.G.M., and Eisel, U.L.M. (2011). Tumor necrosis factor receptor cross-talk. The FEBS journal *278*, 888-898.

Nayak, R.C., Sen, P., Ghosh, S., Gopalakrishnan, R., Esmon, C.T., Pendurthi, U.R., and Rao, L.V.M. (2009). Endothelial cell protein C receptor cellular localization and trafficking: potential functional implications. Blood *114*, 1974-1986.

Nestorowa, S., Hamey, F.K., Pijuan Sala, B., Diamanti, E., Shepherd, M., Laurenti, E., Wilson, N.K., Kent, D.G., and Göttgens, B. (2016). A single-cell resolution map of mouse hematopoietic stem and progenitor cell differentiation. Blood *128*, e20-31.

Ng, A.P., Kauppi, M., Metcalf, D., Di Rago, L., Hyland, C.D., and Alexander, W.S. (2012). Characterization of thrombopoietin (TPO)-responsive progenitor cells in adult mouse bone marrow with in vivo megakaryocyte and erythroid potential. Proceedings of the National Academy of Sciences of the United States of America *109*, 2364-2369.

Ng, A.P., Kauppi, M., Metcalf, D., Hyland, C.D., Josefsson, E.C., Lebois, M., Zhang, J.-G., Baldwin, T.M., Di Rago, L., and Hilton, D.J., et al. (2014). Mpl expression on megakaryocytes and platelets is dispensable for thrombopoiesis but essential to prevent myeloproliferation. Proceedings of the National Academy of Sciences of the United States of America *111*, 5884-5889.

Nilsson, S.K., Johnston, H.M., and Coverdale, J.A. (2001). Spatial localization of transplanted hemopoietic stem cells: inferences for the localization of stem cell niches. Blood *97*, 2293-2299.

Ninos, J.M., Jefferies, L.C., Cogle, C.R., and Kerr, W.G. (2006). The thrombopoietin receptor, c-Mpl, is a selective surface marker for human hematopoietic stem cells. Journal of translational medicine *4*, 9.

Nishikii, H., Kanazawa, Y., Umemoto, T., Goltsev, Y., Matsuzaki, Y., Matsushita, K., Yamato, M., Nolan, G.P., Negrin, R., and Chiba, S. (2015). Unipotent Megakaryopoietic Pathway Bridging Hematopoietic Stem Cells and Mature Megakaryocytes. Stem cells (Dayton, Ohio) *33*, 2196-2207.

Nishimura, S., Nagasaki, M., Kunishima, S., Sawaguchi, A., Sakata, A., Sakaguchi, H., Ohmori, T., Manabe, I., Italiano, J.E., and Ryu, T., et al. (2015). IL-1α induces thrombopoiesis through megakaryocyte rupture in response to acute platelet needs. The Journal of cell biology *209*, 453-466.

Notta, F., Zandi, S., Takayama, N., Dobson, S., Gan, O.I., Wilson, G., Kaufmann, K.B., McLeod, J., Laurenti, E., and Dunant, C.F., et al. (2016). Distinct routes of lineage development reshape the human blood hierarchy across ontogeny. Science (New York, N.Y.) *351*, aab2116.

Oganesyan, V., Oganesyan, N., Terzyan, S., Qu, D., Dauter, Z., Esmon, N.L., and Esmon, C.T. (2002). The crystal structure of the endothelial protein C receptor and a bound phospholipid. The Journal of biological chemistry *277*, 24851-24854.

Ogilvy, S., Metcalf, D., Print, C.G., Bath, M.L., Harris, A.W., and Adams, J.M. (1999). Constitutive Bcl-2 expression throughout the hematopoietic compartment affects multiple lineages and enhances progenitor cell survival. Proc. Natl. Acad. Sci. U.S.A. *96*, 14943-14948.

Olnes, M.J., Scheinberg, P., Calvo, K.R., Desmond, R., Tang, Y., Dumitriu, B., Parikh, A.R., Soto, S., Biancotto, A., and Feng, X., et al. (2012). Eltrombopag and improved hematopoiesis in refractory aplastic anemia. The New England journal of medicine *367*, 11-19.

Osawa, M., Hanada, K., Hamada, H., and Nakauchi, H. (1996). Long-term lymphohematopoietic reconstitution by a single CD34-low/negative hematopoietic stem cell. Science (New York, N.Y.) *273*, 242-245.

Parganas, E., Wang, D., Stravopodis, D., Topham, D.J., Marine, J.C., Teglund, S., Vanin, E.F., Bodner, S., Colamonici, O.R., and van Deursen, J.M., et al. (1998). Jak2 is essential for signaling through a variety of cytokine receptors. Cell *93*, 385-395.

Pariser, D.N., Hilt, Z.T., Ture, S.K., Blick-Nitko, S.K., Looney, M.R., Cleary, S.J., Roman-Pagan, E., Saunders, J., Georas, S.N., and Veazey, J., et al. (2021). Lung megakaryocytes are immune modulatory cells. The Journal of clinical investigation *131*.

Park, H., Park, S.S., Jin, E.H., Song, J.S., Ryu, S.E., Yu, M.H., and Hong, H.J. (1998). Identification of functionally important residues of human thrombopoietin. The Journal of biological chemistry *273*, 256-261.

Passegué, E., Wagers, A.J., Giuriato, S., Anderson, W.C., and Weissman, I.L. (2005). Global analysis of proliferation and cell cycle gene expression in the regulation of hematopoietic stem and progenitor cell fates. The Journal of experimental medicine *202*, 1599-1611.

Passweg, J.R., Baldomero, H., Chabannon, C., Basak, G.W., La Cámara, R. de, Corbacioglu, S., Dolstra, H., Duarte, R., Glass, B., and Greco, R., et al. (2021). Hematopoietic cell transplantation and cellular therapy survey of the EBMT: monitoring of activities and trends over 30 years. Bone marrow transplantation *56*, 1651-1664.

Patel, S.R., Hartwig, J.H., and Italiano, J.E. (2005). The biogenesis of platelets from megakaryocyte proplatelets. The Journal of clinical investigation *115*, 3348-3354.

Paul, F., Arkin, Y., Giladi, A., Jaitin, D.A., Kenigsberg, E., Keren-Shaul, H., Winter, D., Lara-Astiaso, D., Gury, M., and Weiner, A., et al. (2015). Transcriptional Heterogeneity and Lineage Commitment in Myeloid Progenitors. Cell *163*, 1663-1677.

Perié, L., Duffy, K.R., Kok, L., Boer, R.J. de, and Schumacher, T.N. (2015). The Branching Point in Erythro-Myeloid Differentiation. Cell *163*, 1655-1662.

Pietras, E.M., Lakshminarasimhan, R., Techner, J.-M., Fong, S., Flach, J., Binnewies, M., and Passegué, E. (2014). Re-entry into quiescence protects hematopoietic stem cells from the killing effect of chronic exposure to type I interferons. The Journal of experimental medicine *211*, 245-262.

Pietras, E.M., Mirantes-Barbeito, C., Fong, S., Loeffler, D., Kovtonyuk, L.V., Zhang, S., Lakshminarasimhan, R., Chin, C.P., Techner, J.-M., and Will, B., et al. (2016). Chronic interleukin-1 exposure drives haematopoietic stem cells towards precocious myeloid differentiation at the expense of self-renewal. Nature cell biology *18*, 607-618.

Pietras, E.M., Reynaud, D., Kang, Y.-A., Carlin, D., Calero-Nieto, F.J., Leavitt, A.D., Stuart, J.M., Göttgens, B., and Passegué, E. (2015). Functionally Distinct Subsets of Lineage-Biased Multipotent Progenitors Control Blood Production in Normal and Regenerative Conditions. Cell stem cell *17*, 35-46.

Pikman, Y., Lee, B.H., Mercher, T., McDowell, E., Ebert, B.L., Gozo, M., Cuker, A., Wernig, G., Moore, S., and Galinsky, I., et al. (2006). MPLW515L is a novel somatic activating mutation in myelofibrosis with myeloid metaplasia. PLoS medicine *3*, e270.

Plo, I., Bellanné-Chantelot, C., Mosca, M., Mazzi, S., Marty, C., and Vainchenker, W. (2017). Genetic Alterations of the Thrombopoietin/MPL/JAK2 Axis Impacting Megakaryopoiesis. Frontiers in endocrinology *8*, 234.

Porteu, F., Rouyez, M.C., Cocault, L., Bénit, L., Charon, M., Picard, F., Gisselbrecht, S., Souyri, M., and Dusanter-Fourt, I. (1996). Functional regions of the mouse thrombopoietin receptor cytoplasmic domain: evidence for a critical region which is involved in differentiation and can be complemented by erythropoietin. Molecular and cellular biology *16*, 2473-2482.

Prins, D., Park, H.J., Watcham, S., Li, J., Vacca, M., Bastos, H.P., Gerbaulet, A., Vidal-Puig, A., Göttgens, B., and Green, A.R. (2020). The stem/progenitor landscape is reshaped in a mouse model of essential thrombocythemia and causes excess megakaryocyte production. Science advances *6*.

Pronk, C.J.H., Veiby, O.P., Bryder, D., and Jacobsen, S.E.W. (2011). Tumor necrosis factor restricts hematopoietic stem cell activity in mice: involvement of two distinct receptors. The Journal of experimental medicine *208*, 1563-1570.

Purton, L.E., and Scadden, D.T. (2007). Limiting factors in murine hematopoietic stem cell assays. Cell stem cell *1*, 263-270.

Qian, H., Buza-Vidas, N., Hyland, C.D., Jensen, C.T., Antonchuk, J., Månsson, R., Thoren, L.A., Ekblom, M., Alexander, W.S., and Jacobsen, S.E.W. (2007). Critical Role of Thrombopoietin in Maintaining Adult Quiescent Hematopoietic Stem Cells. Cell stem cell *1*, 671-684.

Qian, S., Fu, F., Li, W., Chen, Q., and Sauvage, F.J. de (1998). Primary Role of the Liver in Thrombopoietin Production Shown by Tissue-Specific Knockout. Blood *92*, 2189-2191.

Raadsen, M., Du Toit, J., Langerak, T., van Bussel, B., van Gorp, E., and Goeijenbier, M. (2021). Thrombocytopenia in Virus Infections. Journal of clinical medicine *10*.

Rabe, J.L., Hernandez, G., Chavez, J.S., Mills, T.S., Nerlov, C., and Pietras, E.M. (2020). CD34 and EPCR coordinately enrich functional murine hematopoietic stem cells under normal and inflammatory conditions. Experimental hematology *81*, 1-15.e6.

Racke, F.K., Lewandowska, K., Goueli, S., and Goldfarb, A.N. (1997). Sustained activation of the extracellular signal-regulated kinase/mitogen-activated protein kinase pathway is required for megakaryocytic differentiation of K562 cells. The Journal of biological chemistry *272*, 23366-23370.

Ramasz, B., Krüger, A., Reinhardt, J., Sinha, A., Gerlach, M., Gerbaulet, A., Reinhardt, S., Dahl, A., Chavakis, T., and Wielockx, B., et al. (2019). Hematopoietic stem cell response to acute thrombocytopenia requires signaling through distinct receptor tyrosine kinases. Blood *134*, 1046-1058.

Rekhtman, N., Radparvar, F., Evans, T., and Skoultchi, A.I. (1999). Direct interaction of hematopoietic transcription factors PU.1 and GATA-1: functional antagonism in erythroid cells. Genes & development *13*, 1398-1411.

Rezzoug, F., Huang, Y., Tanner, M.K., Wysoczynski, M., Schanie, C.L., Chilton, P.M., Ratajczak, M.Z., Fugier-Vivier, I.J., and Ildstad, S.T. (2008). TNF-alpha is critical to facilitate hemopoietic stem cell engraftment and function. Journal of immunology (Baltimore, Md. : 1950) *180*, 49-57.

Richardson, J.L., Shivdasani, R.A., Boers, C., Hartwig, J.H., and Italiano, J.E. (2005). Mechanisms of organelle transport and capture along proplatelets during platelet production. Blood *106*, 4066-4075.

Riewald, M., Petrovan, R.J., Donner, A., Mueller, B.M., and Ruf, W. (2002). Activation of endothelial cell protease activated receptor 1 by the protein C pathway. Science (New York, N.Y.) *296*, 1880-1882.

Ritchie, A., Braun, S.E., He, J., and Broxmeyer, H.E. (1999). Thrombopoietin-induced conformational change in p53 lies downstream of the p44/p42 mitogen activated protein kinase cascade in the human growth factor-dependent cell line M07e. Oncogene *18*, 1465-1477.

Roberts, A., Buonocore, L., Price, R., Forman, J., and Rose, J.K. (1999). Attenuated vesicular stomatitis viruses as vaccine vectors. Journal of virology *73*, 3723-3732.

Rodriguez-Fraticelli, A.E., Wolock, S.L., Weinreb, C.S., Panero, R., Patel, S.H., Jankovic, M., Sun, J., Calogero, R.A., Klein, A.M., and Camargo, F.D. (2018). Clonal analysis of lineage fate in native haematopoiesis. Nature *553*, 212-216.

Rojnuckarin, P., Drachman, J.G., and Kaushansky, K. (1999). Thrombopoietin-induced activation of the mitogen-activated protein kinase (MAPK) pathway in normal megakaryocytes: role in endomitosis. Blood *94*, 1273-1282.

Rondina, M.T., Brewster, B., Grissom, C.K., Zimmerman, G.A., Kastendieck, D.H., Harris, E.S., and Weyrich, A.S. (2012). In vivo platelet activation in critically ill patients with primary 2009 influenza A(H1N1). Chest *141*, 1490-1495.

Rongvaux, A., Willinger, T., Takizawa, H., Rathinam, C., Auerbach, W., Murphy, A.J., Valenzuela, D.M., Yancopoulos, G.D., Eynon, E.E., and Stevens, S., et al. (2011). Human thrombopoietin knockin mice efficiently support human hematopoiesis in vivo. Proc. Natl. Acad. Sci. U.S.A. *108*, 2378-2383.

Rosendaal, M., Hodgson, G.S., and Bradley, T.R. (1979). Organization of haemopoietic stem cells: the generation-age hypothesis. Cell and tissue kinetics *12*, 17-29.

Rouyez, M.C., Boucheron, C., Gisselbrecht, S., Dusanter-Fourt, I., and Porteu, F. (1997). Control of thrombopoietin-induced megakaryocytic differentiation by the mitogen-activated protein kinase pathway. Molecular and cellular biology *17*, 4991-5000.

Royer, Y., Staerk, J., Costuleanu, M., Courtoy, P.J., and Constantinescu, S.N. (2005). Janus kinases affect thrombopoietin receptor cell surface localization and stability. The Journal of biological chemistry *280*, 27251-27261.

Russell, E.S. (1979). Hereditary Anemias of the Mouse: A Review for Geneticists. In (Elsevier), pp. 357–459.

Ryabkova, V.A., Churilov, L.P., and Shoenfeld, Y. (2021). Influenza infection, SARS, MERS and COVID-19: Cytokine storm - The common denominator and the lessons to be learned. Clinical immunology (Orlando, Fla.) *223*, 108652.

Sabath, D.F., Kaushansky, K., and Broudy, V.C. (1999). Deletion of the Extracellular Membrane-Distal Cytokine Receptor Homology Module of Mpl Results in Constitutive Cell Growth and Loss of Thrombopoietin Binding. Blood *94*, 365-367.

Sakamoto, A., Tsukamoto, T., Furutani, Y., Sudo, Y., Shimada, K., Tomita, A., Kiyoi, H., Kato, T., and Funatsu, T. (2016). Live-cell single-molecule imaging of the cytokine receptor MPL for analysis of dynamic dimerization. Journal of molecular cell biology *8*, 553-555.

Sangkhae, V., Saur, S.J., Kaushansky, A., Kaushansky, K., and Hitchcock, I.S. (2014). Phosphorylated c-Mpl tyrosine 591 regulates thrombopoietin-induced signaling. Experimental hematology *42*, 477-86.e4.

Sanjuan-Pla, A., Macaulay, I.C., Jensen, C.T., Woll, P.S., Luis, T.C., Mead, A., Moore, S., Carella, C., Matsuoka, S., and Bouriez Jones, T., et al. (2013). Platelet-biased stem cells reside at the apex of the haematopoietic stem-cell hierarchy. Nature *502*, 232-236.

Sato, T., Onai, N., Yoshihara, H., Arai, F., Suda, T., and Ohteki, T. (2009). Interferon regulatory factor-2 protects quiescent hematopoietic stem cells from type I interferon-dependent exhaustion. Nature medicine *15*, 696-700.

Saur, S.J., Sangkhae, V., Geddis, A.E., Kaushansky, K., and Hitchcock, I.S. (2010). Ubiquitination and degradation of the thrombopoietin receptor c-Mpl. Blood *115*, 1254-1263.

Sauvage, F.J. de, Carver-Moore, K., Luoh, S.M., Ryan, A., Dowd, M., Eaton, D.L., and Moore, M.W. (1996). Physiological regulation of early and late stages of megakaryocytopoiesis by thrombopoietin. The Journal of experimental medicine *183*, 651-656.

Schambach, A., Bohne, J., Chandra, S., Will, E., Margison, G.P., Williams, D.A., and Baum, C. (2006). Equal potency of gammaretroviral and lentiviral SIN vectors for expression of O6-methylguanine-DNA methyltransferase in hematopoietic cells. Molecular therapy : the journal of the American Society of Gene Therapy *13*, 391-400.

Schofield, R. (1978). The relationship between the spleen colony-forming cell and the haemopoietic stem cell. Blood cells *4*, 7-25.

Selleri, C., Sato, T., Anderson, S., Young, N.S., and Maciejewski, J.P. (1995). Interferon-gamma and tumor necrosis factor-alpha suppress both early and late stages of hematopoiesis and induce programmed cell death. Journal of cellular physiology *165*, 538-546.

Sezaki, M., Hayashi, Y., Wang, Y., Johansson, A., Umemoto, T., and Takizawa, H. (2020). Immuno-Modulation of Hematopoietic Stem and Progenitor Cells in Inflammation. Frontiers in immunology *11*, 585367.

Shin, J.Y., Hu, W., Naramura, M., and Park, C.Y. (2014). High c-Kit expression identifies hematopoietic stem cells with impaired self-renewal and megakaryocytic bias. The Journal of experimental medicine *211*, 217-231.

Shivdasani, R.A., Fujiwara, Y., McDevitt, M.A., and Orkin, S.H. (1997). A lineage-selective knockout establishes the critical role of transcription factor GATA-1 in megakaryocyte growth and platelet development. The EMBO journal *16*, 3965-3973.

Shivdasani, R.A., Rosenblatt, M.F., Zucker-Franklin, D., Jackson, C.W., Hunt, P., Saris, C.J., and Orkin, S.H. (1995). Transcription factor NF-E2 is required for platelet formation independent of the actions of thrombopoietin/MGDF in megakaryocyte development. Cell *81*, 695-704.

Signer, R.A.J., Magee, J.A., Salic, A., and Morrison, S.J. (2014). Haematopoietic stem cells require a highly regulated protein synthesis rate. Nature *509*, 49-54.

Simsek, T., Kocabas, F., Zheng, J., Deberardinis, R.J., Mahmoud, A.I., Olson, E.N., Schneider, J.W., Zhang, C.C., and Sadek, H.A. (2010). The distinct metabolic profile of hematopoietic stem cells reflects their location in a hypoxic niche. Cell stem cell *7*, 380-390.

Sitnicka, E., Lin, N., Priestley, G.V., Fox, N., Broudy, V.C., Wolf, N.S., and Kaushansky, K. (1996a). The effect of thrombopoietin on the proliferation and differentiation of murine hematopoietic stem cells. Blood *87*, 4998-5005.

Sitnicka, E., Ruscetti, F.W., Priestley, G.V., Wolf, N.S., and Bartelmez, S.H. (1996b). Transforming growth factor beta 1 directly and reversibly inhibits the initial cell divisions of long-term repopulating hematopoietic stem cells. Blood *88*, 82-88.

Sommerkamp, P., Romero-Mulero, M.C., Narr, A., Ladel, L., Hustin, L., Schönberger, K., Renders, S., Altamura, S., Zeisberger, P., and Jäcklein, K., et al. (2021). Mouse multipotent progenitor 5 cells are located at the interphase between hematopoietic stem and progenitor cells. Blood *137*, 3218-3224.

Spangler, J.B., Moraga, I., Mendoza, J.L., and Garcia, K.C. (2015). Insights into cytokine-receptor interactions from cytokine engineering. Annual review of immunology *33*, 139-167.

Spangrude, G.J., Heimfeld, S., and Weissman, I.L. (1988). Purification and characterization of mouse hematopoietic stem cells. Science (New York, N.Y.) *241*, 58-62.

Staerk, J., Defour, J.-P., Pecquet, C., Leroy, E., Antoine-Poirel, H., Brett, I., Itaya, M., Smith, S.O., Vainchenker, W., and Constantinescu, S.N. (2011). Orientation-specific signalling by thrombopoietin receptor dimers. The EMBO journal *30*, 4398-4413.

Starr, R., and Hilton, D.J. (1999). Negative regulation of the JAK/STAT pathway. Bioessays *21*, 47-52.

Subbarao, K., and Roberts, A. (2006). Is there an ideal animal model for SARS? Trends in microbiology *14*, 299-303.

Sugiyama, T., Kohara, H., Noda, M., and Nagasawa, T. (2006). Maintenance of the hematopoietic stem cell pool by CXCL12-CXCR4 chemokine signaling in bone marrow stromal cell niches. Immunity *25*, 977-988.

Sun, S., Jin, C., Si, J., Lei, Y., Chen, K., Cui, Y., Liu, Z., Liu, J., Zhao, M., and Zhang, X., et al. (2021). Single-cell analysis of ploidy and the transcriptome reveals functional and spatial divergency in murine megakaryopoiesis. Blood *138*, 1211-1224.

Sungaran, R., Markovic, B., and Chong, B.H. (1997). Localization and regulation of thrombopoietin mRNa expression in human kidney, liver, bone marrow, and spleen using in situ hybridization. Blood *89*, 101-107.

Syed, R.S., Reid, S.W., Li, C., Cheetham, J.C., Aoki, K.H., Liu, B., Zhan, H., Osslund, T.D., Chirino, A.J., and Zhang, J., et al. (1998). Efficiency of signalling through cytokine receptors depends critically on receptor orientation. Nature *395*, 511-516.

Takizawa, H., Regoes, R.R., Boddupalli, C.S., Bonhoeffer, S., and Manz, M.G. (2011). Dynamic variation in cycling of hematopoietic stem cells in steady state and inflammation. The Journal of experimental medicine *208*, 273-284.

Takubo, K., Nagamatsu, G., Kobayashi, C.I., Nakamura-Ishizu, A., Kobayashi, H., Ikeda, E., Goda, N., Rahimi, Y., Johnson, R.S., and Soga, T., et al. (2013). Regulation of glycolysis by Pdk functions as a metabolic checkpoint for cell cycle quiescence in hematopoietic stem cells. Cell stem cell *12*, 49-61.

Teijaro, J.R., Walsh, K.B., Cahalan, S., Fremgen, D.M., Roberts, E., Scott, F., Martinborough, E., Peach, R., Oldstone, M.B.A., and Rosen, H. (2011). Endothelial cells are central orchestrators of cytokine amplification during influenza virus infection. Cell *146*, 980-991.

Thapa, R., Elfassy, E., Olender, L., Sharabi, O., and Gazit, R. (2022). Rapid Activation of Hematopoietic Stem Cells.

Thomas, E.D., Lochte, H.L., Lu, W.C., and Ferrebee, J.W. (1957). Intravenous infusion of bone marrow in patients receiving radiation and chemotherapy. The New England journal of medicine *257*, 491-496.

Tijssen, M.R., Cvejic, A., Joshi, A., Hannah, R.L., Ferreira, R., Forrai, A., Bellissimo, D.C., Oram, S.H., Smethurst, P.A., and Wilson, N.K., et al. (2011). Genome-wide analysis of simultaneous GATA1/2, RUNX1, FLI1, and SCL binding in megakaryocytes identifies hematopoietic regulators. Developmental cell *20*, 597-609.

Till, J.E., and McCulloch, E.A. (1961). A direct measurement of the radiation sensitivity of normal mouse bone marrow cells. Radiation research *14*, 213-222.

Tomer, A., Harker, L.A., and Burstein, S.A. (1987). Purification of human megakaryocytes by fluorescence-activated cell sorting. Blood *70*, 1735-1742.

Tong, W., Ibarra, Y.M., and Lodish, H.F. (2007). Signals emanating from the membrane proximal region of the thrombopoietin receptor (mpl) support hematopoietic stem cell self-renewal. Experimental hematology *35*, 1447-1455.

Tong, W., and Lodish, H.F. (2004). Lnk inhibits Tpo-mpl signaling and Tpo-mediated megakaryocytopoiesis. The Journal of experimental medicine *200*, 569-580.

Tong, W., Sulahian, R., Gross, A.W., Hendon, N., Lodish, H.F., and Huang, L.J. (2006). The membrane-proximal region of the thrombopoietin receptor confers its high surface expression by JAK2-dependent and -independent mechanisms. The Journal of biological chemistry *281*, 38930-38940.

Tran, T.H., Nguyen, T.L., Nguyen, T.D., Luong, T.S., Pham, P.M., van Nguyen, V.C., Pham, T.S., Vo, C.D., Le, T.Q.M., and Ngo, T.T., et al. (2004). Avian influenza A (H5N1) in 10 patients in Vietnam. The New England journal of medicine *350*, 1179-1188.

Tripic, T., Deng, W., Cheng, Y., Zhang, Y., Vakoc, C.R., Gregory, G.D., Hardison, R.C., and Blobel, G.A. (2009). SCL and associated proteins distinguish active from repressive GATA transcription factor complexes. Blood *113*, 2191-2201.

Tsai, F.Y., and Orkin, S.H. (1997). Transcription factor GATA-2 is required for proliferation/survival of early hematopoietic cells and mast cell formation, but not for erythroid and myeloid terminal differentiation. Blood *89*, 3636-3643.

Tubman, V.N., Levine, J.E., Campagna, D.R., Monahan-Earley, R., Dvorak, A.M., Neufeld, E.J., and Fleming, M.D. (2007). X-linked gray platelet syndrome due to a GATA1 Arg216Gln mutation. Blood *109*, 3297-3299.

Tusi, B.K., Wolock, S.L., Weinreb, C., Hwang, Y., Hidalgo, D., Zilionis, R., Waisman, A., Huh, J.R., Klein, A.M., and Socolovsky, M. (2018). Population snapshots predict early haematopoietic and erythroid hierarchies. Nature *555*, 54-60.

Tzeng, Y.-S., Li, H., Kang, Y.-L., Chen, W.-C., Cheng, W.-C., and Lai, D.-M. (2011). Loss of Cxcl12/Sdf-1 in adult mice decreases the quiescent state of hematopoietic stem/progenitor cells and alters the pattern of hematopoietic regeneration after myelosuppression. Blood *117*, 429-439.

Vadhan-Raj, S., Murray, L.J., Bueso-Ramos, C., Patel, S., Reddy, S.P., Hoots, W.K., Johnston, T., Papadopolous, N.E., Hittelman, W.N., and Johnston, D.A., et al. (1997). Stimulation of megakaryocyte and platelet production by a single dose of recombinant human thrombopoietin in patients with cancer. Annals of internal medicine *126*, 673-681.

Vainchenker, W., and Kralovics, R. (2017). Genetic basis and molecular pathophysiology of classical myeloproliferative neoplasms. Blood *129*, 667-679.

Valet, C., Magnen, M., Qiu, L., Cleary, S.J., Wang, K.M., Ranucci, S., Grockowiak, E., Boudra, R., Conrad, C., and Seo, Y., et al. (2022). Sepsis promotes splenic production of a protective platelet pool with high CD40 ligand expression. The Journal of clinical investigation *132*.

van den Oudenrijn, S., Bruin, M., Folman, C.C., Peters, M., Faulkner, L.B., Haas, M. de, and Borne, A.E. von dem (2000). Mutations in the thrombopoietin receptor, Mpl, in children with congenital amegakaryocytic thrombocytopenia. British journal of haematology *110*, 441-448.

van der Meer, J.W., Barza, M., Wolff, S.M., and Dinarello, C.A. (1988). A low dose of recombinant interleukin 1 protects granulocytopenic mice from lethal gram-negative infection. Proceedings of the National Academy of Sciences of the United States of America *85*, 1620-1623.

Vannini, N., Girotra, M., Naveiras, O., Nikitin, G., Campos, V., Giger, S., Roch, A., Auwerx, J., and Lutolf, M.P. (2016). Specification of haematopoietic stem cell fate via modulation of mitochondrial activity. Nature communications *7*, 13125.

Velten, L., Haas, S.F., Raffel, S., Blaszkiewicz, S., Islam, S., Hennig, B.P., Hirche, C., Lutz, C., Buss, E.C., and Nowak, D., et al. (2017). Human haematopoietic stem cell lineage commitment is a continuous process. Nature cell biology *19*, 271-281.

Vigon, I., Mornon, J.P., Cocault, L., Mitjavila, M.T., Tambourin, P., Gisselbrecht, S., and Souyri, M. (1992). Molecular cloning and characterization of MPL, the human homolog of the v-mpl oncogene: identification of a member of the hematopoietic growth factor receptor superfamily. Proceedings of the National Academy of Sciences of the United States of America *89*, 5640-5644.

Waddington, C.H. (1957). The Strategy of the Genes (Routledge).

Walter, D., Lier, A., Geiselhart, A., Thalheimer, F.B., Huntscha, S., Sobotta, M.C., Moehrle, B., Brocks, D., Bayindir, I., and Kaschutnig, P., et al. (2015). Exit from dormancy provokes DNA-damage-induced attrition in haematopoietic stem cells. Nature *520*, 549-552.

Walz, L., Kays, S.-K., Zimmer, G., and Messling, V. von (2018). Neuraminidase-Inhibiting Antibody Titers Correlate with Protection from Heterologous Influenza Virus Strains of the Same Neuraminidase Subtype. Journal of virology *92*.

Weinreb, C., Rodriguez-Fraticelli, A., Camargo, F.D., and Klein, A.M. (2020). Lineage tracing on transcriptional landscapes links state to fate during differentiation. Science (New York, N.Y.) *367*.

Weissman, I.L., and Shizuru, J.A. (2008). The origins of the identification and isolation of hematopoietic stem cells, and their capability to induce donor-specific transplantation tolerance and treat autoimmune diseases. Blood *112*, 3543-3553.

Wendling, F., Maraskovsky, E., Debili, N., Florindo, C., Teepe, M., Titeux, M., Methia, N., Breton-Gorius, J., Cosman, D., and Vainchenker, W. (1994). cMpl ligand is a humoral regulator of megakaryocytopoiesis. Nature *369*, 571-574.

Wendling, F., Varlet, P., Charon, M., and Tambourin, P. (1986). MPLV: a retrovirus complex inducing an acute myeloproliferative leukemic disorder in adult mice. Virology *149*, 242-246.

Whalen, A.M., Galasinski, S.C., Shapiro, P.S., Nahreini, T.S., and Ahn, N.G. (1997). Megakaryocytic differentiation induced by constitutive activation of mitogen-activated protein kinase kinase. Molecular and cellular biology *17*, 1947-1958.

Whitty, A., and Borysenko, C.W. (1999). Small molecule cytokine mimetics. Chemistry & biology *6*, R107-18.

Wilkinson, A.C., Ishida, R., Kikuchi, M., Sudo, K., Morita, M., Crisostomo, R.V., Yamamoto, R., Loh, K.M., Nakamura, Y., and Watanabe, M., et al. (2019). Long-term ex vivo haematopoietic-stem-cell expansion allows nonconditioned transplantation. Nature *571*, 117-121.

Will, B., Kawahara, M., Luciano, J.P., Bruns, I., Parekh, S., Erickson-Miller, C.L., Aivado, M.A., Verma, A., and Steidl, U. (2009). Effect of the nonpeptide thrombopoietin receptor agonist Eltrombopag on bone marrow cells from patients with acute myeloid leukemia and myelodysplastic syndrome. Blood *114*, 3899-3908.

Wilmes, S., Hafer, M., Vuorio, J., Tucker, J.A., Winkelmann, H., Löchte, S., Stanly, T.A., Pulgar Prieto, K.D., Poojari, C., and Sharma, V., et al. (2020). Mechanism of homodimeric cytokine receptor activation and dysregulation by oncogenic mutations. Science (New York, N.Y.) *367*, 643-652.

Wilson, A., Laurenti, E., Oser, G., van der Wath, R.C., Blanco-Bose, W., Jaworski, M., Offner, S., Dunant, C.F., Eshkind, L., and Bockamp, E., et al. (2008). Hematopoietic stem cells reversibly switch from dormancy to self-renewal during homeostasis and repair. Cell *135*, 1118-1129.

Wilson, A., Murphy, M.J., Oskarsson, T., Kaloulis, K., Bettess, M.D., Oser, G.M., Pasche, A.-C., Knabenhans, C., Macdonald, H.R., and Trumpp, A. (2004). c-Myc controls the balance between hematopoietic stem cell self-renewal and differentiation. Genes & development *18*, 2747-2763.

Winkler, E.S., Bailey, A.L., Kafai, N.M., Nair, S., McCune, B.T., Yu, J., Fox, J.M., Chen, R.E., Earnest, J.T., and Keeler, S.P., et al. (2020). SARS-CoV-2 infection of human ACE2-transgenic mice causes severe lung inflammation and impaired function. Nature immunology *21*, 1327-1335.

Woods, V.M.A., Latorre-Rey, L.J., Schenk, F., Rommel, M.G.E., Moritz, T., and Modlich, U. (2022). Targeting transgenic proteins to alpha granules for platelet-directed gene therapy. Molecular therapy. Nucleic acids *27*, 774-786.

World Health Organization (2002). WHO manual on animal influenza diagnosis and surveillance (World Health Organization).

Wright, D.E., Cheshier, S.H., Wagers, A.J., Randall, T.D., Christensen, J.L., and Weissman, I.L. (2001). Cyclophosphamide/granulocyte colony-stimulating factor causes selective mobilization of bone marrow hematopoietic stem cells into the blood after M phase of the cell cycle. Blood *97*, 2278-2285.

Yamamoto, R., Morita, Y., Ooehara, J., Hamanaka, S., Onodera, M., Rudolph, K.L., Ema, H., and Nakauchi, H. (2013). Clonal analysis unveils self-renewing lineage-restricted progenitors generated directly from hematopoietic stem cells. Cell *154*, 1112-1126.

Yamamoto, R., Wilkinson, A.C., Ooehara, J., Lan, X., Lai, C.-Y., Nakauchi, Y., Pritchard, J.K., and Nakauchi, H. (2018). Large-Scale Clonal Analysis Resolves Aging of the Mouse Hematopoietic Stem Cell Compartment. Cell stem cell *22*, 600-607.e4.

Yamashita, M., and Passegué, E. (2019). TNF-α Coordinates Hematopoietic Stem Cell Survival and Myeloid Regeneration. Cell stem cell *25*, 357-372.e7.

Yamazaki, S., Iwama, A., Takayanagi, S., Morita, Y., Eto, K., Ema, H., and Nakauchi, H. (2006). Cytokine signals modulated via lipid rafts mimic niche signals and induce hibernation in hematopoietic stem cells. The EMBO journal *25*, 3515-3523.

Yeaman, M.R. (2014). Platelets: at the nexus of antimicrobial defence. Nature reviews. Microbiology *12*, 426-437.

Yokota, T., Oritani, K., Butz, S., Kokame, K., Kincade, P.W., Miyata, T., Vestweber, D., and Kanakura, Y. (2009). The endothelial antigen ESAM marks primitive hematopoietic progenitors throughout life in mice. Blood *113*, 2914-2923.

Yoshihara, H., Arai, F., Hosokawa, K., Hagiwara, T., Takubo, K., Nakamura, Y., Gomei, Y., Iwasaki, H., Matsuoka, S., and Miyamoto, K., et al. (2007). Thrombopoietin/MPL signaling regulates hematopoietic stem cell quiescence and interaction with the osteoblastic niche. Cell stem cell *1*, 685-697.

Yu, V.W.C., Yusuf, R.Z., Oki, T., Wu, J., Saez, B., Wang, X., Cook, C., Baryawno, N., Ziller, M.J., and Lee, E., et al. (2017). Epigenetic Memory Underlies Cell-Autonomous Heterogeneous Behavior of Hematopoietic Stem Cells. Cell *168*, 944-945.

Zhang, C.C., Kaba, M., Ge, G., Xie, K., Tong, W., Hug, C., and Lodish, H.F. (2006). Angiopoietin-like proteins stimulate ex vivo expansion of hematopoietic stem cells. Nature medicine *12*, 240-245.

Zhang, C.R.C., Nix, D., Gregory, M., Ciorba, M.A., Ostrander, E.L., Newberry, R.D., Spencer, D.H., and Challen, G.A. (2019). Inflammatory cytokines promote clonal hematopoiesis with specific mutations in ulcerative colitis patients. Experimental hematology *80*, 36-41.e3.

Zhang, J., Niu, C., Ye, L., Huang, H., He, X., Tong, W.-G., Ross, J., Haug, J., Johnson, T., and Feng, J.Q., et al. (2003). Identification of the haematopoietic stem cell niche and control of the niche size. Nature *425*, 836-841.

Zhao, J.L., Ma, C., O'Connell, R.M., Mehta, A., DiLoreto, R., Heath, J.R., and Baltimore, D. (2014). Conversion of danger signals into cytokine signals by hematopoietic stem and progenitor cells for regulation of stress-induced hematopoiesis. Cell stem cell *14*, 445-459.

Zhou, B.O., Ding, L., and Morrison, S.J. (2015). Hematopoietic stem and progenitor cells regulate the regeneration of their niche by secreting Angiopoietin-1. eLife *4*, e05521.

Zhu, F., Feng, M., Sinha, R., Seita, J., Mori, Y., and Weissman, I.L. (2018). Screening for genes that regulate the differentiation of human megakaryocytic lineage cells. Proceedings of the National Academy of Sciences of the United States of America *115*, E9308-E9316.

Zimmet, J.M., Ladd, D., Jackson, C.W., Stenberg, P.E., and Ravid, K. (1997). A role for cyclin D3 in the endomitotic cell cycle. Molecular and cellular biology *17*, 7248-7259.

Zsebo, K.M., Williams, D.A., Geissler, E.N., Broudy, V.C., Martin, F.H., Atkins, H.L., Hsu, R.-Y., Birkett, N.C., Okino, K.H., and Murdock, D.C., et al. (1990). Stem cell factor is encoded at the SI locus of the mouse and is the ligand for the c-kit tyrosine kinase receptor. Cell *63*, 213-224.

Zufferey, A., Speck, E.R., Machlus, K.R., Aslam, R., Guo, L., McVey, M.J., Kim, M., Kapur, R., Boilard, E., and Italiano, J.E., et al. (2017). Mature murine megakaryocytes present antigen-MHC class I molecules to T cells and transfer them to platelets. Blood advances *1*, 1773-1785.

Acknowledgement

Starting and developing on my PhD project was a remarkable experience that has provided me with countless opportunities to develop and grow as a research scientist, teacher and as a person. This amazing time of challenges and breakthroughs would not have been possible with the continued support of the following mentors, colleagues, collaborators, friends, family, and my boyfriend.

First of all, I would like to thank you, **Ute**. I am deeply grateful for the support, trust, patients, and confidence you put in me. The freedom to pursue my own ideas in our project. You have provided me with an excellent atmosphere and workplace in the PEI to experience the term research. Thank you for being critical and challenging to bring out the best possible of myself.

I would like to thank **Angelika Schnieke** for taking over the supervision at the Technische Universität München. Moreover, I would like to thank the members of my thesis examination committee, **Angelika Schnieke**, **Benjamin Schusser** and the **Claudia Waskow** for taking the time to read and evaluate my thesis.

Furthermore, I would like to thank all the members of my thesis committee **Veronika von Messling**, **Christian Buchholz**, **Ute Modlich**, and **Angelika Schnieke** for asking excellent questions and the support.

Next, I would like to give a *big thank* you and applause to the current and former members and students of the **Modlich group** who contributed to such an amazing research atmosphere, and for their endless help! I would especially like to thank **Saskia**, for passing on all knowledge and projects that I was able to continue working on. Thanks to the essential core of the group **Franziska** for the constant lab and mental support and taking care of the mouse colonies. **Katharina**, **Tanja**, **Simon P.**, **Julia F**, **Julia B** and **Vanessa** for all the experimental and scientific contribution, proofreading of manuscript and coffee/tea breaks! All the students I directly or indirectly supervised, thank you for bringing fresh energy, ideas, cakes and joy to our group. Thanks to: **Julia A.**, **Stella, Yiwei, Luise, Tim, India, Eva, Simon B., Magdalena, Christian M., Melissa, Nora, Sabrina, Vanessa,** and **Theresa.**

Another big thank you goes to the **von Messling / Pfaller group** who started this outstanding project to combining virology and hematopoietic stem cell biology. Thanks to **Veronika von Messling** and **Christian Pfaller** for the great discussion and the willingness of all of us to learn new things from each other. Thanks to **Lisa** without your personality and positive working atmosphere it would not have been possible to start the influenza project. **Yvonne, Kevin** and **Svetlana** who always have provided me a helping hand during the experiments with the mice.

Especially **Svetlana**, without you we would not have been able to answer the reviewer's questions!

Lacra, I can't be more great full that you have the magic hands for transplantation at all hours of the day and endless patients to analyze CFUs together, thank you so much. Thank you to the Ivics group, **Zoltan** and **Csaba** for bringing RNA-sequencing to the PEI and the computer power to analyze tons of FC data. Thanks to all the people and friends from different divisions at the PEI for the inspiring and motivating atmosphere but also for being there when you need a break: Thanks to **Olga, Nina, Iris, Johanna, Arne, Alexander,** and **Oliver**.

Next, I would like to say thank you FACS core facility for providing me with excellent machines and unforgettable knowledge about the Aria Fusion! Thanks to **Sven** and **Jörg**. The **animal caretakers** and **veterinarians** who took care of the mice and the fun moments in the PEI37. A big thank you goes to the **histology ladies**, providing me insight and tips from the beginning until the end of organ preparation.

What can I say? Thank you, **Fenia**, for the awesome work hours, coffee breaks, and the joy of discuss science and all other topic in life. You**, Esther, Ian and Melanie** motivated me to enjoy and stay in research and made the DKFZ Sommerfest 2022 unforgettable. Thanks to **Mick Milsom** and **Marieke Essers** for the outstanding collaboration experience!

Thanks to all people, I have met in the scientific community during the time at conferences: **Gülce**, **Nina** and **Kerstin**.

Ein großer Dank geht an meine Eltern **Guido** und **Gudrun**, dass ihr mir durch Eure fortwährende Unterstützung, aber auch die Freiheit ermöglicht hab meine eigenen Ziele und Wünsche zu verfolgen und jetzt zu erreichen. An meine Schwester **Veronika** vielen Dank für das Wachhalten bei nächtlichen Heimfahrten vom PEI. **Sonja, Desiree** und **Andrea –** Freunde, die man immer Erreichen und Belagern kann und die einem immer die richtige Idee ins Ohr setzen. Einen Dank an alle Freunde und Bekannten, die mich mit vielleicht nicht durch ersichtliche Hilfe unterstützt haben, die ich aber hier gerne erwähnen möchte.

Zum Schluss möchte ich mich bei der Person danken, die mich ohne jegliche Erklärung und mit unendlichem Verständnis aufgefangen und unterstützt hat. Mir immer das Gefühl gegeben hat „Du kannst alles erreichen!“: **Max**. Danke Dit.